DOI: 10.1070/RCR4866

Quantum chemical methods in charge density studies from X-ray diffraction data †

Alexander A. Korlyukov,[a, b] Yulia V. Nelyubina [a]

[a] *A.N.Nesmeyanov Institute of Organoelement Compounds, Russian Academy of Sciences, ul. Vavilova 28, 119991 Moscow, Russian Federation*
[b] *N.I.Pirogov Russian National Research Medical University, ul. Ostrovityanova 1, 117997 Moscow, Russian Federation*

Single-crystal X-ray diffraction studies are among the best experimental methods for elucidating the structure of chemical compounds. Recently, their focus has been shifted towards extracting information on chemical bonding features and related valuable properties of these compounds from the analysis of charge density distribution obtained in high-resolution X-ray diffraction experiments; the latter are possible only for a limited number of well-ordered crystals of small molecules. In this review, the hybrid approaches are described that introduce quantum chemical methods into the refinement of X-ray diffraction data. Their use significantly extends the range of systems suitable for charge density studies (such as polypeptides, metal-organic frameworks, inclusion compounds and others) and the scope of problems that they solve, *viz*., from protein structure refinement to determination of thermodynamic or other wave function-derived properties of crystals. The potential of these hybrid approaches and prospects for their future applications are discussed.
The bibliography includes 322 references.

Contents

1. Introduction 677
2. The basics of single-crystal X-ray diffraction 679
3. The basics of high-resolution X-ray diffraction studies 682
4. Databases of experimental multipole parameters 689
5. Quantum chemical calculations of X-ray structure factors 692
6. Databases of theoretical multipole parameters 696
7. Calculations of anisotropic displacement parameters of atoms 702
8. The Hirshfeld atom refinement 705
9. X-Ray constrained wave function refinement 708
10. Conclusion 710

1. Introduction

Single-crystal X-ray crystallography is based on the interaction of X-ray radiation with electrons and is widely regarded as main experimental method for molecular structure determination. Already in the early stage of development of the method it became clear that one can obtain information on not only atomic coordinates and types of atoms (and, correspondingly, bond lengths, bond angles or other structural data that can be used to establish structure – property correlations), but also the electron density (ED) distribution in crystals,[1] which is responsible for their properties in accordance with the Hohenberg – Kohn theorem.[2] Realization of such a strategy became possible long after,[3] first of all, due to the development of theoretical approaches (*e.g.*, the multipole model [4] and Bader's quantum topological theory 'Atoms in molecules' [5]) that involve

A.A.Korlyukov. Doctor of Chemistry, Professor RAS, Leading Researcher at the Laboratory for X-ray Diffraction Studies at the INEOS RAS and Principal Researcher at the Department of Medicinal Chemistry and Toxicology at the RNRMU.
Telephone: +7(499)135 – 9214, e-mail: alex@xrlab.ineos.ac.ru
Current research interests: crystal chemistry, quantum chemistry, theory of the structure of matter, materials science.
Yu.V.Nelyubina. Doctor of Chemistry, Head of the Centre for Molecular Structure Studies at the INEOS RAS.
Telephone: +7(499)135 – 6568, e-mail: unelya@ineos.ac.ru
Current research interests: crystal chemistry, quantum chemistry, theory of the structure of matter, materials science, molecular magnetism, targeted design.

Received 10 October 2018
Translation: A.M.Raevskiy

† Dedicated to Vladimir Grigorievich Tsirelson. A prominent Russian physicist, one of the first experts in the application of X-ray diffraction to studies of chemical bonding in crystals, he recently celebrated his 70th birthday.

© 2019 Uspekhi Khimii, Russian Academy of Sciences and Turpion Ltd.

the description and interpretation of the charge density distribution from the available X-ray diffraction data.

To date,[6] high-resolution single-crystal X-ray diffraction studies‡ represent a method that is rather widely used[9–14] and can compete with quantum chemical calculations. These studies provide detailed information on the nature of chemical bonds[15] and related properties of chemical compounds including the reactivity, optical, magnetic, transport properties, *etc.*[16–19] Recently, there has been an increase in the number of high-resolution X-ray diffraction studies, first of all, due to the availability of powerful laboratory and synchrotron sources of X-ray radiation, the design of new types of detectors and progress in hardware and software. This led to the situation where certain researchers cast some doubt on the value of such studies out of context of particular problems in chemistry or materials science.[20]

Despite this fact, high-resolution single-crystal X-ray diffraction studies still cannot be treated as routine ones since they imply collection of an array of X-ray diffraction data that meet much more stringent requirements than those applied to the data obtained in conventional X-ray diffraction experiments. The main criterion that distinguishes high-resolution X-ray diffraction data from conventional-quality ones is the angular resolution that should be as high as possible. However, the boundary between high- and 'conventional'-resolution X-ray diffraction data is not clearly specified. The International Union of Crystallography recommends that the minimum angular resolution, $\sin\theta/\lambda$ (θ and λ are respectively the angle of incidence and the wavelength of the primary wave), should be at least 0.6 $Å^{-1}$, which corresponds to a minimum interplanar spacing $d = 0.81$ Å. Usually, one has $\sin\theta/\lambda = 0.7$ $Å^{-1}$ for routine X-ray diffraction experiments and $\sin\theta/\lambda > 1$ $Å^{-1}$ ($d < 0.5$ Å) for high-resolution ones.

Not only resolution, but also the accuracy of measurement of the observed reflection intensities is of paramount importance to high-resolution single-crystal X-ray diffraction studies. To increase the accuracy, one should minimize the effects of certain factors, first of all, temperature, which influences thermal motion of atoms, and some other related to the physical nature of the crystal (*e.g.*, absorption of radiation by atoms). This goal can be achieved by carrying out high-resolution X-ray diffraction experiments at temperatures that should be as low as possible in the former case and using tunable synchrotron radiation in the latter case. However, liquid helium and cryogenic equipment are expensive and therefore experiments at $T < 80$ K are rare, while a synchrotron is not always available and has its pros and cons.[21] This significantly reduces the number of systems available for high-resolution X-ray diffraction studies. Indeed, a routine X-ray diffraction experiment requires only a single crystal to determine the structure of compounds of different nature from elements to DNA. Contrary to this, high-resolution X-ray diffraction studies are mainly used in the case of well-ordered crystals composed of small molecules (usually, the constituent elements are no heavier than zinc). A few examples where compounds containing heavier elements (*e.g.*, antimony,[22–24] tin,[25,26] gold,[27] lanthanides[28–30] or actinides,[31–34]) were studied only confirm this rule. Often, high-resolution X-ray diffraction data can be collected for certain individual crystals. However, stringent requirements for such crystals (no disordering, twinning, strong absorption, extinction, *etc.*) preclude further extension of high-resolution X-ray diffraction studies to certain classes of practically valuable systems including biomacromolecules, metal-organic frameworks, inclusion compounds as well as series of related compounds, although research activity in this field would help to reveal general trends and establish structure–property correlations[35] for further application in materials science[19] and biosciences.[36]

The difficulties mentioned above can be overcome using hybrid approaches that combine quantum chemical methods and partial (or complete) refinement of X-ray diffraction data. This does not imply the use of lattice constants and atomic coordinates determined from X-ray diffraction data as the initial approximation to subsequent quantum chemical calculations (for details, see a review[37]). Quantum chemical calculations of isolated molecules, supramolecular fragments and crystals provide information on the electronic structure that is hard or impossible to obtain with sufficiently high accuracy using routine X-ray diffraction experiments. Note that calculations of crystals are performed more rarely because of long computing time and high computational cost. Since quantum chemical methods do not go beyond the scope of theoretical concepts that are basic to high-resolution X-ray diffraction studies, one can introduce important corrections to improve the informativity and reliability of the results of analysis of experimental ED distribution in the crystal. An example is provided by conventional normalization of X–H bond lengths when no neutron diffraction data are available. Quantum chemical methods allow one to study systems that can be characterized by only conventional- and lower-resolution X-ray diffraction data, *viz.*, biomacromolecules,[38,39] metal-organic frameworks,[18,40] ionic liquids,[41] *etc.*

At present, almost all hybrid approaches described in this review are widely used by researchers who work in the field of high-resolution X-ray diffraction studies. The development of user-friendly software (*e.g.*, Olex2 program§) has made the hybrid methods available to a much larger research community whose members work in other fields of X-ray crystallography. For these readers, we put emphasis on the potential and limitations of high-resolution X-ray diffraction studies and on the criteria for reliability of the experimental ED distribution thus obtained. The review begins with a brief survey of the theoretical basis of single-crystal X-ray diffraction. This is not a didactive or instructional description since excellent textbooks[42,43] and monographs[44–46] are available. It is first of all addressed to researchers who are low-skilled in this field of science and seek to expand their knowledge.

Notations are as follows:

A — absorbed radiation;

a, b, c — tabulated constants;

α — phase factor;

BB — electron density building blocks;

BLYP — exchange-correlation functional by Becke, Lee, Yang and Parr;

‡ High-resolution X-ray diffraction studies, as this is termed in Russian scientific literature.[7,8]

§ Current version of Olex program for refinement of X-ray diffraction data.

B_{atom} (k) — matrix of root-mean-square displacements of kth atom;
c — coefficient in the molecular orbitals as linear combination of atomic orbitals (MO LCAO) approximation;
CIF — crystallographic information file;
CP — critical point;
d — resolution;
d^f — fractal dimension;
DED — deformation ED;
DFT — density functional theory;
Δ — desired accuracy;
E — potential energy of harmonic oscillator;
ED — electron density;
$\mathbf{e}(k|j\mathbf{q})$ — unit vector corresponding to kth component of the eigenvector $\mathbf{e}(j\mathbf{q})$ and normal mode along the wave vector;
E_0 — vibrational energy at equilibrium point; EDA — energetic decomposition analysis (method for evaluation of interaction energy between different molecular fragments);
ELF — electron localization function;
ELI — electron localizability indicator;
ELMAM — experimental library of multipolar atom model;
ELMO — extremely localized molecular orbitals;
EP/MM — exact potential/multipole moment method;
ε — factor specifying the orthogonality of orbitals;
F_{calc} — calculated X-ray structure factor;
f_i — atomic scattering factor;
F_i^C — X-ray structure factor in the Hirshfeld model;
f_{ij} — force constants;
F_{hkl}, $F(\mathbf{s})$, $F_0(\mathbf{s})$ — X-ray structure factors;
F_{obs}, F_i^{exp} — measured X-ray structure factors;
$f(\mathbf{s})$ — X-ray structure factor in fractional coordinates;
Φ — total deviation;
$|\Psi\rangle$ — wave function;
Ψ_j — wave function of a noninteracting part of a crystal;
GGA — generalized gradient approximation;
GOF — goodness of fit;
h — Planck constant;
h, k, l — Miller indices;
HAR — Hirshfeld atom refinement;
I — intensity of reflection;
IAM — independent atom model;
INVARIOMS — invariant atoms;
I_0 — intensity of a plane wave;
$I_{\mu\nu}^g$ — static scattering integral;
k_B — Boltzmann constant;
κ, κ' — expansion – contraction parameters in the multipole model;
L — tensor describing atomic librations;
L — (i) Lagrangian, (ii) Lorentz factor;
LDA — local density approximation in DFT;
LOL — localized-orbital locator;
λ — primary wavelength;
λ_i — Lagrange multiplier;
m_k — mass of kth atom;
μ — (i) absorption coefficient; (ii) reduced mass of harmonic oscillator;
NoMoRe — normal mode refinement;
N_r — number of reflections included in the refinement;
N_p — number of refined parameters;
P — polarization factor;
P_{core} — core electron population;
P_{lm} — population of a multipole;
$P_{\mu\nu}^q$ — element of the density matrix;
P_{val} — population of spherically symmetric valence shell;
$\mathbf{q}$ — wave vector;
R — R-factor;
r — generalized coordinate;
RDA — residual density analysis;
$\mathbf{r}_e$, $\mathbf{r}$ — vectors describing positions of the primary and secondary wave, respectively;
r_{ij} — force constant coordinates;
$\langle \Delta r_i^2 \rangle$ — root-mean-square deviation of ith atom from its equilibrium position;
R_l — radial function;
ρ_0 — electron density for the unique part of the unit cell;
ρ_i^0 — electron density of noninteracting spherical atoms;
ρ_{IAM} — ED distribution function;
$\rho_{MM}(\mathbf{r})$ — static ED distribution function obtained from multipole refinement;
ρ^{mol} — the molecule electron density;
ρ^{pro} — the promolecule electron density;
$\rho(\mathbf{r})$ — ED distribution function;
$\Delta\rho(\mathbf{r})$ — deformation electron density;
$\mathbf{s}$ — scattering vector;
$\mathbf{S}$ — tensor describing atomic screw motion;
s — scale factor;
S — trace of a matrix;
SBFA — synthon based fragment approach;
S_{TLS} — vibrational entropy of crystal;
σ — standard deviation;
$T(h)$ — Debye – Waller factor;
t — path length of a beam in the crystal;
T — tensor describing atomic translational motion;
TLS — Schomaker – Trueblood rigid body model;
θ — angle of incidence of primary wave;
U — tensor describing anisotropic thermal vibrations;
$\langle u^2 \rangle$ — root-mean-square amplitude of atomic displacements;
U_{ij} — anisotropic displacement parameters (components of tensor U);
UBDB — the University at Buffalo pseudoatom databank;
UHF — unrestricted Hartree – Fock method;
V — the volume of the crystal;
V_{cell} — the unit cell volume;
v_i — frequency of ith harmonic oscillator;
w — weighting factor;
χ^2 — factor divergence;
$X_i(\xi, |F_i|)$ — the function that includes extinction and depends on empirical parameter ξ;
ξ — difference function;
$\omega_j(\mathbf{q})$ — normal mode frequency;
XCW — X-ray constrained wave function fit;
XWR — X-ray constrained wave function refinement.

2. The basics of single-crystal X-ray diffraction

X-Ray diffraction analysis is based on the kinematic theory of diffraction [42, 47] which deals with elastic coherent scattering of X-rays by lattice electrons. The crystal lattice is treated as infinite system of static spherical atoms that are regularly (periodically) arranged in the 3D space. This is the so-called spherical atom model used to describe X-ray diffraction of crystals. The kinematic theory ignores inter-

ference of the primary (incident) and secondary (scattered) waves as well as multiple interaction of waves with the lattice atoms.

To take into account the nature of the crystal interacting with X-rays, an improved dynamical theory was developed [48] that also accounts for multiple interference of secondary waves. Within the framework of the dynamical theory one can exactly describe all physical phenomena responsible for the differences between theoretical and experimental X-ray diffraction intensities. In turn, the kinematic theory can be improved by introducing corrections calculated using the dynamical theory.

Calculations of X-ray diffraction intensities within the framework of the kinematic theory require knowledge of the X-ray scattering power of the *i*th atom compared to an electron. A measure of the scattering power of an isolated atom is called the atomic scattering factor f_i (Fig. 1) and represents a monotonically decreasing function equal to the number of electrons in the atom at $\sin\theta/\lambda = 0$,

$$f_i = \left\{ \sum a \exp\left[b \left(\frac{\sin\theta}{\lambda} \right)^2 \right] \right\} + c \qquad (1)$$

where a, b, c are tabulated constants and θ and λ are respectively the angle of incidence and the wavelength of the primary wave. Most software for X-ray structure refinement uses the a, b and c values determined using the wave functions of spherical atoms or ions obtained from Hartree–Fock calculations.[49]

The atomic scattering factors rapidly decrease with increasing θ. The major contribution to the atomic scattering factor comes from valence electrons at small angles θ and from inner-shell (core) electrons at larger θ (usually, at $\sin\theta/\lambda > 0.6$ Å^{-1}).

In the kinematic theory the intensity of X-ray radiation scattering by all atoms in the unit cell compared to an electron is given by

$$I_{\text{cell}} = \left[I_0 \left(\frac{\mathbf{r}_e^2}{\mathbf{r}^2} \right) \frac{1 - \cos^2 2\theta}{2} \right] |F_{hkl}|^2 \qquad (2)$$

where I_0 is the intensity of the plane wave interacting with the electron; $\mathbf{r}_e$ and $\mathbf{r}$ are respectively the vectors describing positions of the primary and secondary waves scattered by the electron; $|F_{hkl}|$ is the amplitude of the secondary wave scattered by the atoms in the unit cell (compared to the scattering by one electron). The coordinates of the *i*th atom are specified using the indices of lattice planes h, k, l (so-called Miller indices) and the fractional coordinates representing fractions of corresponding lattice constants

$$F_{hkl} = \sum f_i \{ \cos\left[2\pi(hx_i + ky_i + lz_i)\right] + \\ + \mathrm{i}\sin\left[2\pi(hx_i + ky_i + lz_i)\right] \} \qquad (3)$$

This complex quantity (for a certain set of indices h, k, l) is called the structure factor. For centrosymmetric crystals the imaginary part of the structure factor equals zero, while for non-centrosymmetric ones it specifies the intensity of so-called anomalous scattering which is used to determine the atomic structure of large biomolecules and the absolute configuration of chiral compounds.

The structure factor is the Fourier transform of the ED distribution function $\rho_{x,y,z}$ in the unit cell of a crystal

$$F_{hkl} = \int_{V_{\text{cell}}} \{ \rho_{x,y,z} \exp\left[\mathrm{i}2\pi(hx + ky + lz)\right] \} \mathrm{d}V \qquad (4)$$

where x, y, z are the coordinates of an arbitrary point in the unit cell of a crystal of volume V_{cell}. Practically, one can measure only the intensities of diffraction maxima (reflections) that are proportional to the squared moduli of corresponding structure factors

$$F_{hkl} = |F_{hkl}| \mathrm{e}^{\mathrm{i}\alpha} \qquad (4a)$$

The loss of phase factors α is the essence of the phase problem in X-ray crystallography.

Having determined the structure factors F_{hkl}, applying a Fourier transform to them allows one to obtain the ED distribution function $\rho(r)$ in the unit cell of a crystal

$$\rho(r) = \frac{1}{V_{\text{cell}}} \sum_{hkl} F_{hkl} \exp\left[-\mathrm{i}2\pi(hx + ky + lz)\right] \qquad (5)$$

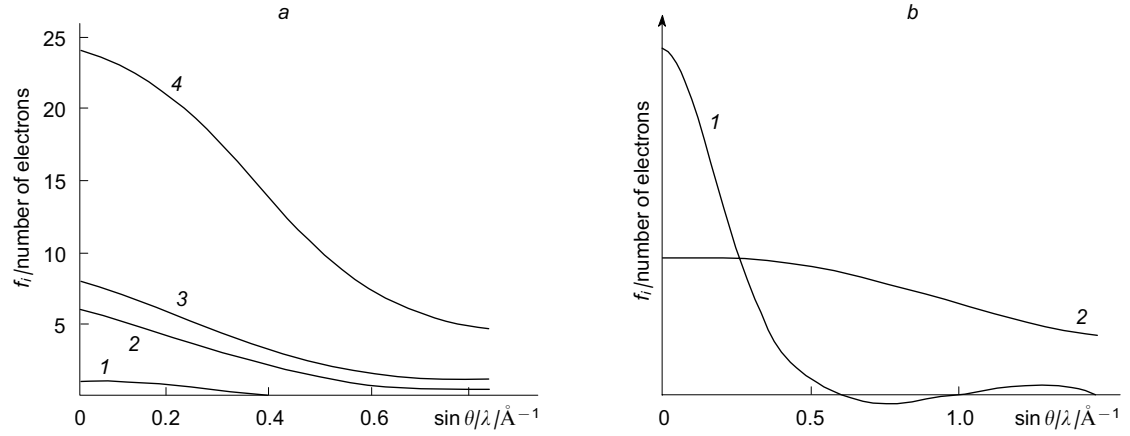


Figure 1. Atomic scattering factor plotted *vs.* $\sin\theta/\lambda$ for different atoms (*a*) and electrons (*b*).[47]
(*a*) H (*1*), C (*2*) and O (*3*) atoms; Fe^{2+} ion (*4*); (*b*) valence (*1*) and core (*2*) electrons.

This expression implies summation of infinite number of structure factors. However, real X-ray diffraction experiments give finite sets of structure factors and the ED calculated from them always differs from the theoretical ED corresponding to infinitely large values of the indices h, k, l. As a consequence, one deals with inaccurate determination of atomic coordinates and the appearance of ED maxima that do not match the atomic positions (Fourier series truncation error). The discrepancies observed can be to some extent compensated by increasing the resolution of X-ray diffraction experiments, *e.g.*, by going to high-resolution studies.

The kinematic theory gives an approximate description of the diffraction of X-rays travelling through a real crystal since it ignores thermal vibrations of atoms that cause the scattering intensity to decrease and occur even at 0 K. This feature is taken into account by the parameter called the Debye–Waller factor which represents the root-mean-square displacement of the ith atom from its equilibrium position

$$U_i = \langle \Delta r_i^2 \rangle \tag{6}$$

where r is the generalized coordinate.

Assuming independent and isotropic atomic vibrations in crystals (the latter means equal vibrational amplitudes along all directions), the expression for the atomic scattering factor takes the form

$$f_{\text{exp}} = f_{\text{theor}} \exp\left[-8\pi^2 U_i \left(\frac{\sin\theta}{\lambda}\right)^2\right] = f_{\text{theor}} T(h) \tag{7}$$

where $T(h)$ is the individual atomic temperature factor (Debye–Waller factor). Generally, $T(h)$ is the Fourier transform of the probability density to locate the atom at a certain point. Since the Debye–Waller factor depends on the angle θ, the difference between the theoretically calculated and experimentally observed intensity of X-ray diffraction increases with the angle of incidence of the primary wave. The influence of temperature on $T(h)$ manifests itself in a decrease in the amplitude of thermal vibrations of atoms with decreasing temperature. This is the main reason for carrying out low-temperature X-ray diffraction studies.

In the isotropic approximation, the Debye–Waller factor depends on the generalized root-mean-square displacement of an atom from its equilibrium position and ignores the anisotropy of atomic displacements. A more complicated model used at present treats the temperature factor as a 3×3 tensor having six nonzero components (U_{ij}) representing amplitudes of atomic vibrations along the directions x, y, z. Graphically, this corresponds to an ellipsoid. Within the framework of this approximation one can analyze low-frequency atomic vibrations and their static and dynamic disorder. Unfortunately, anisotropic approximation is almost inapplicable to hydrogen atoms since their scattering power is very low (see Fig. 1).

In some cases, especially, in high-temperature X-ray diffraction experiments the anisotropic approximation appears to be insufficient. As an example, Fig. 2 presents the probability density function for two silver atoms in the mineral $Ag_4MnSb_2S_6$. At present, the International Union of Crystallography recommends to use the so-called Gram–Charlier expansion. The harmonic temperature factor can be expanded in a series in such a manner that the

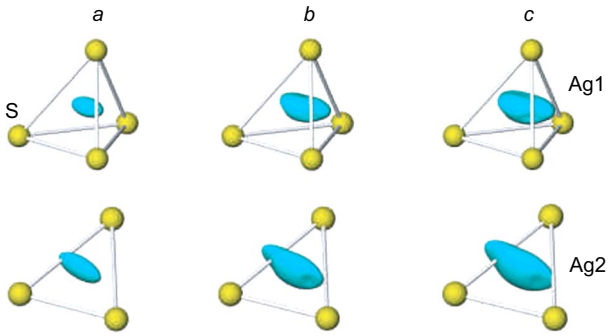


Figure 2. Non-harmonic probability density isosurfaces of silver atoms in the mineral samsonite $Ag_4MnSb_2S_6$ at different temperatures.[50]
T/K: 100 (*a*), 293 (*b*) and 400 (*c*).

even members of the series are real quantities while odd members are imaginary ones.[51] Expressions for the temperature factor are too complicated and the physical sense of certain members of the series is lost. Usually, the first- and second-order derivatives having 10 and 15 nonzero components, respectively, are taken into account. As a rule, these temperature factors (or anharmonicity) are analyzed using graphical methods (see Fig. 2).

Not only thermal motion of atoms, but also absorption of X-ray radiation by the crystal can lead to a decrease in the intensity of X-ray diffraction compared to that calculated within the framework of the kinematic theory. Absorbed radiation (A) depends on the nature of constituent atoms (as additive function of the mass absorption coefficient of the ith atom) as well as on the shape and size of the atoms

$$A = V^{-1} \int_V \exp(-\mu t) \mathrm{d}V \tag{8}$$

where V is the volume of the crystal, μ is the absorption coefficient and t is the beam path length in the crystal.

The observed discrepancy can be partially compensated by introducing an appropriate correction. In most present-day X-ray diffraction experiments this can be achieved by analyzing the dependence of the beam intensity on the so-called azimuthal angle or by choosing an isometric crystal and(or) a smaller-size crystal.

Structural defects whose surface and bulk distributions are unknown also considerably contribute to the decrease in the intensity of X-ray radiation scattered by real crystals. This leads to deviations of experimentally measured intensities from theoretical values for different angles θ. Treatment of the crystal as a totality of small domains having the structure of a perfect crystal and disordered relative to one another allows one to minimize the discrepancies mentioned above by introducing a correction called the Lorentz factor (L)

$$L = \frac{1}{\sin 2\theta} \tag{9}$$

which depends on the angle θ similarly to the polarization factor (P)

$$P = \frac{1 + \cos^2 \theta}{2} \tag{10}$$

In some cases (usually, for highly symmetric crystals of inorganic compounds) the experimentally measured intensities of the so-called strong reflections (most intense diffraction maxima) and those predicted by the kinematic theory can differ appreciably. The reason is extinction resulting from double diffraction ignored by the kinematic theory. Extinction is in some sense similar to additional absorption. In X-ray diffraction experiments it is taken into account by introducing an extinction correction as function of a refined parameter (extinction coefficient). It depends on the size of building blocks (primary extinction) in the crystal and on the extent of crystallographic disorientation of these blocks relative to one another (secondary extinction) and takes different values for different reflections. Experimentally, extinction can be reduced using smaller crystals (by analogy with absorption) or by dividing large building blocks into smaller ones by polishing or quenching the crystal (*e.g.*, by placing it in a liquid nitrogen jet followed by rapid removal of the crystal from the jet).

A perfect structure model implies excellent agreement between the reflection intensities (I) measured in X-ray diffraction experiments and those calculated with inclusion of all corrections mentioned above. The structure refinement procedure is reduced to minimization of the observed deviations by the least squares method ($I \propto |F_{hkl}|^2$)

$$\Phi = \sum w\left(I_{\text{obs}} - |sF_{\text{calc}}|^2\right)^2 \tag{11}$$

where Φ is the total deviation; w is the weighting factor related to the measurement accuracy of structural amplitudes for weak and strong reflections; and s is the scale factor.

Usually, structure solution methods (among them, the direct method based on exact specification of phases of the check reflections is most widely used) allow one to determine positions of heavy atoms that make a major contribution to X-ray radiation scattering intensity. Lighter atoms (*e.g.*, H) are localized iteratively by comparing the 'instantaneous' ED distribution function calculated from the structure factors for the 'running' (currently known) structural fragment with the ED distribution function obtained from the experimentally measured reflection intensities. The latter is the essence of the inverse problem in X-ray crystallography.

At present, correctness of the structure model is tested using various criteria including statistical ones (so-called R-factors) [52] and the goodness of fit (GOF). A conventional R-factor (R) characterizes only the difference between theoretically calculated ($|F_{\text{calc}}|$) and experimentally measured ($|F_{\text{obs}}|$) structural amplitudes

$$R = \frac{\sum ||F_{\text{obs}}| - |F_{\text{calc}}||}{\sum |F_{\text{obs}}|} \tag{12}$$

A similar quantity can be calculated using squared structural amplitudes (F^2_{hkl}) or reflection intensities (I). Since reflections of different intensity make different contributions to the R-factor, the weighted R-factor (wR_2, or R_w) is often used

$$wR_2 = \sqrt{\frac{\sum w(F^2_{\text{obs}} - F^2_{\text{calc}})^2}{\sum w(F^2_{\text{obs}})^2}} \tag{13}$$

where w is the weighting factor. The R and wR_2 values are calculated for all measured reflections and for the strongest reflections whose intensities are two- or fourfold standard deviation. The admissible R-factor values are to a great extent determined by the maximum angle θ, although by the general sense they should tend to zero. Since the R-factors do not characterize the reliability of the structure model from the standpoint of the least-squares minimization of deviations, the GOF value is also used. The latter parameter should tend to unity. A too low GOF value is indicative of a large number of reflections whose intensities are comparable with the measurement error,[53]

$$\text{GOF} = \frac{\sqrt{\sum w(F^2_{\text{obs}} - F^2_{\text{calc}})^2}}{N_{\text{r}} - N_{\text{p}}} \tag{14}$$

where N_{r} is the number of reflections included in the refinement and N_{p} is the number of refined parameters. Usually, these are the coordinates of symmetrically unique atoms, their anisotropic thermal parameters and the scale factor. Among other refined parameters, there are the extinction coefficient, occupations of atomic positions (*e.g.*, for disordered structural fragments), *etc*. As a rule, the number of refined parameters should be at least tenfold smaller than the number of reflections.

In addition to statistical criteria for correctness (or quality) of a structure model, other criteria can be used, *e.g.*, the maximum or minimum residual ED, the absence of anomalies in thermal parameters ($U < 0$ or $U \gg 0$) or the absence of large differences between $|F_{\text{obs}}|$ and $|F_{\text{calc}}|$ for certain reflections (*e.g.*, due to ignored extinction), root-mean-square errors in measurement of bond lengths, *etc*. The results of modern X-ray diffraction studies are presented in electronic form as crystallographic information files (CIF).[54] The process is highly automated owing to the development of, *e.g.*, the standalone PLATON program [55] or its online version;¶ however, an expert opinion of high-skilled specialists in X-ray diffraction analysis is just as important as three decades ago.[56]

3. The basics of high-resolution X-ray diffraction studies

The ED distribution in a crystal obtained by solving the inverse problem of X-ray crystallography includes information concerning not only atomic types and positions (they correspond to ED maxima), but also the character of atom–atom interactions. An analysis of these interactions requires modification of X-ray diffraction experiments [57] aimed to accurately measure the intensities of a large number of reflections. First of all, one should collect an array of X-ray diffraction data with high angular resolution (*e.g.*, $\theta > 50^\circ$ for Mo K_α-radiation). In this case the major contribution to the atomic scattering factors (see Fig. 1) comes from core electrons localized within a small spatial

¶ See http://journals.iucr.org/services/cif/checkcif.html, last accessed on January 15, 2019.

domain surrounding the atomic nucleus; the number of core electrons exceeds that of valence electrons starting with atoms of the third-row elements.

Since the 1970s, this fact has been used for more accurate determination of atomic coordinates during the so-called high-angle refinement ($\theta > 30-40$);[8] this step was basic to the first high-resolution X-ray diffraction studies. To observe reflections at high angles θ, one should (i) go to low-temperature experiments, which reduce the amplitudes of thermal motion of atoms and related effects (anharmonicity and diffuse scattering)[9] and improve the signal-to-noise ratio for high-angle reflections and (ii) use higher-brilliance sources of X-ray radiation[21] and detectors with high dynamic range.[58]

Valence electrons are involved in the formation of chemical bonds. Their contribution to scattering of X-ray radiation begins to dominate only at small angles θ (see Fig. 1); therefore, it is of great importance to evaluate the intensities of corresponding reflections as accurately as possible. At present, this can be achieved by measuring the intensities of same reflections many times and subsequent averaging of the experimental values. The procedure also makes possible a more accurate calculation of the absorption correction; otherwise, one can deal with the appearance of residual ED maxima and distortion of anisotropic displacement parameters. This is of particular importance for the studies of inorganic compounds containing atoms of heavy elements (starting with the fourth-row elements).[59] For such compounds, extinction occurs more frequently. Taking account of high symmetry of their crystals, extinction can significantly distort information on the distribution of valence electrons, which is contained in a few low-angle reflections. Unfortunately, the available methods for solving this problem (see above) regularly lead to a decrease in the intensities of weaker reflections at high angles θ.

In high-resolution X-ray diffraction studies much more attention is paid to instrumental errors. For instance, empirical corrections are applied for, *e.g.*, thermal diffuse scattering[60] (it introduces errors into atomic displacement parameters and corresponding ED maxima) and low-energy photon contamination (it is due to permeation of low-energy photons through focusing multilayer optics[61] and subsequent distortion of the intensity of certain reflections); in the latter case, an alternative is to decrease the intensity of X-ray radiation using Al foil).[62]

However, the development of high-resolution X-ray diffraction studies as a particular field of X-ray crystallography is first of all due to the shift away from the spherical atom model rather than methodological aspects. Indeed, this model ignores the ED redistribution upon formation of chemical bonds or the presence of lone electron pairs.

The first attempts to introduce aspherical effects into the description of atomic parameters date back to the 1960s;[63–65] however, it is the Hansen–Coppens model[4] proposed more recently that is widely used in modern high-resolution studies. Within the framework of this model the ED distribution in the unit cell is given by a superposition of independent atomic contributions, so-called pseudoatoms[64]

$$\rho(\mathbf{r}) = \sum_i \rho_i(\mathbf{r}) \qquad (15)$$

where ρ_i is the contribution of each independent atom.

The ED function of each pseudoatom, ρ_i, has two spherically symmetric components corresponding to the core and valence electrons (as in the spherical atom model), and an aspherical contributoin $\rho_d(\kappa'\mathbf{r})$ that describes deformation of the valence shells

$$\rho_i(\mathbf{r}) = P_{core}\rho_{core}(\mathbf{r}) + P_{val}\,\kappa^3\,\rho_{val}(\kappa\mathbf{r}) + \rho_d(\kappa'\mathbf{r}) \qquad (16)$$

where $\rho_{core}(\mathbf{r})$ and $\rho_{val}(\kappa\,\mathbf{r})$ are tabulated spherically symmetric functions obtained for isolated atoms from Hartree–Fock calculations carried out without[49] or with inclusion of relativistic effects.[66,67] In the Hansen–Coppens model the aspherical component $\rho_d(\kappa'\mathbf{r})$ of the pseudoatom is specified using multipole expansion and represents a combination of radial functions (R_l) and spherical harmonics (y_{lm})

$$\rho_d(\kappa'\mathbf{r}) = \sum_l \kappa'^3 R_l(\kappa'\mathbf{r}) \sum_{m=-l}^{l} P_{lm} y_{lm}(\mathbf{r}/r) \qquad (17)$$

where l is an analogue to the orbital quantum number and P_{lm} are the populations of the multipoles describing deformation of the electron shell of the atom.

This expression is an analogue to the solution of the Schrödinger equation for hydrogen-like atom within the framework of the Born–Oppenheimer approximation. The radial functions are of the Slater or Gaussian type, obtained from quantum chemical calculations of isolated atoms including density functional theory (DFT) calculations.[66,67]

Generally, spherical harmonics are solutions to the Laplace equation; they are specified in rather complicated manner using associated Legendre functions in spherical coordinates (see, *e.g.*, a monograph[68]). However, the Hansen–Coppens model uses real spherical harmonics corresponding to multipoles (monopoles, dipoles, quadrupoles, *etc.*). Depending on the l and m values ($m = 0, \pm l$; both are integers), graphical analogues to different multipoles are the s, p, d, f, *etc.* orbitals. In practice, the multipole expansion is usually truncated at $l = 4$ (hexadecapole level); this is similar to truncation of the Fourier series in X-ray crystallography. In those rare cases where an atom occupies a site with cubic symmetry, cubic harmonics are used instead of spherical ones (see, *e.g.*, Ref. 69).

Expressions (15)–(17) allow one to obtain the ED distribution in the crystal in analytical form upon refinement of the populations of spherically symmetric valence shell P_{val}, the multipole parameters P_{lm} responsible for its deformation (the sum of P_{lm} with fixed core electron population P_{core} equals the total number of electrons in the atom) and corresponding expansion–contraction parameters κ and κ' (in theory, one parameter for each l value)[70] using the structure factors collected in high-resolution X-ray diffraction experiments. This is static ED distribution (separated from thermal motion by deconvolution) rather than dynamic one obtained upon summation of structural amplitudes in routine X-ray diffraction studies. The static ED distribution can be directly compared with the ED distribution obtained by quantum chemiatry methods.[71] The spherical atom model with anisotropic approximation of thermal motion common in X-ray crystallography uses up to 10 parameters per atom (taking account of site occupancy). Unlike this, the number of refined parameters in the Hansen–Coppens model can be as large as 66 including 25 parameters to describe the anharmonicity of

thermal motion using the Gram–Charlier expansion; this requires measurements of much larger number of structure factors and is achieved in high-resolution X-ray diffraction experiments.

Although the multipole model is very popular (compromise between 'flexibility' and 'local character'), it has some disadvantages.[72] The most important drawback is the use of atom-centred diffuse functions that overlap with neighbouring functions. This makes the description of the ED distribution in the region of chemical bonds less accurate, especially, for organometallic and coordination compounds where this distribution is very flat.[73] This problem can be solved only upon rejection of the pseudoatom concept, while other disadvantages of the Hansen–Coppens multipole model are to some extent taken into account in various modifications of this model. For instance, low 'flexibility' of the widely used radial functions R_l is compensated by using tabulated values of the expansion–contraction parameters κ' obtained from multipole refinement using theoretical structure factors that are not influenced by experimental errors.[74]

Conventional multipole model is based on the 'frozen core' approximation, which ignores deformation of the core electron shells of an atom upon formation of chemical bonds. This can lead to difficulties in the description of the ED distribution for heavy elements. Indeed, the number of core electrons in the heavy-element atoms much exceeds the number of valence electrons. To overcome these difficulties, the core electron population P_{core} and the corresponding expansion–contraction parameter (κ_{core}) is refined within the framework of the extended Hansen–Coppens model.[75] The contribution of core electrons to the ED of a pseudoatom can then be divided into two[76] (or more[77]) components (method of separated core shells) up to refinement of each electron shell separately as the sum of spherical and aspherical contributions specified by corresponding multipole expansion.[32] In fact, this procedure implies refinement of several atoms occupying the same site, which can hamper further analysis of the ED distribution.[76] Unfortunately, this automatically leads to enormous increase in the number of structure factors that cannot always be collected even in high-resolution X-ray diffraction experiments.

Although conventional multipole model and its extended versions provide flexible tools to describe the ED distribution function for a crystal, realistic results are not ensured. Methodologically, the least-squares refinement of all possible parameters can be numerically unstable owing to correlations between the multipole populations and anisotropic displacement parameters of atoms. It can also lead to transition to a nearest energy minimum at which the values of certain parameters are far from being physically meaningful despite small *R*-factor and low maximum (minimum) residual ED values. Therefore, one should impose constraints[78] on the multipole populations taking into account the approximate symmetry of atomic position or equate parameters of atoms that are in the same chemical environment.

The multipole model also allows one to carry out structure refinement in different manner, *e.g.*, to refine all parameters simultaneously or in group-by-group fashion. As a consequence, the results concerning chemical bonding in the crystal of the same compound can be different depending on the scientific school to which the authors belong (*cf.*, for example, the results reported in Refs 79 and 80). A particular problem is to describe the ED distribution for hydrogen atoms characterized by low scattering power which becomes negligible even at small $\sin\theta/\lambda$ ratios (see Fig. 1). In modern high-resolution studies[81] positions and isotropic displacement parameters of hydrogen atoms are usually determined using Stewart's generalized X-ray scattering factor[82] during high-angle multipole refinement (*e.g.*, $\sin\theta/\lambda < 0.6$ Å^{-1}) followed by elongation of the X–H bonds to tabulated values derived from neutron diffraction data.[83]

Taking account of anisotropic displacement parameters for hydrogen atoms is also of great importance for correct description of the bonds that do not involve the H atoms.[84] Traditionally, this is done using the simple hydrogen atom displacement estimator (SHADE) approach[85] based on analysis of a large array of neutron diffraction data for related compounds. However, other strategies are also available.[86] For instance, the anisotropic displacement parameters of H atoms obtained from refinement of the expansion–contraction parameter κ using constant conventional X–H distances (see Ref. 83) followed by refinement of hydrogen atomic positions at constant κ value were only slightly different from those determined using neutron diffraction data.[33] Usually, the multipole parameters of hydrogen atoms are used to refine the populations of monopole, dipole and quadrupole whose *z* axis is aligned with the bond line;[81] the κ' (in some cases, also κ) parameters corresponding to the multipoles are obtained from theoretical calculations.[74]

A similar situation observed for the alkali and alkali-earth metal cations is also due to small contribution to the scattering from their valence electrons, which decreases to zero at $\sin\theta/\lambda \approx 0.15$ Å^{-1}. This precludes the refinement of the multipole populations and, usually, the contribution of spherically symmetric valence ED P_{val} and its expansion–contraction parameter κ for these cations. Successful attempts to refine P_{val} and κ are rare. This was done for, *e.g.*, K^+ using the atomic scattering factor of neutral potassium atom[87] and for Cs^+ using the method of separated core shells (see above).[32]

Yet another issue related to atomic displacement parameters is as follows. The case in point is that the multipole refinement can be augmented with anharmonic description of thermal motion within the framework of the Gram–Charlier formalism using 25 additional refined parameters.[21,88] Although this enables a more correct description of static ED distribution in the crystal (Fig. 3),[33,89] this description is often used to decrease the *R*-factors and residual ED even in the absence of anharmonic atomic vibrations.

Until recently, the dependence of the results of multipole refinement on the choice of refined parameters and on the refinement procedure was accentuated by the fact that no objective measures of the reliability of the ED distribution function thus obtained were available. It should be noted that so far, subjective criteria based on the experience and professional skills of researchers rather than statistical criteria play an important role when evaluating the results of multipole refinement. By and large, the reliability and quality of a structure model are determined as in the case of routine X-ray diffraction experiments, *i.e.*, using the *R*-factors, GOF and the residual ED maxima (or minima). In addition, high-resolution X-ray diffraction studies involve an analysis of anisotropic displacement parameters of

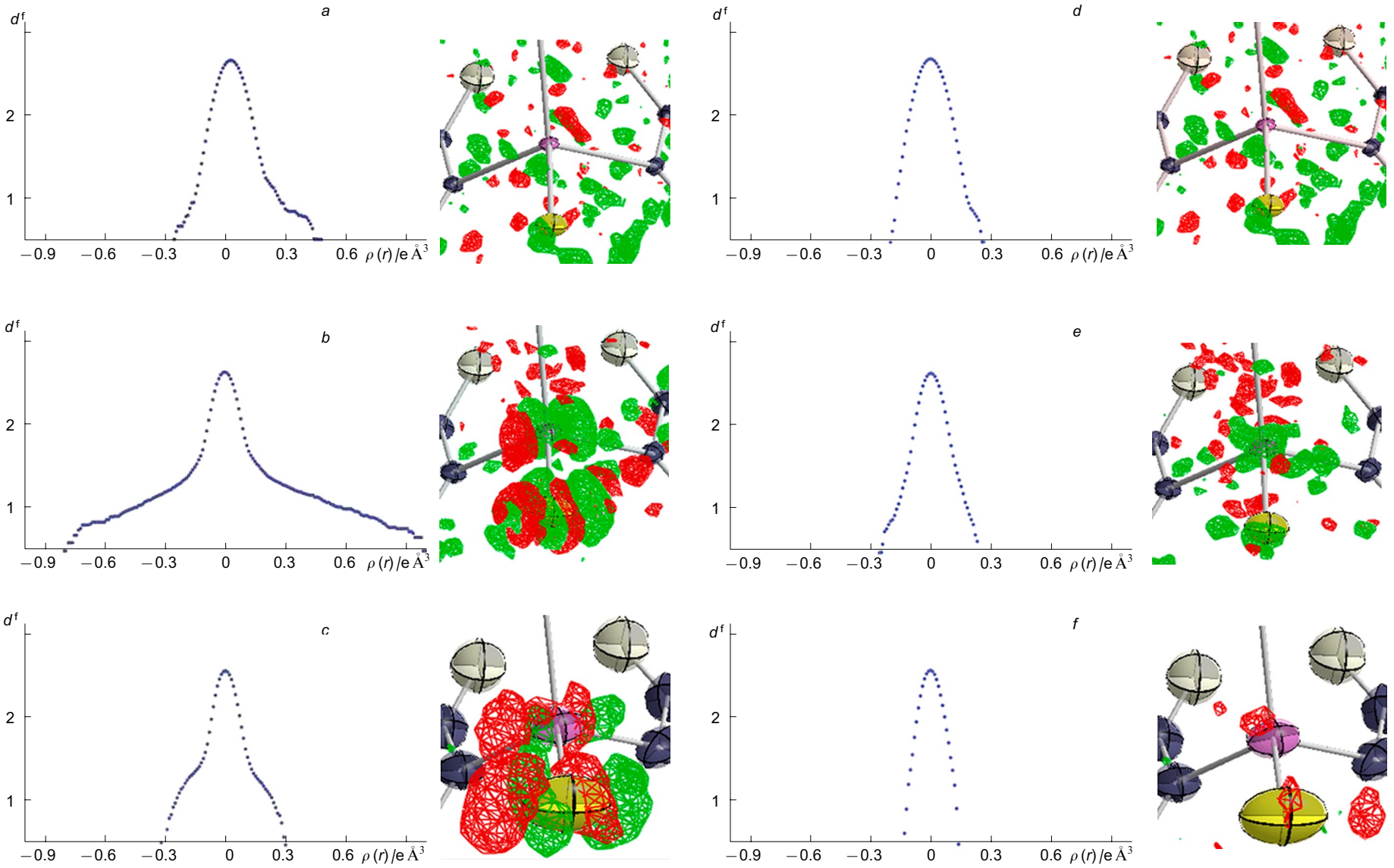


Figure 3. Residual ED distribution near phosphorus (*a*–*c*) and sulfur (*d*–*f*) atoms in 9-(diphenylthiophosphinoyl)anthracene crystal calculated taking into account (right) and ignoring (left) anharmonic atomic motions at different temperatures.[89] Negative and positive ED regions are given in red and green, respectively. Results of residual density analysis, or $\rho_0(d^f)$ diagrams (see below) are also presented.
T/K: 15 (*a*, *d*), 100 (*b*, *e*) and 293 (*c*, *f*).

atoms using the Hirshfeld rigid-bond test,[90] according to which the amplitudes of vibrational motion of two atoms along the line of their mutual bond should be nearly equal. For atoms with close masses the maximum admissible difference between the root-mean-square atomic displacements is 10^{-3} Å^2; much larger values are indicative of incorrect description of the ED asphericity or disorder that was ignored.

Besides, a traditionally important role is played by visual analysis of the deformation ED (DED) representing the difference between the experimental ED distribution and the superposition of noninteracting spherical atoms placed in the same positions as those occupied by atoms in the crystal (so-called procrystal model or, generally, promolecule model[91]),

$$\Delta\rho(\mathbf{r}) = \rho_{MM}(\mathbf{r}) - \rho_{IAM}(\mathbf{r}) \quad (18)$$

where $\rho_{MM}(\mathbf{r})$ and $\rho_{IAM}(\mathbf{r})$ are the static ED distribution functions obtained from the multipole refinement and using the spherical atom model, respectively. As a result, the DED distribution is also static (effects of thermal motion are excluded) and can be directly compared with the ED distribution obtained from quantum chemical calculations. In both cases, it should agree with commonly accepted concepts of chemical bonding. For instance, there should be at most one DED maximum near the midpoint of covalent C–C bond. For covalent polar bonds, the DED maximum should be shifted towards the electronegative atom. The pattern of the DED maxima should also be qualitatively consistent with the model for repulsion between the electron pairs of the valence shell. For instance, a carbonyl oxygen atom should be characterized by two DED maxima and the angle between them should be equal to $\sim 120^\circ$.

A qualitative description of the DED distribution for transition-metal, lanthanide and actinide atoms is hard to obtain. As to 3d transition metals, one should expect that the number and pattern of DED maxima nearly match those of d orbitals of the metal under study taking account of the formal oxidation state.

Deviations from these rules (especially, the appearance of additional DED maxima) can be indicative of incorrect ED distribution model obtained after the multipole refinement and (or) low quality of the X-ray diffraction data array. The DED function does not suffer from finite resolution of the experimental set of structure factors (*i.e.*, truncation of the Fourier series); however, it depends on the choice of the promolecule model, which is to some extent arbitrary (*e.g.*, atoms in one or another oxidation state are used).

This led to the situation where direct methods for analysis of static ED distribution are widely used, *e.g.*, topological approaches[92] and first of all, Bader's quantum topological theory 'Atoms in Molecules' (AIM).[5] This theory is based on physically substantiated division of the ED distribution function in real space into non-overlapping domains, each of them being unambiguously associated with a certain atom (atomic basin). The properties of each atom (volume, charge, electrostatic moments, *etc.*) can be evaluated by integrating corresponding functions over the atomic basin. In the AIM theory interatomic interactions are closely related to topology of the ED distribution function, that is, the set and types of bond critical points (BCP) at which the gradient of the electron density is zero. According to Bader's theory, four types of BCP are possible for a crystal depending on the curvature of the ED function along the principal axes:

— the (3,−3)BCP is characterized by negative curvature along all the three axes and corresponds to nuclear positions;

— the (3,−1)BCP, or the saddle point (curvature along one axis is positive); the presence of the (3,−1)BCP and a gradient trajectory (bond path) passing through this point is the necessary condition for a chemical bond (generally, the necessary condition for stabilizing interaction between a pair of atoms); recently, the bond paths have been attributed to exchange-correlation energy channels;[93]

— the (3,+1)BCP and (3,+3)BCP are characterized by positive curvature along two and three principal axes, respectively, being indicative of cyclic or polyhedral atomic structure.

The values of the ED distribution function and functions derived from it (*e.g.*, the Laplacian, electronic energy density,[94] ellipticity, *etc.*) at the (3,−1)BCP allow one to describe the character of interatomic interactions and in some cases to evaluate their energies, in particular, using a semiquantitative correlation with the kinetic energy density[95] or a derived quantity, the potential energy density[96] at the (3,−1)BCP.[97,98] Certain authors cast some doubt on the correctness of the energies thus evaluated and on the possibility to use them for quantitative description of the contributions of individual intermolecular interactions in the crystal; however, the total energy of these interactions is in reasonable agreement with the binding energies obtained from quantum chemical calculations or with the experimentally measured enthalpies of sublimation[99–103] of compounds of different chemical nature.

Besides, static ED distribution can be used to obtain the electrostatic potential, kinetic energy density of electrons and related functions including electron localization function (ELF),[104] localized-orbital locator (LOL),[105] binding entropy,[106] transition-metal d-orbital occupancies,[107,108] dipole (and higher multipole) moments of the molecules,[109] as well as to evaluate the energy of electrostatic interaction between molecules in crystals.[110] Corresponding parameters can also serve as criteria for correctness of the ED distribution model obtained after multipole refinement of X-ray diffraction data.

Recently, statistical criteria[111] have been increasingly widely used. Historically, construction of normal probability plots is one of the first methods for analysis of errors in experimental data.[112] It is based on the fact that a real distribution of a certain quantity (in X-ray crystallography, this is the ratio of the difference $F^2_{obs} - F^2_{calc}$ to the squared standard deviation σ) can be plotted against the expected distribution of the same quantity assuming its normal distribution. The expected and experimental distributions are plotted on the abscissa and ordinate, respectively. If errors are distributed randomly (Gaussian distribution), the plot is a straight line with a slope of unity and some deviations near the lower left and upper right corners (Fig. 4). Marked deviations from this line are indicative of systematic errors caused by the quality of the single crystal, instrumental errors, problems in processing primary data or inappropriate description of the ED in the refined model (*e.g.*, neglect of certain multipole or expansion–contraction parameters, anharmonicity of thermal vibrations, *etc.*).

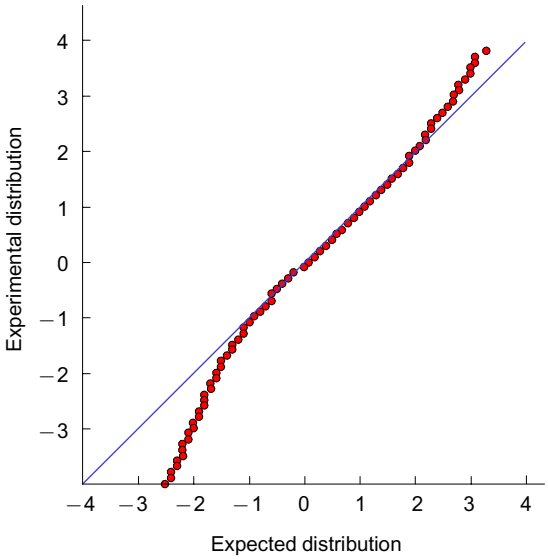


Figure 4. Normal probability plot for estrone.[57]

Construction of so-called DRK plots (see †) is a more widely used method for evaluating the quality of high-resolution X-ray diffraction data or the ED distribution derived from them. In this case, no high skills in statistical methods of analysis are required. A DRK plot is a simple plot of the $\sum F^2_{obs}/\sum F^2_{calc}$ ratio against $\sin\theta/\lambda$. Ideally, this ratio should not differ from unity. However, since all experiments and all models always include errors, small deviations from unity (within 2%) are admitted. When these deviations become larger than 5%, either the array of X-ray diffraction data or the ED distribution model is erroneous. As an example, Fig. 5 presents the plot of $\sum F^2_{obs}/\sum F^2_{calc}$ *vs.* $\sin\theta/\lambda$ for estrone,[57] which clearly demonstrates that the largest errors are observed for high-θ reflections, being due to overestimation of the intensities of these reflections.

Yet another type of plots used in high-resolution X-ray studies[111] was proposed[113] by the author who works in macromolecular X-ray crystallography. In this field there is an urgent problem of averaging the intensities of equivalent reflections owing to possible decomposition of crystals exposed to synchrotron radiation. Assuming that the X-ray diffraction data set obeys the Poisson distribution, the measurement error (σ) for each reflection is determined by the instrumental measurement error ($\sigma_{counting}$) and two constants (K_1 and K_2) that depend on the type of detector and on the software used for intensity averaging,

$$\sigma = K_1\sigma^2_{counting}K_2I^2 \qquad (19)$$

In the ideal case, the plot of I/σ against I [or the $(I/\sigma)_{asymptotic}$ plot] is a sigmoidal 'curve' passing from the lower left to the upper right corner of the plane of reference (Fig. 6 *a*). Noticeable deviations from this 'curve' may be evidence for the lack of synchronization during rotation of the sample about the goniometer ϕ axis in the continuous scan mode, while the presence of an asymptotic limit

† This type of plots is aimed to visualize statistical regularities of the distribution of measured values. In the case of single-crystal X-ray diffraction these are the reflection intensities or X-ray structure factors.

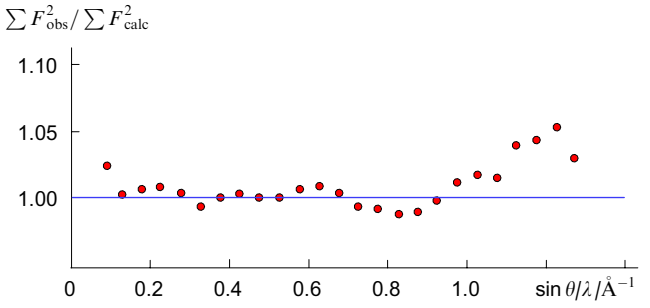


Figure 5. A DRK plot for estrone.[57]

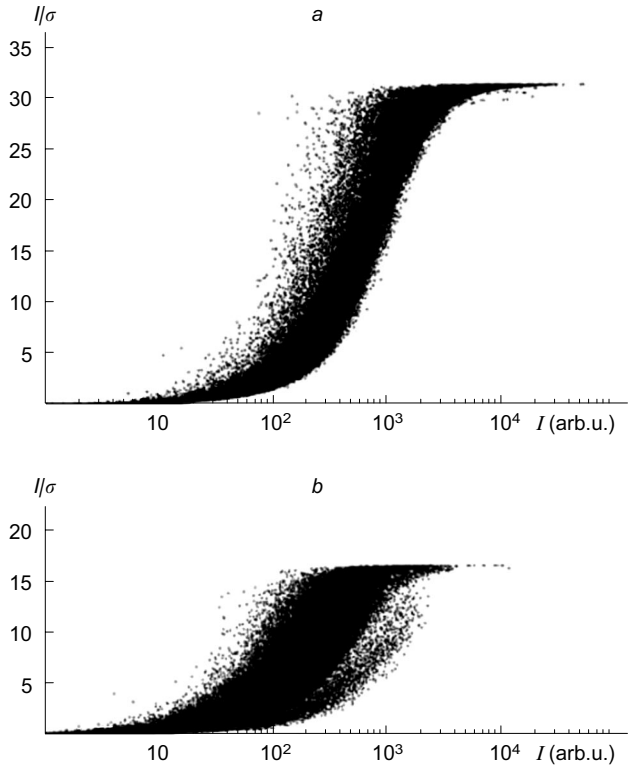


Figure 6. $(I/\sigma)_{asymptotic}$ plots for 'good' (*a*) and 'bad' (*b*) X-ray diffraction data array.[113]

suggests errors in reflection intensity measurements (Fig. 6 *b*). Having collected all data sets under identical conditions, a possible source of errors is the dynamic range of the detector, which is insufficient for intensity measurements of strong reflections.

One more statistical method for revealing systematic errors in high-resolution X-ray diffraction experiments is to analyze the Bayesian conditional probability plots.[114–116] It is based on the assumption that the residual (ξ), *i.e.*, the difference between the observed and calculated reflection intensities ($I_{obs}-I_{calc}$) divided by the standard deviation $\sigma(I_0)$, is independent of the resolution, the measured reflection intensities and other parameters of the experiment. As an example, Fig. 7 presents the plot of ξ against angular resolution of X-ray diffraction data for roxythromycin,[114] which represents an array of points. Would all reflection intensities be measured with the same accuracy, the plane

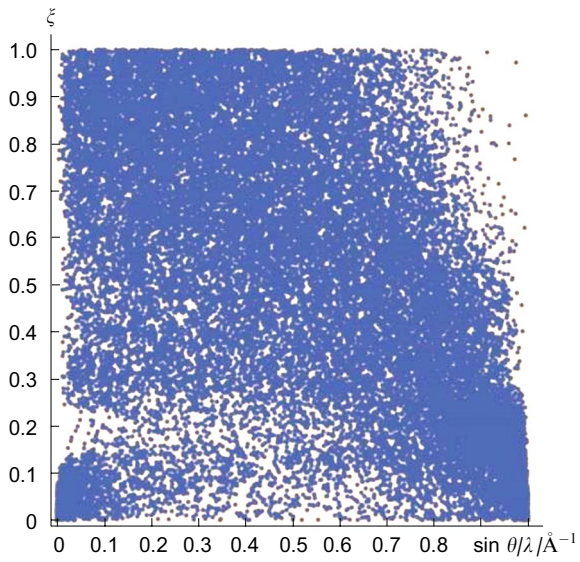


Figure 7. ξ-*vs.*-$\sin\theta/\lambda$ plot for the data set for roxythromycin.[114]

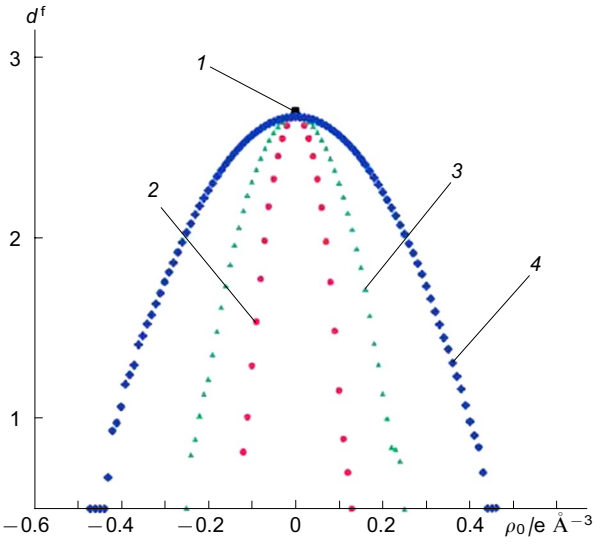


Figure 8. Fractal dimension d^f plotted *vs.* residual density ρ_0 at different ρ_1 values.
ρ_1 = 0 (*1*), 0.222 (*2*), 0.444 (*3*) and 0.888 (*4*).[117]

should be uniformly filled with points. However, the plot for roxythromycin exhibits two different features, *viz.*, 'thickening' of points at the lower right corner and 'loosening' at the upper right corner. This pattern of the plot originates from errors in the averaging of equivalent and multiply measured reflections corresponding to small $\sin\theta/\lambda$ values. Probably, the errors are due to the fact that certain reflections were collected on peripheral regions of the detector.

The most widely used approach is called residual density analysis (RDA) [117] based on the maximum entropy method. For a correct structure model, the residual ED distribution is assumed to be Gaussian (random) and thus exhibits no

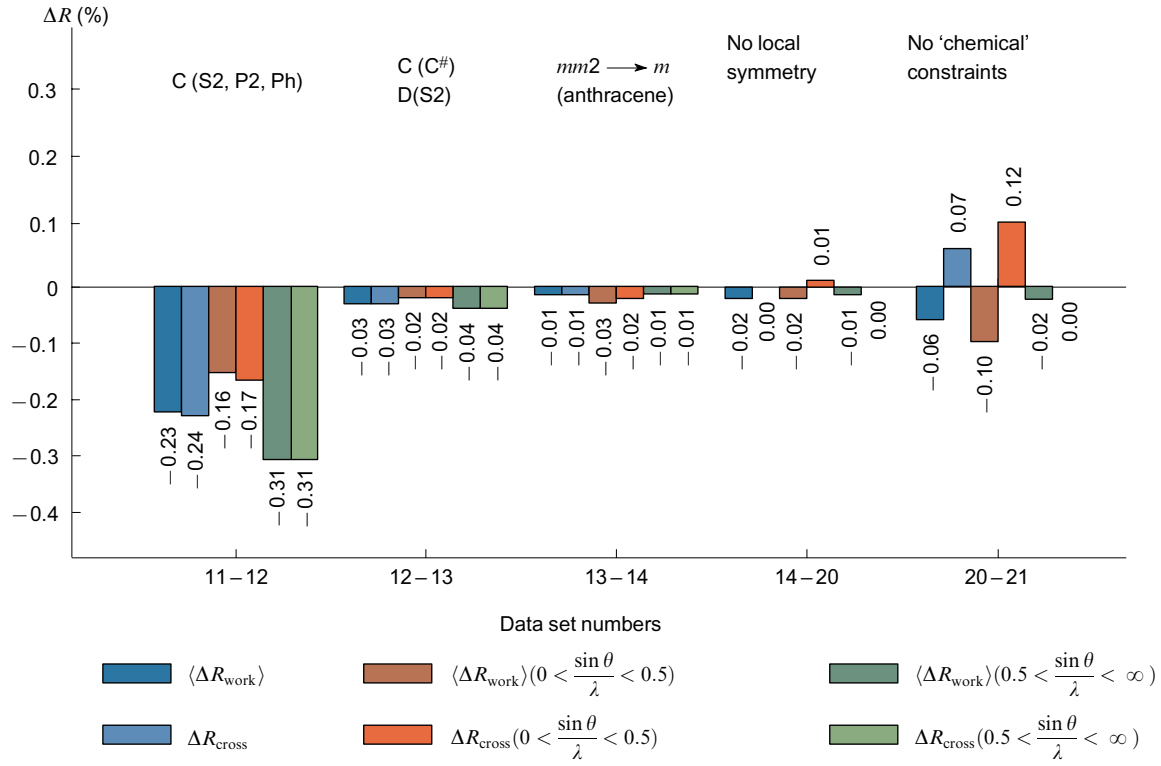


Figure 9. ΔR values for the different refinement steps of the anthracene structure.[118]
R_{work} is the *R*-factor calculated for the entire data array; R_{cross} is the *R*-factor calculated for the training set; and C$^{\#}$ denotes six additional types of carbon atoms.

maxima and(or) minima concentrated in a certain region, *e.g.*, near a halogen atom. The method involves calculations of the volumes of the regions confined by the isosurface with a specified residual ED value (ρ_0). For a perfect structure model, the residual ED distribution presents no structural information ($\rho_0 = 0$), whereas for imperfect models, systematic errors lead to a decrease in the volume of the isosurfaces corresponding to $\rho_0 = 0$ compared to the isosurfaces corresponding to $\rho_0 \neq 0$. The results of RDA are presented as a plot of the fractal dimension (d^f) against ρ_0, so one can assess to which extent the character of the residual ED distribution differs from Gaussian. This can be illustrated taking $S(NBu^t)_3$ as an example. A set of idealized structure factors calculated [117] for the $S(NBu^t)_3$ crystal with a resolution, $\sin\theta/\lambda$, of 1.14 $Å^{-1}$ was contaminated with random 'noise' specified using the parameter ρ_1. An increase in the noise (Fig. 8) to simulate experimental errors led to a marked increase in the width of the error distribution curve. Analogously, the character of the dependence of d^f on ρ_0 characterized the correctness of various parameters of the Hansen–Coppens multipole model. For instance, an arbitrary variation of the parameter κ, or the monopole population, noticeably increased the asymmetry of the plot.

Among the most recent improvements in the field of statistical criteria for quality of high-resolution X-ray diffraction data, there is the cross-validation method. It was proposed [78] to divide these data sets into complementary subsets. One of them (training set) is used to derive the error model, while the other are used to validate the model by gradually adding(removing) refined parameters and constraints taking account of local symmetry of atoms and(or) resolution. Then, the other subset is used as the training set and the process is repeated iteratively. The main goal of the cross-validation technique is to choose the optimum multipole refinement strategy that uses a not too large number of refined parameters. Although unconstrained refinement of a larger number of parameters from X-ray diffraction data decreases the *R*-factors and residual ED values, the values thus obtained can be physically unrealistic and the ED distribution model cannot correspond to a local potential energy minimum.

The results of the cross-validation treatment are presented as 'shashlik-like' [118] plots of changes in *R*-factors depending on the refined parameters and(or) constraints imposed (Fig. 9). These plots allow one to determine the parameters whose refinement leads to improvements in the ED distribution model; however, they provide almost no information on the quality of the X-ray diffraction data set. In this case, one should simultaneously use a combination of the statistical criteria described above.

4. Databases of experimental multipole parameters

There are various methods for quality assessment of the ED distribution function obtained in high-resolution X-ray diffraction experiments; however, they only make it possible to reveal instrumental errors or the nature of the problems related to the quality of the crystal, and to partially eliminate some of them (*e.g.*, diffuse scattering or absorption of X-ray radiation) by applying relevant corrections. Unfortunately, thermal motion or disordering of atoms and, as a consequence, low scattering power of the crystal preclude the attainment of high resolution necessary to obtain a reliable ED distribution within the framework of the multipole refinement of X-ray diffraction data.

This problem is urgent for research into materials whose properties (*e.g.*, transport ones) originate from random occupation of the same crystallographic site by two different kinds of atoms or to partial occupation of site, as well as for investigations of biomacromolecules since they are large and contain flexible or disordered fragments. The possibility to solve this issue (and to some extent formalize the multipole refinement process, as a kind of a 'side product') appeared after the development of approaches that describe deformation of an atom upon formation of covalent bonds using the multipole parameters (P_{lm}, P_v, κ and κ') taken from the results of high-resolution X-ray diffraction studies of compounds whose crystals are free from the drawbacks mentioned above. This description of the ED distribution function in crystals is called the transferable aspherical atom model by analogy with the spherical atom model.[119]

The transferable aspherical atom model is based on the assumption of transferability of the multipole parameters of an atom having the same chemical environment (*e.g.*, nitrogen atom in the nitro group) in different molecules. This model is intimately connected with the central concept in chemistry, according to which certain atoms or functional groups impart specific chemical and physical properties to compounds and allow one to predict their behaviour in chemical reactions.[92] In turn, this means that atoms or functional groups formed by them in different molecules to a great extent retain the characteristic ED distribution that can be described using pseudoatoms in the Hansen–Coppens multipole model (or discrete atomic contributions within the framework of Bader's theory mentioned above).[120]

The idea of transfer of just the multipole parameters became customary to X-ray diffraction studies [11] first of all since the multipole model provides a local frame of reference for each pseudoatom.[121] This makes it possible to unambiguously choose the local axes for pseudoatoms in different molecules and to minimize the number of the multipole parameters used to describe the ED distribution in the atom by imposing local symmetry constraints.[78] Transfer of fixed parameters to another molecule where the atom is in the same chemical environment (*i.e.*, forms covalent bonds of the same nature with the same atoms) is in essence equivalent to their normalization to the most probable values.[122] Subsequent refinement of atomic positions and thermal displacement parameters in the transferable aspherical atom model [119] offers a number of advantages over not only the spherical atom model, but also the multipole refinement. On the one hand, the refined parameters are the same for both the transferable aspherical atom model and routine X-ray diffraction experiments aimed at structure determination; however, the former allows one to take account of probable redistribution of the electron density owing to the formation of chemical bonds by atoms or to the presence of lone electron pairs. Consequently, this approach does not require high-resolution X-ray diffraction data and is suitable for large or disordered systems and for systems with low scattering power.

The authors of the pioneering study [123] tried to improve the accuracy of determination of anisotropic displacement parameters in the anthracene and naphthalene crystals and used pseudoatoms obtained from high-resolution X-ray diffraction experiment for a related compound, perylene.

A logical extension of this approach was building a data bank of experimental multipole parameters [121] that includes the populations P_{val} and P_{lm} up to $l = 3$ and the corresponding expansion–contraction parameters [κ and κ' in expression (16), respectively] for atoms in small peptide molecules. Corresponding parameters were transferred [121, 124] to atoms in the same chemical environment in oligopeptides that were inappropriate for high-resolution X-ray diffraction studies due to low scattering power (even at $d < 1$ Å, which is not always attainable for macromolecules). The problem of electrical neutrality of the oligopeptide molecule appearing after transfer of monopole populations for atoms from different peptides was solved either by their normalization [121] to the values for neutral atoms or by refinement using the available experimental data.[124]

This approach made it possible to describe the ED distribution in oligopeptide crystals with the accuracy that much exceeded the accuracy for the spherical atom model with respect to the main criteria for refinement quality (*R*-factors, residual ED, violation of Hirshfeld rigid-bond test and reasonable values of anisotropic displacement parameters). Extension of this approach to proteins [125] including those containing disordered fragments (say nothing of bound water molecules) [126] for the first time allowed one to more correctly determine their structure and the distribution of electrostatic potential playing an important role in protein binding to small (*e.g.*, drug) molecules from X-ray diffraction data collected in routine experiments.[127]

Based on the results of these studies, the experimental library of multipolar atom model (ELMAM) was developed[128] for the atoms containing in all 20 natural amino acid molecules and proteins (Fig. 10). In the ELMAM database, each record for chemically equivalent atoms represents a set of averaged multipole parameters (taking account of local symmetry constraints in order to minimize the number of parameters necessary to describe the ED distribution) obtained from the multipole refinement of high-resolution low-temperature X-ray data for certain amino acids and small peptides. A set of parameters was assigned to an atom using a group of criteria characterizing its chemical environment, namely, the number and nature of atoms to which the atom of interest is covalently bonded and the type of these bonds (single, double, aromatic). The problem of electrical neutrality upon data transfer from the ELMAM database to the molecule under study was solved automatically by uniformly distributing the excess (or deficient) charge over all atoms in the molecule. For protein molecules composed of very large number of atoms, these changes appeared to be even smaller than the standard deviation in the determination of P_{val} for small molecules;[126] this is of importance for correct assessment of electrostatic properties of proteins from the corresponding charges.[126]

In all cases the use of the ELMAM database in the refinement of positional and thermal displacement parameters of atoms from X-ray diffraction data gave more accurate information on the structure of biomacromolecules than conventional spherical atom model. The most striking example is provided by the results of unconstrained refinement of anisotropic displacement parameters and X–H distances compared to those obtained upon normalization to commonly accepted neutron diffraction values, as is

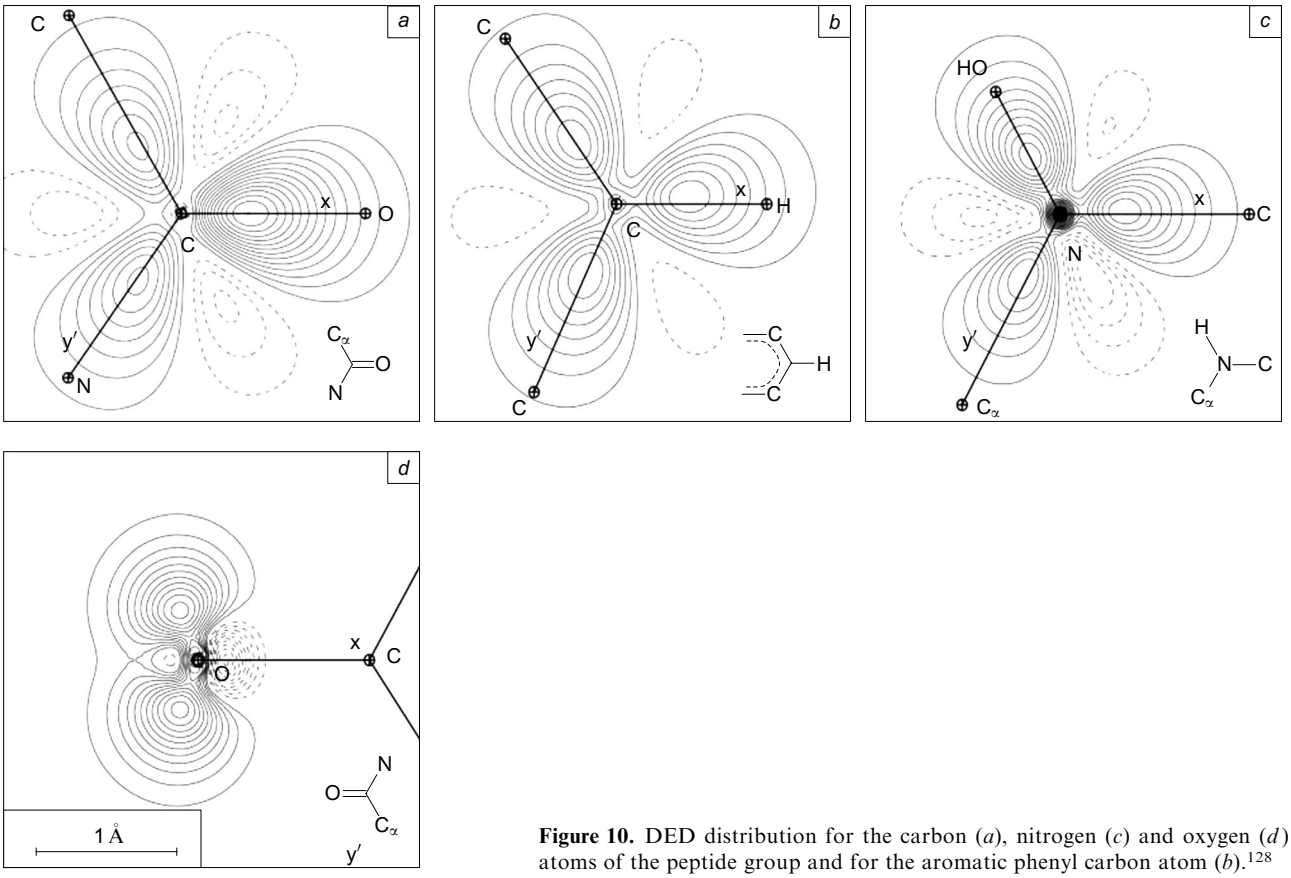


Figure 10. DED distribution for the carbon (*a*), nitrogen (*c*) and oxygen (*d*) atoms of the peptide group and for the aromatic phenyl carbon atom (*b*).[128]

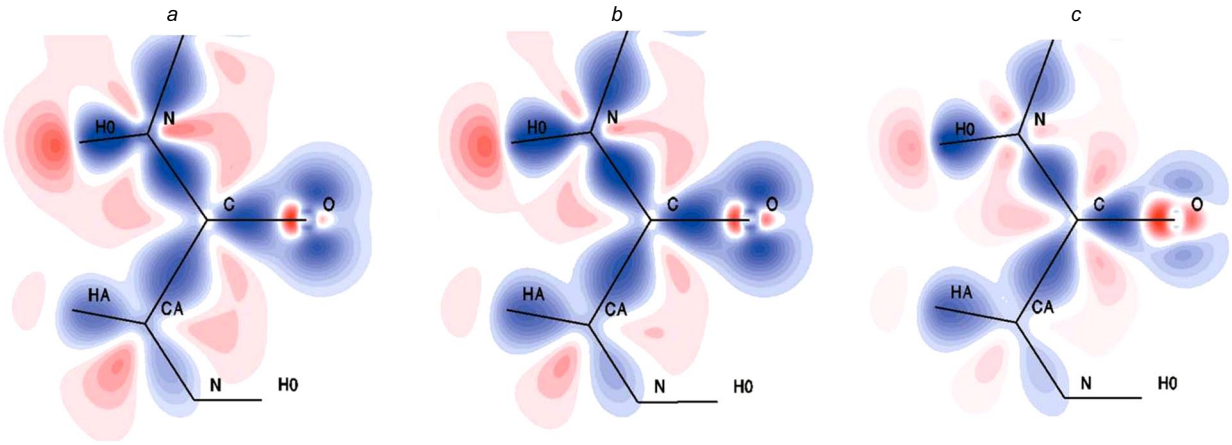


Figure 11. DED distribution near the peptide bond: transferred from the ELMAM database (*a*), after ELMAM constrained multipole refinement of X-ray diffraction data (*b*) and after multipole refinement starting from the spherical atom model (*c*).[126]

traditionally done in high-resolution X-ray diffraction studies.[128] The multipole populations from the ELMAM database also appeared to be a better initial approximation for subsequent multipole refinement of X-ray diffraction data of sufficiently high resolution (at $d < 0.7$ Å) (Fig. 11) than the spherical atom model, which in some cases led to a local minimum.[128] It was proposed to use this approximate ED distribution to analyze peculiar features of chemical bonding in proteins, including the description of intermolecular interactions responsible for the secondary structure of proteins.[129]

A more recent and larger database, ELMAM2,[130] covers a broad range of organic compounds. Utilization of ELMAM2 seems to be a possible alternative to the multipole refinement of high-resolution X-ray diffraction data.[131] It also provides a more accurate distribution of the dynamic ED which includes the effects of thermal motion[132] in contrast to the static ED described using the multipole model [see expressions (15)–(17)].

The ELMAM2 database includes averaged multipole parameters for a larger number of model compounds previously studied by high-resolution X-ray diffraction at low temperatures. Certain model compounds now contain atoms with $Z > 10$ that were not included in the ELMAM database. Yet another important distinction from the ELMAM concerns the description of hydrogen atoms in these compounds, *viz.*, not only the monopole population, but also the population of a quadrupole whose Z axis is aligned with the X–H bond is now refined and thermal motion is treated as anisotropic using the SHADE method.[85] In addition, the multipole parameters are selected automatically taking into account the chemical nature of the atom, local symmetry, number and type of nearest neighbours to the second (for hydrogen atoms) or third (for oxygen atoms) sphere, as well as geometric parameters (bond lengths and bond angles) and then transferred from the ELMAM2 database.[133]

Taking account of these improvements, ELMAM2 rapidly became a convenient tool for X-ray diffraction studies of organic small molecules and macromolecules. Indeed, it is better than the spherical atom model and is at least competitive with the multipole refinement of high-resolution X-ray diffraction data, being free from the main limitations of these methods. The quality of the structure model thus obtained can be confirmed in exactly the same manner as for routine X-ray diffraction experiment, *i.e.*, using the *R*-factors and residual ED values, while the reliability of the corresponding ED distribution can be confirmed using all criteria utilized in modern high-resolution X-ray diffraction studies (see above).

It is also commonly accepted to compare the distribution thus obtained with the results of multipole refinement of high-resolution X-ray diffraction data (or X-ray structure factors obtained from quantum chemical calculations of crystals; see below).[130] This can be done by comparing the numerical values of the ED or DED (for better clarity) at each point of the unit cell, the similarity index for two tensors of anisotropic displacement parameters and the convergence factors of topological parameters of the ED [numerical values of various functions at the (3,–1)BCP within the framework of Bader's theory].[131] One can also use the atomic charges evaluated from the monopole population P_{val} or by integrating the ED over the atomic basin, the dipole and quadrupole moments, the electrostatic potential distribution (including its distribution over the molecular surface), the electrostatic interaction energy and the correlation coefficients of any parameter mentioned above determined using two ED models.[130] Although the multipole refinement from high-resolution X-ray diffraction data is always more preferable, the use of the multipole parameters of atoms from the ELMAM2 database allows one to describe the ED distribution in crystals of organic compounds (from small molecules to proteins) with reasonable accuracy and thus extend the field of research to systems that were previously inaccessible.

Yet another version of the ELMAM and ELMAM2 databases is claimed[134] to be an individual database of experimental multipole parameters. Unlike the ELMAM and ELMAM2 where the effect of crystal environment on molecules is included indirectly (first of all, since the multipole parameters of the model compounds were determined from experimental data for crystals), the modified database uses larger structural fragments that form stable supramolecular motifs, so-called synthons and is termed as synthon based fragment approach (SBFA). It was assumed that synthons are more appropriate to describe frequently

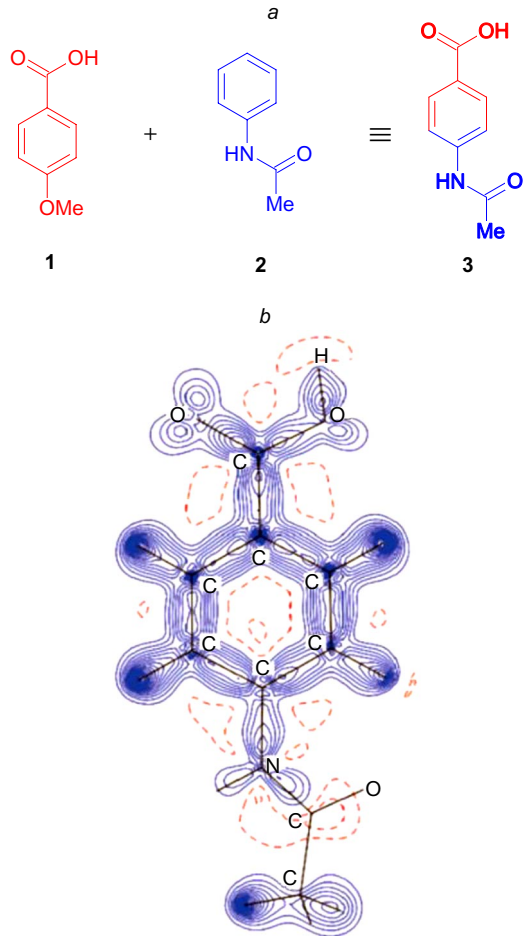


Figure 12. Assembling a molecule from model compounds (*a*) and the SBFA-derived DED distribution in the molecule (*b*).[134]

occurring intermolecular interactions, *e.g.*, hydrogen bonds[134] involving peptide groups in proteins, nucleic acids and many other biomacromolecules (Fig. 12). Since then the SBFA database was augmented with synthons assembled through weaker interactions; it is also used to study multicomponent systems[135] including polymorphism in them.[136]

A clearly seen disadvantage of the SBFA approach compared to the transfer of multipole parameters from the ELMAM and ELMAM2 databases consists in subjective choice of chemically reasonable fragments[135] used as building blocks (see Fig. 12). This makes the SBFA approach less versatile and significantly reduces the range of compounds to be studied; therefore, the SBFA database is of limited use.[137]

Creation of databases of experimental multipole parameters was of great importance since in some cases it gave the ED distribution for systems that were inaccessible to both high-resolution X-ray diffraction studies (*e.g.*, for proteins having flexible fragments and disordered domains) and quantum chemical calculations (*e.g.*, proteins since their molecules are too large). Application of the databases in question also extended the range of problems to be solved in X-ray crystallography and quantum chemistry — from protein structure refinement to protein binding to small (*e.g.*, drug) molecules. However, the application field of the databases of experimental multipole parameters is limited because crystals of many model compounds necessary for database provisioning are inappropriate for high-resolution X-ray diffraction studies. Besides, the results of multipole refinement can be influenced by the experimental errors and the ED smearing caused by thermal motion of atoms, which cannot always be separated from the static ED distribution described by the multipole model.

A possible route to solve these issues is to use the multipole parameters determined from theoretical structure factors obtained from quantum chemical calculations instead of high-resolution experimental data sets. It should be noted that the possibility to calculate the structure factors was available more than three decades ago;[138] however, reliable methods and user-friendly software were developed only recently.

5. Quantum chemical calculations of X-ray structure factors

Theoretical X-ray structure factors calculated only from the unit cell parameters and atomic coordinates (these are not always necessary)[139] are widely used in modern X-ray diffraction studies to confirm the reliability of experimental ED distribution in the crystal.[140] They are not influenced by the errors associated with the nature of crystals (low scattering power, disordering, absorption of X-ray radiation, twinning, *etc.*), experimental errors (diffuse X-ray scattering or permeation of low-energy photons through focusing multilayer optics) and thermal motion of atoms. However, the theoretical structure factors also 'suffer' from finite resolution (Fourier series truncation) that is specified by the researcher depending on a particular goal (see, *e.g.*, Ref. 141) and from errors introduced into corresponding ED distribution by the Hansen–Coppens multipole model[72] used to refine the X-ray diffraction data. On the one hand, this allows one to correctly compare the theoretical and experimental ED distributions.[140] On the other hand, one can reveal artifacts originating from drawbacks of the multipole model[73,139] by comparing the theoretical ED distribution with the results of analysis of the wave function obtained from quantum chemical calculations.

Theoretical basis of quantum chemical calculations of X-ray structure factors from the ED distribution function for a crystal was laid in the 1960–1970s;[138] however, details of practical implementation depend on the basis set used. The structure factor $f(\mathbf{s})$ depends on the scattering vector $\mathbf{s}$ defined using the Miller indices *hkl*. Going to the basis of crystal cell (fractional coordinates) and omitting *hkl* for brevity, the structure factor is given by:[142]

$$f(\mathbf{s}) = \int \rho(bbr) \exp(-\mathrm{i}sr)\mathrm{d}r \qquad (20)$$

Correspondingly, the ED can be expressed through the sum of contributions of the products of the density matrix elements $P^{g}_{\mu\nu}$ by the atomic orbitals χ^{0}_{μ} (the origin is at 0) and χ^{g}_{ν} (the origin is shifted to g unit cells),

$$\rho(\mathbf{r}) = \sum_{\mu,\nu,g} P^{g}_{\mu\nu}\, \chi^{0}_{\mu}\, \chi^{g}_{\nu} \qquad (21)$$

Combining Eqns (20) and (21), one gets the expression for the static structure factor $[F_0(\mathbf{s})]$, which depends on the

density matrix elements $P^g_{\mu\nu}$, and the static scattering integral $I^g_{\mu\nu}(\mathbf{s})$,

$$F_0(\mathbf{s}) = \sum_{\mu,\nu,g} P^g_{\mu\nu} I^g_{\mu\nu}(\mathbf{s}) \quad (22)$$

The static scattering integral is determined by the integration domain (*i.e.*, explicitly depends on coordinates) and can be treated as the product of integrals calculated separately for each coordinate,

$$I^g_{\mu\nu}(\mathbf{s}) = I^{g_x}_{\mu\nu}(s_x)\, I^{g_y}_{\mu\nu}(s_y)\, I^{g_z}_{\mu\nu}(s_z) \quad (23)$$

$$I^{g_x}_{\mu\nu}(s_x) = \int_{-\infty}^{+\infty} (x - x_A)^m \left\{ \exp\left[-\alpha(x - x_A)^2 (x - x_B - g_x)^n\right] \right\} \times$$

$$\times \left\{ \exp\left[-\beta(x - x_B - g_x)^2\right] \right\} \left[\exp(-\mathrm{i}s_x x)\right] \mathrm{d}x \quad (24)$$

where α and β are the exponents of Gaussian functions related to the orbitals $\mu(A)$ and $\nu(B)$ centred at the coordinates x_A and $x_B + g_x$, while the power coefficients m and n are specified by the Gaussian functions.

However, this approach was of limited use since it required representation of the wave function by combination of Gaussian atomic orbitals described using split-valence basis sets or N-zeta basis sets ($N = 2-5$). In particular, implementation of this approach in the CRYSTAL program package,[143] which has been long (see, *e.g.*, Ref. 144) and most widely used to this end, precluded the use of Slater functions or taking account of relativistic effects. These calculations of structure factors are simple for crystals of compounds containing atoms of Period 1 – 3 elements and a relatively small number of atoms in the unit cell; however, their computational cost becomes very high in certain other cases.

Thus it was logical to modify these studies in order to extend them to other types of basis sets, first of all, plane waves.[145, 146] They are used to describe the valence electrons, while the core electrons are described using various types of pseudopotentials or spherical harmonics depending on how is the method implemented in different program packages. Although separate determination of structure factors accelerates the calculations (especially, if the VASP software is used),[145] they lead to some difficulties in further refinement of the structure factors within the framework of the multipole model; therefore, full-electron Gaussian basis sets still remain more preferable.[147]

Emphasize that the structure factors in question are static and thus cannot be used to analyze thermal motion and(or) disorder in crystals because the atomic displacement parameters are zero in this case. The dynamic structure factor is given by the product of expression (22) by the temperature factor $T(h)$ [see formula (7)]; however, obtaining $T(h)$ values is not a trivial task.

In the pioneering study[148] of urea crystal each structure factor value was multiplied by the Debye – Waller factor calculated from the average U_i value obtained in the X-ray diffraction experiment.[149] Such a simulation of thermal motion of atoms followed by multipole refinement of theoretical structure factors gave the ED distribution that was similar to experimental one (in terms of R-factors, deformation ED and topological parameters of the ED distribution function for intra- and intermolecular interactions) and could be used to analyze the anisotropy of atomic displacements by comparing experimental and calculated U_{ij} values.

Theoretical structure factors were first of all used to study crystals of elemental substances taking into account the fact that quantum chemical calculations of periodic systems take longer time than those of isolated molecules. For instance, diamond, silicon and germanium form covalent bonds[150] that cannot be correctly described by the multipole model. As a consequence, only semiquantitative agreement between the experimental and theoretical (calculated in the local density approximation, LDA) ED distributions and the Laplacian was obtained. The corresponding values at the (3, −1)BCP differed by 10% – 30%; it was of importance to calculate as many structure factors per refined parameter as possible by choosing a balance between the resolution and computing time. Similar conclusions were made in the studies of binary [MgO,[151] NaF and LiF (Ref. 152)] and more complex [NH_4F and NH_4HF_2 (Ref. 149)] inorganic compounds where most chemical bonds have ionic nature, and the difference between the ED and Laplacian at the (3, −1)BCP is even smaller. Although the multipole refinement of theoretical structure factors has certain drawbacks, it is a workhorse to check the correctness of experimental ED distribution and to reveal instrumental errors or effects that were only partially included in processing X-ray diffraction data (*e.g.*, diffuse X-ray scattering).[148]

An example is provided by the study of molecular iodine crystal[98] characterized by strong absorption of X-ray radiation. In spite of close values of the topological parameters of the theoretical and experimental ED distributions, the latter demonstrated artifacts in the region of the lone electron pair of iodine atom. Therefore, further studies of electrostatic potential and evaluation of the intermolecular interaction energy were carried out using the theoretically calculated structure factors. An important conclusion drawn in that study[98] was the necessity of taking into account relativistic effects for heavy elements since their neglect introduces errors into the ED distribution function, which is especially noticeable when analyzing the second derivative of this function.

A study[153] of noble-gas (Kr and Xe) crystals deserves particular attention. Conventional DFT approximations describe weak van der Waals interactions in these crystals with insufficient accuracy. The results of refinement of the structure factors calculated in two approximations, LDA and generalized gradient approximation (GGA), were different. The former led to more diffuse ED function and larger value of this function at the (3, −1)BCP of intermolecular interactions compared to the GGA approximation; however, the latter gave a better description of core electrons. Both methods fairly well reproduced the topological parameters of the ED function obtained from standard-resolution X-ray diffraction data ($2\theta < 60^\circ$ owing to numerous difficulties in growing high-quality single crystals of these noble gases) using a model[154] with refinement of the population and the expansion – contraction parameter of spherically symmetric valence shell of the atom.

Theoretical structure factors were used in the studies of not only crystals of elemental substances and inorganic compounds, but also organic crystals,[37] starting with the pioneering investigation of urea.[148] In some cases the multi-

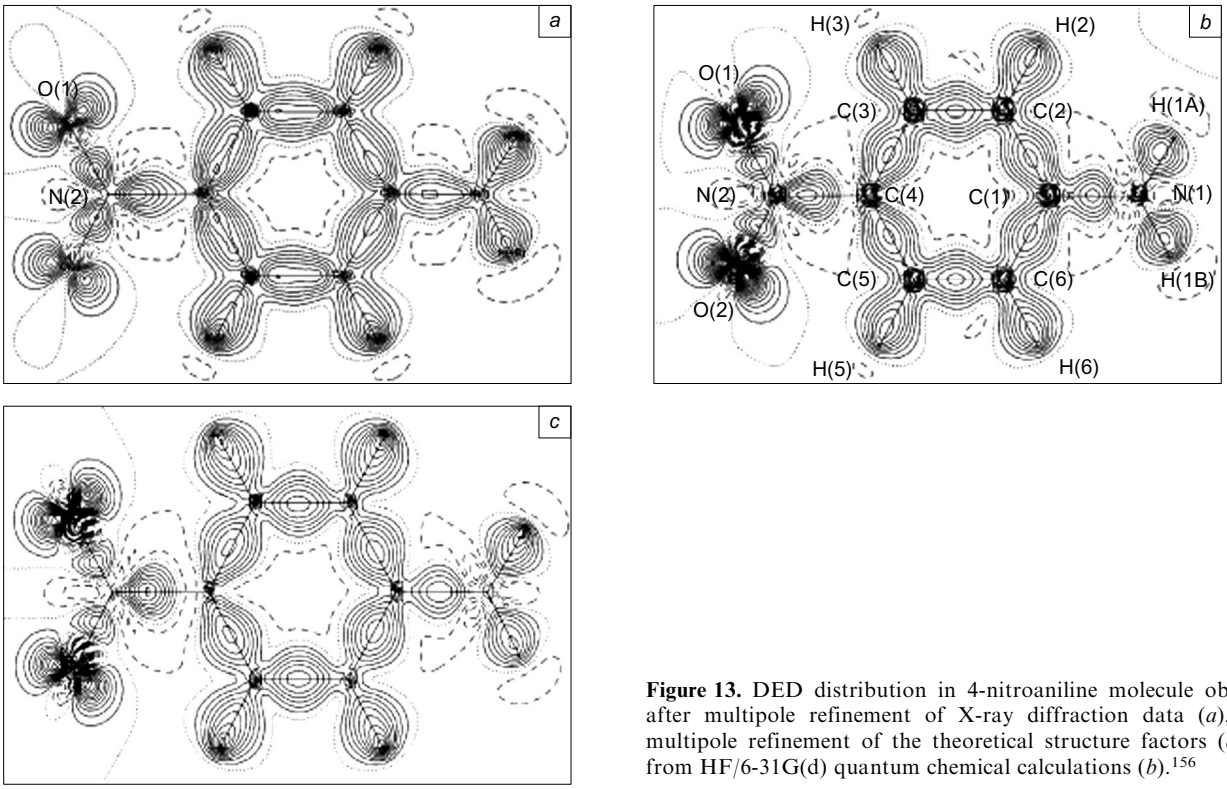


Figure 13. DED distribution in 4-nitroaniline molecule obtained after multipole refinement of X-ray diffraction data (*a*), after multipole refinement of the theoretical structure factors (*c*) and from HF/6-31G(d) quantum chemical calculations (*b*).[156]

pole refinement of structure factors was the only way to obtain the ED distribution in the crystal (see, *e.g.*, Ref. 155); however, the main goal was to assess the correctness of experimental data.[140] In particular, a study [156] of 4-nitroaniline crystal showed that the ED distribution obtained upon refinement of high-resolution X-ray diffraction data was in good agreement (within 5%) with that obtained from quantum chemical calculations. However, the Hessian eigenvalues along certain bond lines (λ_3) differed twofold and more. This difference was explained by disadvantages of the multipole model that was used to obtain the experimental ED distribution. A comparison with the results of the multipole refinement of theoretical structure factors (Fig. 13) shows much less pronounced differences, especially near nuclear sites.

Quantum chemical calculations of periodic systems are also employed to analyze the interaction density.[140] This quantity is the difference between the ED distribution in the crystal and the superposition of electron densities in non-interacting molecules; calculations of the latter do not require knowledge of the unit cell parameters or atomic coordinates.

Of course, the use of theoretical structure factors has its own drawbacks due to the difficulties in the description of thermal motion of atoms (see above) and to the dependence on the level of theory chosen for quantum chemical calculations (Hartree – Fock or DFT methods, different basis sets, taking account of relativistic corrections). When studying compounds containing atoms of Period 1 – 2 elements, this dependence is not so critical as in the case of heavier elements [98] (a few publications are available, see, *e.g.*, Ref. 157). This is most probably due to the lack of full-electron basis sets and difficulties with inclusion of relativistic corrections in the CRYSTAL program package,[143] which is most widely used in calculations of periodic systems.[158]

To this end, pseudopotentials can also be used. This approach is implemented in the VASP program package [145] and aimed to solve the problem of description of core electrons since heavy-element atoms are abundant in core electrons. An illustrative example is provided by a study [158] on refinement of theoretical structure factors for the hexachlorobenzene crystal. To reproduce the results of high-resolution X-ray diffraction experiment,[159] the ED distribution for atomic cores was quantum chemically calculated in a specific manner. The first step involved calculations for a crystal where positions of real atoms in the hexachlorobenzene molecule were occupied by noble-gas atoms (He for Period 2 elements and Ne for Period 3 elements). Then, the structure factors thus obtained were added to the structure factors calculated for the valence electron density. However, subsequent multipole refinement of the structure factors revealed artifacts in the region of chlorine nuclei (Fig. 14). To remove them, a transition was made from static to dynamic structure factors using expression (7) and average U_i values from the X-ray diffraction data. Eventually, the experimental ED distribution in the hexachlorobenzene crystal was reproduced within 5% – 10% for topological parameters of covalent bonds and 10 – 15% for intermolecular interactions. The discrepancies observed are systematic, although being within the limits of experimental error.

This method for calculations of theoretical structure factors is not time- or labour-consuming and represents an alternative to high-resolution X-ray diffraction studies, especially for compounds containing atoms of elements characterized by strong absorption of X-ray radiation (*e.g.*, bromine [160] or selenium [161]). However, the authors [161] restricted themselves to the multipole refinement of the structure factors calculated for valence electrons and gave

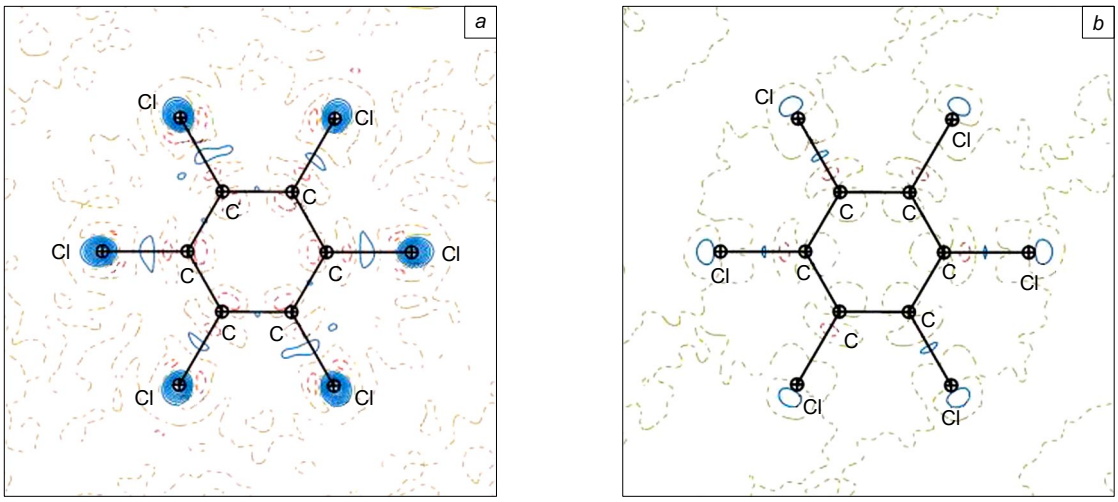


Figure 14. Residual ED distribution in hexachlorobenzene molecule obtained upon multipole refinement of static (*a*) and dynamic (*b*) theoretical structure factors.[158]

a brief description of the results obtained. Probably, this technique for obtaining all-electron structure factors gives unsatisfactory results for compounds containing atoms of for elements of 4th and subsequent periods. Besides, this is not a user-friendly method since it requires separate quantum chemical calculations for the core and valence electrons.

In spite of the development of new approaches and user-friendly software for calculations of theoretical structure factors, they are not widely used by researchers who work in crystal chemistry and quantum chemistry. This is first of all due to the fact that is it more convenient to analyze the ED distribution obtained immediately from quantum chemical calculations of a crystal and not waste time by performing the multipole refinement since the choice of optimum strategy is a rather complicated task even for high-skilled specialists in high-resolution X-ray diffraction studies (see above). Unfortunately, quantum chemical calculations of crystals with large unit cell parameters are very labour-consuming.

However, one should analyze only the ED distribution in the molecule, *e.g.*, if intermolecular interactions are weak or less important from the standpoint of the problem to be solved.[73] In this case, the static structure factors can be obtained from the wave function calculated for isolated molecule rather than calculations of the crystal structure using periodic boundary conditions. This option is implemented in the DENPROP program package.‡ The molecule is placed in a large unit cell with user-defined parameters to exclude the interaction with neighbouring molecules and then the structure factors are calculated numerically or in analytical form[138] for the specified molecular geometry using Gaussian or Slater basis sets.

Among various examples of utilizing the molecular structure factors of organometallic and coordination compounds that form crystals with unit cell parameters and thus are difficult for quantum chemical calculations of periodic systems and high-resolution X-ray diffraction studies, two should be emphasized.[73, 139] A comparison of the data on peculiar features of chemical bonding in transition-metal complexes obtained immediately from analysis of the wave functions of isolated molecules with the results of corresponding multipole refinements revealed physically unmeaningful artifacts in the ED distribution (*viz.*, interactions that do not actually occur)[73] that are solely due to the drawbacks of the multipole model (Fig. 15).

Molecular structure factors calculated for compounds containing gallium[76, 77] and rare-earth element atoms[141] (here, relativistic effects should be taken into account) were also used to evaluate the possibility to describe the polarization of core electrons using the Hansen–Coppens model. For instance, the multipole refinement of high-resolution X-ray diffraction data for a compound of monovalent gallium[76] resulted in a rather large maximum of the residual ED (0.9 e) at the Ga position (Fig. 16*a*). This feature is related to neither absorption of X-ray radiation by the sample nor anharmonicity of thermal motion of atoms. The refinement of theoretical structure factors gave a similar result, thus being indicative of incorrect refinement strategy. The problem was solved using the extended Hansen–Coppens multipole model[75] with refinement of the core populations P_{core} and the corresponding expansion–contraction parameters κ_{core} up to the refinement of each electron shell in the atom (method of separated core shells).[76] This enabled a much better description of the ED distribution (Fig. 16*b*) including the accumulation of valence density in the Ga lone pair region. As in the case of a related Ga(III) compound,[77] it was of importance to refine the all-electron structure factors rather than only the structure factors corresponding to valence electrons as was done in, *e.g.*, the studies of the bromo- and selenium-containing compounds mentioned above.[160, 161]

The theoretical ED distribution in the yttrium, scandium and lanthanum complexes was obtained analogously.[141] Its analysis showed that polarization of core electrons in the metal atom upon the formation of chemical bonds can be revealed only using the refinement within the framework of the model of separated core shells from ultrahigh-resolution theoretical structure factors

‡ A program package for topological analysis of the ED distribution function that is also suitable to calculate the structure factors from analytical ED distribution function.[162]

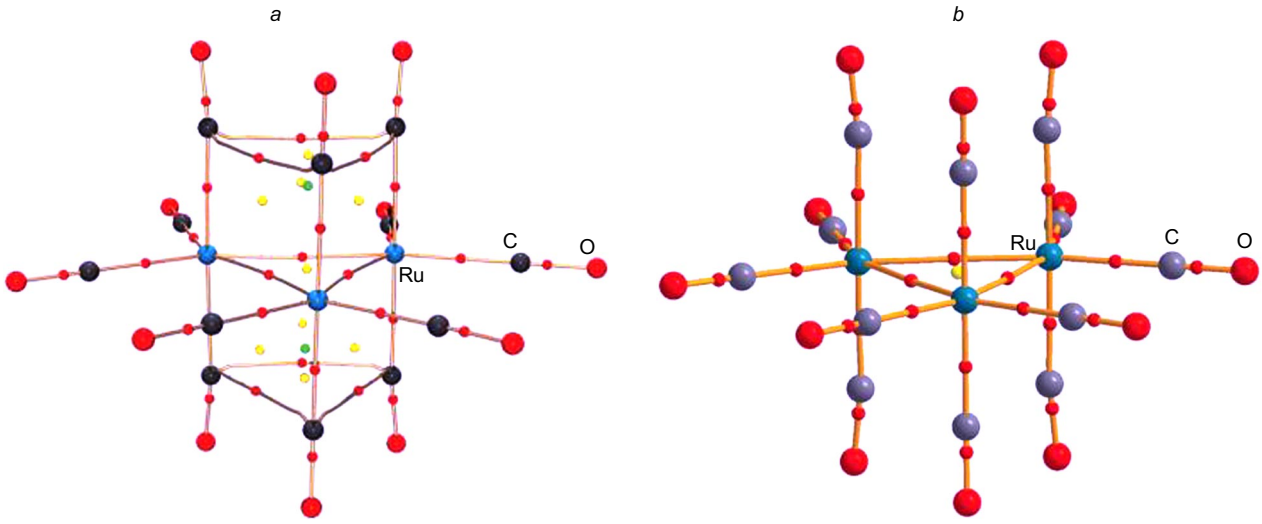


Figure 15. Molecular graph of the $Ru_3(CO)_{12}$ complex obtained from the results of topological analysis of the ED distribution after multipole refinement of the structure factors (*a*) and from the results of PBE0/cc-pVTZ quantum chemical calculations (*b*).[73]
The ED distribution critical points are shown as red spheres for (3, −1)CP, as yellow spheres for (3, +1)CP and as green spheres for (3, +3)CP.

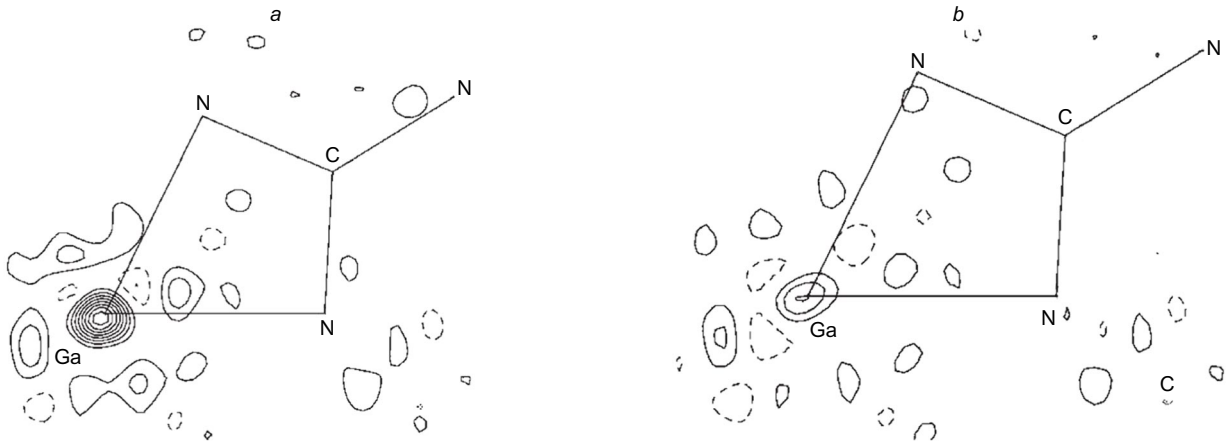


Figure 16. Residual ED Distribution near Ga^+ ion obtained after multipole refinement of the structure factors using one (*a*) and c two (*b*) expansion–contraction parameters for core electrons.[76,77]

($\sin\theta/\lambda < 1.8$ Å^{-1}). However, this effect was also disclosed and the core populations P_{core} for two core shells of Ga atom evaluated using X-ray diffraction data with a resolution of $\sin\theta/\lambda < 1.1$ Å^{-1}.[76]

Generally, the results of the multipole refinement of theoretical structure factors agree well with the results of high-resolution X-ray diffraction studies. Each of the two approaches has its own drawbacks. The former depends on the approximation chosen, on the basis set and on whether or not electron correlation or relativistic effects are included. The latter is influenced by the quality and nature of the crystal, the experimental error and thermal motion of atoms. Quantum chemical calculations of molecular crystals using no periodic boundary conditions are much less computationally expensive, especially, if van der Waals intermolecular interactions are weak; however, problems with the description of large molecular systems, such as biomacromolecules, still persist in this case. Nevertheless, the possibility to calculate the molecular structure factors gave an impetus to the development of methods that utilize databases of theoretically calculated multipole parameters.

6. Databases of theoretical multipole parameters

Creation of databases of theoretical multipole parameters[163] calculated using the transferable aspherical atom model[119] is a logical continuation of the idea of transferability of pseudoatoms obtained in high-resolution X-ray diffraction studies. This type of databases retain all advantages of the databases of experimental multipole parameters [first of all, ELMAM (Ref. 128) and ELMAM2 (Ref. 130)], being free from the key drawback of the 'predecessors', *viz.*, the necessity to have high-resolution X-ray diffraction data for each model compound. Since only a few small-molecule crystals meet stringent requirements for samples for high-resolution X-ray diffraction studies, the databases of exper-

imental multipole parameters remain of limited use. At the same time, the theoretical structure factors, with a user-defined resolution, can be calculated for any isolated molecule or for a molecule of interest in certain crystalline environment using quantum chemistry methods (see above). They depend to some extent on the computational method;[141] however, the multipole refinement of theoretical structure factors gives the valence-shell and multipole populations (P_{val} and P_{lm}, respectively) as well as corresponding expansion – contraction parameters (including κ' for the hydrogen atoms that are traditionally not included in the refinement from X-ray diffraction data[74]) that are free from experimental errors and not influenced by thermal motion of atoms, thus being obviously advantageous over experimental multipole parameters.

This approach is able to generate a necessary set of pseudoatoms in the desired chemical environment (usually, nearest neighbours[163]) at reasonable time. As in the case of the ELMAM and ELMAM2 databases, pseudoatoms are transferred to the molecule of interest and their values remain fixed in the refinement of positional and displacement parameters from the available X-ray diffraction data including low-resolution data ($d > 0.7$ Å).

Strictly speaking, the ED distribution function in the crystal obtained from such a hybrid refinement cannot be treated as experimental. Although all functions in expression (18) describing deformation of the ED upon the formation of chemical bonds (analysis of the ED is the subject of high-resolution X-ray diffraction studies) are described theoretically[72] except the populations of multipole parameters, in this case they were also taken from the results of quantum chemical calculations. However, application of the ELMAM and ELMAM2 databases of experimental multipole parameters is based on the essentially the same normalization of the multipole parameters to the most probable values. Using the theoretical multipole parameters as the most probable values, one can even more extend the range of accessible systems and thus obtain the ED distribution in the corresponding crystal. Since historically the most interest in this respect was aroused by biomacromolecules, successful studies of these objects using the ELMAM and ELMAM2 databases gave an impetus to the creation of databases of theoretical multipole parameters.[164, 165] It should be noted that the asphericity of the ED distribution can be described using an alternative method based on augmentation of conventional independent spherical atom model with additional spherical scatterers placed in the regions of chemical bonds and lone electron pairs.[166] However, in this case the number of refined parameters is considerably larger than when using the TAAM, so the application field of the technique is limited to macromolecular structure determination.

To date, two databases of theoretical multipole parameters are available, *viz*., the University at Buffalo pseudoatom databank (UBDB)[163] and the invariom (from 'invariant atoms') database.[167] The key difference between them[119] is that in the former the multipole parameters are averaged over the results of B3LYP/6-31G(d,p) calculations of a series of related compounds carried out using fixed geometric parameters retrieved from the Cambridge Structural Database,[168] while in the latter they were calculated for a certain model compound upon geometry optimization at the B3LYP/D95 + + (3df, 3pd) level of theory. Therefore, only the theoretical multipole parameters from the UBDB database take into account, although indirectly, the influence of crystalline environment by using the molecular geometry obtained from X-ray diffraction data (note that corresponding changes in the molecular ED distribution are small and lie within the limits of experimental error).[36] The multipole parameters correspond to the structure factors for the valence electron shells whose deformation is described by the conventional multipole model in the 'frozen core' approximation. In this case, the atomic scattering factors rapidly decrease with increasing the $\sin\theta/\lambda$ ratio (see Fig. 1), which allows one to reduce the computational cost.[163]

The concept of invariom uses all-electron structure factors,[167] probably, since there is no need to carry out quantum chemical calculations of series of compounds for subsequent averaging, as in the case of UBDB. Yet another important distinction between the databases in question concerns the way for solving the problem of electrical neutrality of the molecule to which corresponding multipole parameters are transferred. The excess (or deficient) charge from invariom is uniformly distributed over all atoms in the molecule, just as in the ELMAM database,[121] while the method implemented in the UBDB database is more reliable since it takes into account how accurately the atomic charges were determined in the model compounds (similarly to the ELMAM2, see Ref. 133). The lengths of the bonds involving hydrogen atoms are also specified in different manner. Correct localization of H atoms is needed to describe, *e.g*., the electrostatic properties. In the UBDB database, these bond lengths are normalized to conventional neutron diffraction values by analogy with the ELMAM and ELMAM2 databases, while in the invariom database they are normalized to the values obtained upon molecular geometry optimization of the model compound.

In spite of the distinctions mentioned above, both databases of theoretical multipole parameters are based on calculations of the structure factors for pseudoisolated molecules placed in a rather large unit cell (usually, a pseudocubic cell with an edge of 30 Å).[164] First of all, they were created to be used in biomacromolecular studies, although in different manner. Namely, the main goal was to evaluate the interaction energies for UBDB and to obtain more accurate structural data for the invariom database.[36] Noteworthy, there is an interplay between these goals since reliable estimation of the properties of a system from the ED distribution requires accurately determined atomic coordinates and anisotropic displacement parameters of atoms in the crystal.

Chronologically, the UBDB database[163] was created earlier than the invariom database, probably, for some reasons related to successful application of the ELMAM and ELMAM2 databases to describe the electrostatic properties of biomacromolecules.[127, 129] The UBDB database includes the multipole parameters P_{val} and P_{lm} up to $l = 4$ and the corresponding expansion – contraction parameters κ and κ' calculated for atoms of small peptide molecules (Fig. 17). Compared to the ELMAM database, which includes the influence of crystal packing in more explicit form, the UBDB database gives a less accurate description of atomic charges and the electrostatic potential distribution in the polypeptide molecules to which corresponding multipole parameters were transferred.[169] However, the electrostatic interaction energies thus determined were in good agreement with the results of high-level quantum

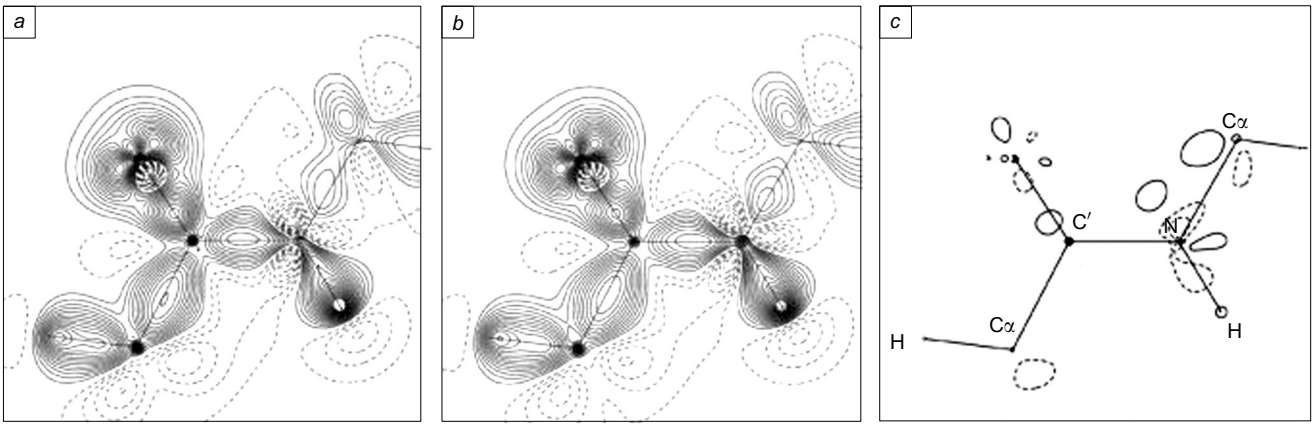


Figure 17. Deformation ED distribution near the peptide bond obtained after conventional multipole refinement (*a*) and after transfer from the UBDB databank (*b*) and the difference between *a* and *b* (*c*).[163]

chemical calculations[170] where they were evaluated using a more accurate approach based on the ED distribution, *viz.*, the so-called exact potential/multipole moment (EP/MM) method.[110] It was developed by the researchers who created the UBDB database, is currently in use and involves more accurate and time-consuming calculations of the Coulomb interaction integral for pseudoatoms at short distances (up to 4.5 Å) and a faster, although less accurate, evaluation of this integral using the multipole approximation at long distances.

The UBDB database and its extended version, UBDB2011, combined with the EP/MM method is actively used to study electrostatic binding of proteins and oligo(poly)peptides[171] as well as DNA, RNA and related biomacromolecules[172] to one another and to small molecules including drugs.[164] The accuracy of evaluation of electrostatic interaction energies using this approach ($\sim$4 kJ mol^{-1})[173] is much better than that provided by conventional force fields[174] whose applicability is limited because of high computational cost of *ab initio* quantum chemical methods or DFT methods for large systems.

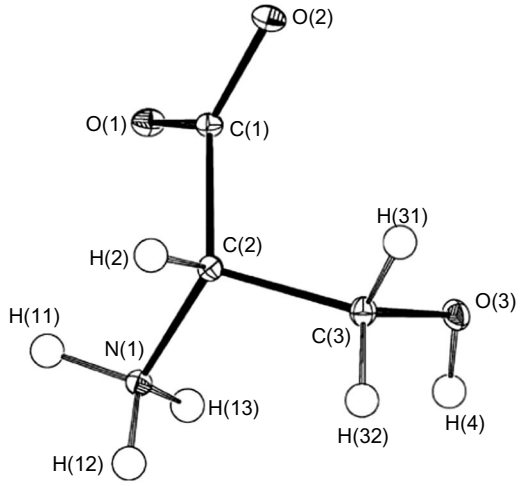
Having collected high-resolution X-ray diffraction data ($d \leqslant 0.85$ Å) for biomacromolecules (this occurs rarely), the theoretical multipole parameters from the UBDB database can be used as the starting point for their refinement to obtain the ED distribution[168] similarly to the experimental multipole parameters from the ELMAM and ELMAM2 databases. If only low-resolution data are available, the UBDB database allows one to more accurately (compared to the spherical atom model) describe the molecular geometry and anisotropic displacement parameters of atoms,[38] which are close to the results of conventional multipole refinement or to neutron diffraction data,[175] and to locate hydrogen atoms, which is a sophisticated problem in macromolecular X-ray crystallography.

However, it is recommended[175] to use the UBDB database and the TAAM in the studies of biomacromolecules only if high-resolution X-ray diffraction data ($d < 1$ Å) are available and the proportion of disordered fragments and solvent molecules in the crystal is relatively low. To obtain more accurate positional and anisotropic displacement parameters of atoms in small molecules, it is also desired to attain a higher resolution ($d \leqslant 0.65$ Å); however, even if this is impossible, the UBDB database describes the structure much more accurately than the spherical atom model.[176] As a consequence, one can, *e.g.*, evaluate the normal mode frequencies and thus the vibrational entropy of the crystal[177] from the X-ray diffraction data that are formally suitable for structure determination purposes only.

The UBDB database can be also be used to describe the ED distribution in disordered fragments[178] that are intrinsically present in biomacromolecules. In this case reliable evaluation of electrostatic interaction energies even for small molecules requires tabulated values of the expansion–contraction parameters κ' derived from the refinement of theoretical structure factors.[74] However, the ED distribution in the crystal obtained using the UBDB database is somewhat different from that obtained after multipole refinement of high-resolution X-ray diffraction data.[178] This discrepancy is systematic and first of all observed in the regions near atomic nuclei. Therefore, corresponding anisotropic displacement parameters of atoms cast some doubt in spite of the fact that they are more accurate than those obtained using the spherical atom model. On the other hand, unlike the invariom database, the UBDB database was initially optimized to evaluate the electrostatic properties of biomacromolecules rather than to solve the problem in question.

The concept of invarioms was introduced[167] following the creation of the UBDB database. The model systems for calculating the molecular structure factors and subsequent determination of multipole parameters included fragments containing only the atom of interest and its nearest neighbours (and atoms bonded to them in the case of aromatic systems),[179] while other positions were occupied by hydrogen atoms (Fig. 18). In this case, each atom, depending on its chemical environment (nature of atoms to which it is covalently bonded, and type of these bonds — single, double, aromatic), can be assigned a uniquely specified set of theoretical multipole parameters called the invariom.

By analogy with the UBDB database, having transferred corresponding invarioms and refined positional and thermal displacement parameters of atoms in a molecule of interest from the available X-ray diffraction data, one gets more accurate results compared to the spherical atom model,[179] especially for hydrogen atoms. Besides, such a refinement allows one to reconstruct the ED distribution including the dynamic ED distribution (using invarioms as the source of



Atom	Invariom	Model compound
O(1)	O1.5c[1.5o1c]-	$MeCOO^-$
O(2)	O1.5c[1.5o1c]-	$MeCOO^-$
O(3)	O1c1h	MeOH
N(1)	N1c1h1h1h+	$MeNH_3^+$
C(1)	C1.5o1.5o1c	$MeCOO^-$
C(2)	C1n1c1c1h	Me_2CHNH_2
C(3)	C1o1c1h1h	$MeCH_2OH$
H(2)	H1c	CH_4
H(11)	H1n	NH_3
H(12)	H1n	NH_3
H(13)	H1n	NH_3
H(31)	H1c	CH_4
H(32)	H1c	CH_4
H(4)	H1o	H_2O

Figure 18. Molecular structure of D,L-serine and the model compounds used to calculate corresponding invariom.[182]

exact anisotropic displacement parameters[180] or as the starting point for further refinement[181]) in the molecule and to assess its properties. These can be the electrostatic potential, the dipole moment, topological parameters of bonds and integrated parameters of atoms within the framework of Bader's theory[167] that are traditionally determined in high-resolution X-ray diffraction studies. Using invarioms to determine these properties, there is no need to have high-resolution X-ray diffraction data; however, for reliable evaluation of anisotropic displacement parameters of atoms including temperature-dependent ones[123] it is recommended that $d < 1.0$ Å.[182]

The concept of invarioms[167] is basic to the invariom database which includes theoretical multipole parameters P_{val} and P_{lm} up to $l = 4$ and the corresponding expansion–contraction parameters κ and κ' for all atoms and all types of chemical environment (see Fig. 18) that occur in natural amino acids.[39] In addition to a more accurate molecular structure and anisotropic displacement parameters,[165] the invariom database makes it possible to obtain the ED distribution in protein and oligopeptide crystals within a reasonable period of time from conventional-resolution X-ray diffraction data only,[183] although in the case of proteins the requirements are somewhat more stringent ($d \leqslant 0.85$ Å).[184] The difference between the results obtained and those of multipole refinement of high-resolution data ($d > 0.4$ Å) was within the limits of experimental error.

As a logical continuation of these studies the invariom approach was used to evaluate the electrostatic properties of macromolecules (first of all, their dipole moments and peculiar features of the electrostatic potential distribution)[184,185] and their binding to small drug molecules.[186] It should be noted that, similarly to UBDB, the invariom database[178] provides reasonable agreement with the experimentally measured dipole moments (the results thus determined are better than those obtained from the unconstrained refinement of multipole parameters from X-ray diffraction data, which traditionally leads to overestimation[109]). However, the TAAM is not the best choice for higher-order moments.[187] The invariom database is less appropriate for evaluating the electrostatic interaction energy compared to the UBDB database, which was specially designed for this purpose.[119] Current research activity in this field[188] concerns the use of invarioms to develop transferable charges for fast calculations of electrostatic properties of biomacromolecules instead of force fields that require quantum chemical (even semiempirical) calculations, which is not always possible for large systems.

Main application fields of the UBDB database still include research into biomacromolecules and evaluation of electrostatic interaction energy.[189] The latter can be done rather accurately by combining the UBDB database and the EP/MM method. However, the focus of studies of the ED distribution using the invariom database rapidly shifted towards small organic molecules.[190] For instance, it was proposed[191] to use invarioms to determine the absolute configuration of chiral molecules containing only atoms of light elements (C, H, N, O) that are characterized by low intensity of anomalous scattering [see expression (3)] and to improve the accuracy of estimation of the Flack parameter,[192] a key criterion for correctness of the absolute configuration provided that the molecule contains atoms of heavier elements (*e.g.*, chlorine).[193] It should be noted that simultaneous unconstrained refinement of the multipole populations and Flack parameter is not recommended even using high-resolution X-ray diffraction data since it can lead to incorrect evaluation of phases in non-centrosymmetric space groups for which the absolute configuration is usually determined.[191]

The description of the ED distribution in crystals of small organic molecules and biomacromolecules using the invariom approach gave more accurate values of anisotropic displacement parameters[182,194–198] compared to the spherical atom model. The results obtained were comparable with those of multipole refinement of high-resolution X-ray diffraction data (Fig. 19). A similar situation was also observed in the case of isotropic displacement parameters of hydrogen atoms,[195] which are usually assumed to be 1.2- or 1.5-fold larger than those of the non-hydrogen atoms that the H atoms are 'riding' on within the framework of the 'riding model' used in X-ray crystallography.

Unlike the spherical atom model, the refinement of isotropic displacement parameters of hydrogen atoms using tabulated invarioms and the X–H distances taken from the results of quantum chemical calculations of model molecules led to satisfactory agreement with the results of

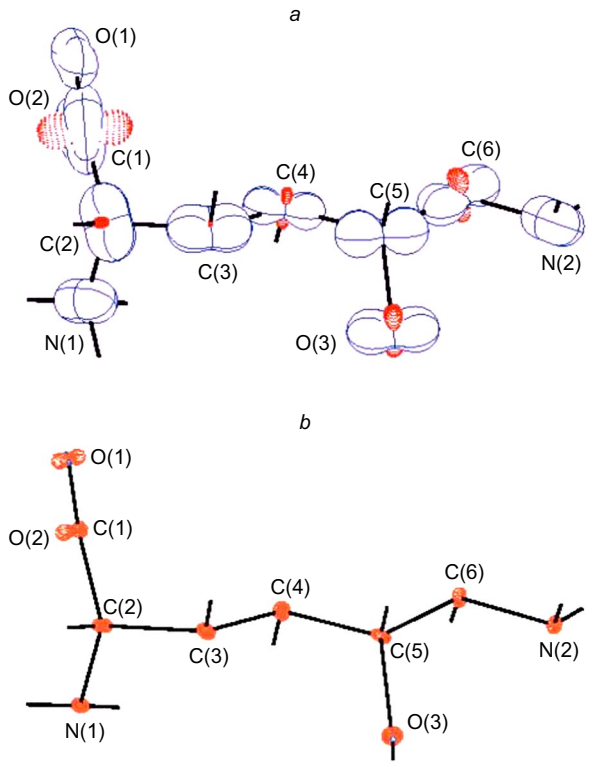


Figure 19. PEANUT representation [198] of the root-mean-square-displacement difference surfaces characterizing the difference between the atomic displacement parameters obtained using invarioms and the spherical atom model (*a*) and the multipole refinement (*b*).[182]

neutron diffraction studies of corresponding organic compounds.[195] Unfortunately, this approach is unsuitable for evaluation of anisotropic displacement parameters of hydrogen atoms [196] since it requires highly accurate measurements of reflection intensities at small angles θ, which can lead to overparameterization and unrealistic values of anisotropic displacement parameters of H atoms characterized by very low scattering power. However, normalization of these parameters to certain values taken from other sources (including the invariom database) [197] in the refinement of H-atom coordinates allows one to obtain the X–H bond lengths that agree well with neutron diffraction data.

Research activity in this field (see above) led to the development of a method for extracting information on the ED distribution and derived properties of organic crystals from normal-resolution X-ray diffraction data.[199] The method uses the ability of invarioms to accurately evaluate the molecular geometry and the atomic displacement parameters (by analogy with a classical study by Coppens, who took the atomic displacement parameters from neutron diffraction data).[3] The refinement of multipole populations using positional and anisotropic displacement parameters fixed to the values from the invariom refinement makes it possible to study the electrostatic potential distribution and to evaluate the atomic charges and volumes, the dipole moments of molecules, as well as the energies of hydrogen bonds [200, 201] and even weak intermolecular interactions [103, 202] using normal-resolution X-ray diffraction data sets collected at room temperature or using Cu K_α-radiation, which is unsuitable for high-resolution studies.

The accuracy of determination of the parameters described above appeared to be comparable with that of conventional multipole refinement of high-resolution X-ray diffraction data. In particular, the differences between the topological parameters of covalent bonds [ED and Laplacian values at corresponding (3, –1)BCPs] did not exceed the transferability indices of the same fragment between different molecules.[203] Moreover, high-resolution X-ray diffraction data can be distorted by errors that in some cases are hard to identify (due to, *e.g.*, low degree of twinning),[204] here, the invariom approach is more appropriate than conventional multipole refinement, which can lead to unrealistic ED distribution in the crystal.

Recent advances in the design of powerful sources of synchrotron radiation and new highly sensitive detectors of X-ray radiation that allow a large set of reflection intensities to be collected within a short period of time (a few minutes) and the invariom database including the multipole parameters for various chemical environments offer great prospects for screening of series of compounds.[205] Using the invariom database, one can obtain the electrostatic potential distribution for each member of the series or evaluate the dipole moment of its molecule in the crystal;[109] these parameters are of great importance for understanding the biological activity of pharmaceuticals.[206]

The difference between two ED distributions (so-called difference ED distribution) obtained from the results of multipole refinement of high-resolution X-ray diffraction data and using the invariom database reveals, *e.g.*, rotational disorder of hydrogen atoms or thermal-induced disorder influencing only H atoms (Fig. 20).[207] Both of them are difficult to disclose if no high-resolution data are available. This is a challenge for high-resolution X-ray diffraction studies since one can obtain unphysical ED distribution [208] owing to correlations with thermal motion of atoms. It should be noted that the invariom description of the disordered fragment does not require the refinement of additional parameters except those available in the spherical atom model and, correspondingly, measurement of a large set of reflection intensities in order to retain the necessary ratio between the number of reflections and the number of parameters.

A similar approach,[209] which is also based on the difference ED distribution, makes it possible to extract an approximate 'interaction density' from X-ray diffraction data. The case in hand is the difference between the real ED distribution in the crystal and the superposition of ED of noninteracting molecules that can be described using invarioms. Thus the 'interaction density' characterizes the influence of crystalline environment which, in particular, manifests itself as an increase in the dipole moment of a molecule in the crystal relative to the gas-phase value.[109] However, it should be noted that the multipole model *per se* does not reproduce peculiar features of the 'interaction density' in crystals.[137]

In spite of the advantages of the invariom database for analysis of various geometric parameters and properties of small molecules it was mainly used in the studies of organic compounds; the only exception was a study of alkali metal salts.[210] The next major step was to be the transition to, *e.g.*, 3d metal compounds playing an important role in biomacromolecules [165] and various materials. However, extension of the invariom database to these compounds is complicated by the fact that coordination bonds with metal ions do not

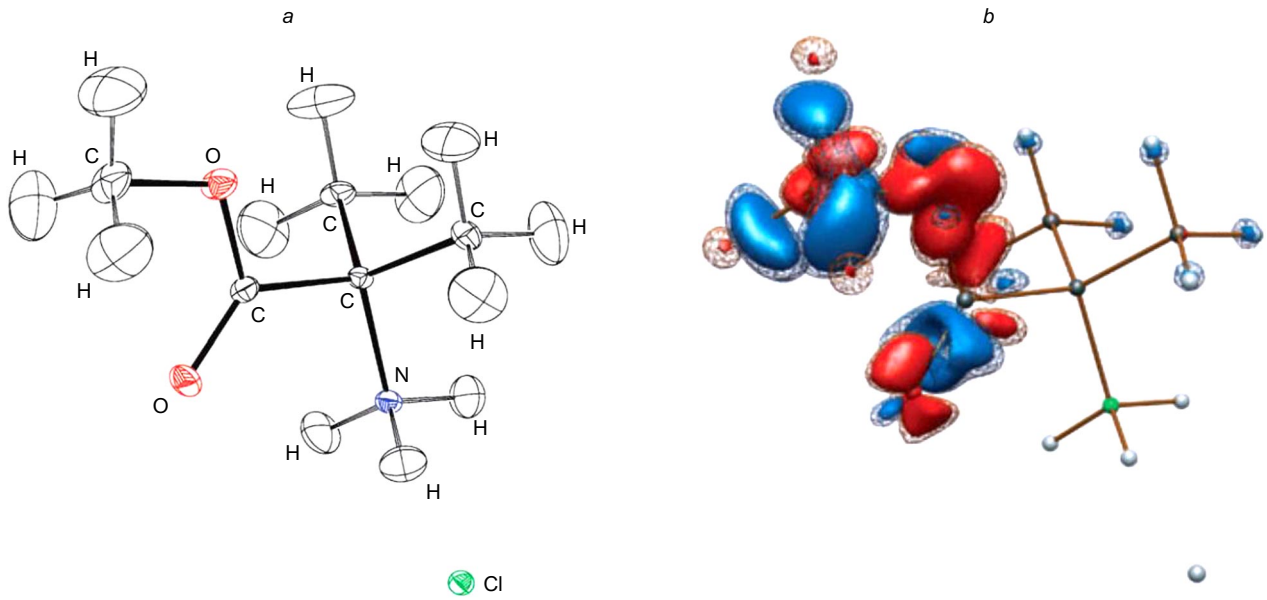


Figure 20. Methyl-2-aminoisobutyrate hydrochloride: an ORTEP representation of the molecule at 10 K (*a*) and the difference ED distribution in this molecule at 100 K (*b*) obtained by subtracting the invariom-refined ED distribution from the ED distribution obtained after multipole refinement of high-resolution X-ray diffraction data.[207]

meet the transferability requirements for local atomic geometry.[190] This led to essential modification of the invariom concept.[211] The new, generalized invariom database was used to obtain a more accurate molecular geometry;[190] however, the multipole parameters were eventually refined from theoretical structure factors calculated for the entire molecule without geometry optimization.

The full-molecular version is not versatile since it is not based on the use of databases; however, it retains certain advantages of the TAAM. It also implies refinement of positional and displacement parameters of atoms in the molecule under study using the available X-ray diffraction data at fixed multipole populations taken from the results of quantum chemical calculations of molecular structure factors. Application of the full-molecular version made it possible to determine the nature of 3d metals (this is not always possible in X-ray crystallography[211]) and even to evaluate the populations of metal ion 3d orbitals in complexes[212] from normal-resolution X-ray diffraction data.

It was found that the description of only organic fragments of coordination compounds using the invariom approach is sufficient to analyze the properties of sophisticated systems like metal-organic frameworks.[40] The electrostatic potential distribution thus obtained can throw light on certain peculiar features of the bonding of metal-organic frameworks to guest molecules (Fig. 21). In this connection mention should be made of a conceptually close but little known 'electron density building block' (BB) approach[18] which treats the ED of the entire metal-organic framework as superposition of the EDs of isolated metal ions (connectors) and organic linkers taking into account aspherical ED distribution in the latter. The BB database includes the

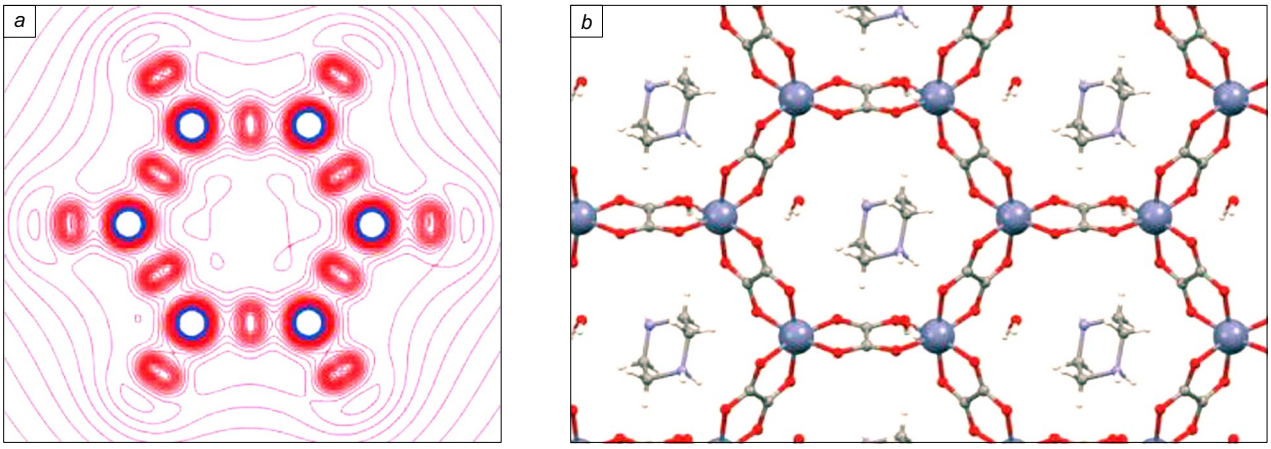


Figure 21. Electrostatic potential distribution in the metal-organic framework (*a*) obtained using the electron density building block approach[18] and the binding site for piperazine guest molecules (*b*).

results of the multipole refinement of theoretical structure factors for the organic molecules used to assemble metal-organic frameworks and spherically symmetric 3d metal ions. Although simplified, this approach enables a rather accurate evaluation of not only the electrostatic potential distribution in the system, but also the energy of the interaction with guest molecules using an original technique [18] and establishment of the most probable binding sites (Fig. 21).

Unlike the ELMAM and ELMAM2 databases of experimental multipole parameters, the invariom and UBDB databases ignore the influence of crystalline environment. Nevertheless, they correctly reproduce the geometry and anisotropic displacement parameters in small-molecule crystals and biomacromolecules as well as the ED distribution and derived properties, *viz.*, the electrostatic potential, the dipole moment, the topological parameters of chemical bonds and the integral parameters of atoms within the framework of Bader's theory. Besides, the UBDB database gives the most accurate estimates of electrostatic interaction energy.[119] Owing to ready availability of quantum chemical calculations of small molecules used for provisioning of theoretical databases, they offer greater prospects for studies of the ED distribution and derived properties (from reactivity to nonlinear optical, magnetic, transport, *etc.*) of not only individual compounds, but also classes of compounds that are regarded as inappropriate for high-resolution X-ray diffraction studies even taking account of recent methodological advances.

They also allow one to carry out systematic studies using series of related compounds [35] to search for general regularities and to construct prognostic models within reasonable periods of time in contrast to quantum chemical calculations of crystals or simply large systems. For instance, the invariom database was used to plot the electrostatic potential distribution on the van der Waals surfaces of nine fluoroquinolone antibiotic molecules [213] using only X-ray diffraction data obtained from routine experiments. This suggested that similarity of the electrostatic potential distributions and molecular dimensions underlie the biological activity of the compounds under study. The UBDB database was used to improve the accuracy of determination of geometric parameters (especially for hydrogen atoms) in crystals of ten uracil derivatives.[214] The cohesive energies and the inter-layer bonding energies calculated using the TAAM atomic coordinates behave better than those computed using conventional spherical atom model when compared with the cohesive energies determined using the optimized geometries. In addition, the ED distribution obtained as side product allowed one to classify weak F···F interaction detected in the crystal of fluorinated uracil derivative as halogen bond [215] that contributes largely to stabilization of the crystal packing.

However, it should be noted that the results described above were attained either using quantum chemical methods (for uracil derivatives) or these methods can be used instead of refinement of positional and displacement parameters of atoms from X-ray diffraction data at fixed values of theoretical multipole parameters (for fluoroquinolones). However, these studies are scarce [35] in spite of almost unlimited opportunities to study the ED distribution in crystals of related compounds provided by the corresponding databases (especially, the invariom database since invarioms can be calculated for an atom in any chemical environment).

In the future one can expect an increase in the number of such studies using databases of multipole parameters since these databases are convenient tools for solving particular problems in materials science.[20] For instance, a systematic analysis of the ED distribution in crystals of a wide range of 1-alkyl-3-methylimidazolium salts was carried out for the first time only recently using the invariom database.[216] These compounds are practically important ionic liquids that were traditionally treated as inaccessible to electron density studies. The results obtained allowed one to formulate a simple approach to the explanation for and prediction of the melting points of 1-alkyl-3-methylimidazolium salts, their stability and the possibility to form a liquid-crystalline phase.[41]

A distinct advantage of the invariom database used in the charge density studies is user-friendly software and first of all the MoleCoolQT program.[217] Its features include automated selection of necessary invarioms and generation of input files for further refinement using the XD program that is traditionally used in high-resolution X-ray diffraction studies. The invariom database was incorporated into the APEX3 software [218] for Bruker diffractometers and crystal structure solution and refinement. Practical application of the UBDB database of multipole parameters is somewhat complicated since the input files [§] for further refinement are generated using commands given in the command-line mode.

7. Calculations of anisotropic displacement parameters of atoms

Obtaining reliable information on the properties of compounds from experimental ED distribution 'separated' from thermal motion of atoms in the crystal is closely related to accurate evaluation of anisotropic atomic displacement parameters.[84] For non-hydrogen atoms, they can be determined with sufficient accuracy from the multipole refinement of high-resolution X-ray diffraction data, which is often complicated by anharmonicity or diffuse scattering,[9] or using the UBDB and invariom databases (see above). However, location of hydrogen atoms and refinement of their displacement parameters still remains the central problem in X-ray crystallography. Even in high-resolution studies positions of H atoms are specified by normalizing the X–H bond lengths to the standard values obtained from gas-phase neutron diffraction studies,[81] while anisotropic displacement parameters are usually evaluated by the SHADE method [219] (the most recent version of SHADE is implemented in the SHADE3 program.[85]

Within the framework of this approach, the motion of atoms in the crystal is described by the sum of two independent contributions corresponding to atomic vibrations in the molecule (U_{ij}^{int}) and to the motion of the entire molecule (U_{ij}^{ext}) in the mean field produced by other molecules

$$U_{ij} = U_{ij}^{\text{int}} + U_{ij}^{\text{ext}} \quad (25)$$

§ See http://harker.chem.buffalo.edu/group/databank.htm, last accessed on January 15, 2019.

where U_{ij} are the components of the tensor U that describes anisotropic thermal vibrations.

In molecular crystals, atoms form strong intramolecular bonds, while intermolecular interactions are much weaker; this allows one to divide atomic vibrations into high-frequency 'internal' vibrations caused by, *e.g.*, deformation of chemical bonds and low-frequency 'external' vibrations induced by correlated motion of molecules and simultaneously involving more than one unit cell. Since X-ray diffraction studies are traditionally carried out at 100 K and higher temperatures, it is just 'external' vibrations that make the major contribution to anisotropic displacement parameters. Unfortunately, they are difficult to measure by spectroscopic methods. However, for lighter hydrogen atoms one should also take into account 'internal' vibrations that are almost temperature independent.

In the SHADE method the contribution of 'internal' vibrations to anisotropic displacement parameters of hydrogen atoms is evaluated using a database that includes the root-mean-square amplitudes of atomic displacements in various functional groups (*e.g.*, in methyl or hydroxyl groups) determined for a wide range of organic compounds by neutron diffraction [219]

$$U_{ij}^{\text{int}} = \sum_k \langle u^2 \rangle_k \mathbf{e}_k \, \mathbf{e}_k^{\text{T}} \tag{26}$$

where $\langle u^2 \rangle$ are the root-mean-square amplitudes of atomic displacements along the direction specified by the unit vector $\mathbf{e}_k$ in the orthogonal frame of reference.

Evaluation of the second term in expression (25) is based on analysis of anisotropic displacement parameters U_{ij} of non-hydrogen atoms using the Schomaker – Trueblood rigid body model [220] implemented in the THMA11 program.¶ This model treats thermal motion of atoms in the crystal as combination of several types of motion of the entire molecule

$$U = TLS \tag{27}$$

where U is the tensor describing anisotropic thermal vibrations of atoms and T, L and S are the tensors describing atomic translational motion, atomic librations and atomic screw motion, respectively. Expressions for these tensors can be found in, *e.g.*, Ref. 222. However, only a few molecules can be considered as 'rigid'. In this case, the problem can be solved using the segmented rigid body model, according to which a molecule is represented by a set of rigid fragments that rotate relative to one another. Expression (27) is augmented with the corresponding tensor. Components of each tensor are determined by the least-squares fitting of anisotropic displacement parameters, U_{ij}, of non-hydrogen atoms to the X-ray diffraction data.

In the quantum mechanical harmonic oscillator approximation [223] the root-mean-square amplitudes of atomic displacements $\langle u^2 \rangle$ can be used to calculate the corresponding vibrational frequencies of the entire molecule [224]

$$\langle u^2 \rangle = \frac{h}{8\pi^2 \mu \nu} \coth \frac{h\nu}{2k_{\text{B}}T} \tag{28}$$

Here μ is the reduced mass of the harmonic oscillator and ν is the oscillation frequency. Taking into account the fact that the oscillation frequency and the atomic displacement amplitude are inversely related, the contribution of low-frequency 'external' vibrations to anisotropic atomic displacement parameters will dominate with increasing temperature. These frequencies can be used to evaluate the vibrational entropy of the crystal [177] provided that high-resolution X-ray diffraction data are available:

$$S_{TLS}(T) = R \sum_i \left\{ \frac{h\nu_i}{k_{\text{B}}T} \left[\exp\left(\frac{h\nu_i}{k_{\text{B}}T} \right) - 1 \right]^{-1} - \right. \tag{29}$$

$$\left. - \ln \left[1 - \exp\left(-\frac{h\nu_i}{k_{\text{B}}T} \right) \right] \right\}$$

where ν_i is the frequency of the ith harmonic oscillator.

Unfortunately, most molecules (especially, conformationally flexible molecules containing atoms of third- and later-period elements) execute low-frequency, large-amplitude anharmonic vibrations. In this case it is impossible to calculate the S tensor (or its trace, see Ref. 222) even if the T and L tensors are known. The trace of the matrix S can be calculated from X-ray diffraction data using an approach [225, 226] which allows one to determine the temperature-dependent and temperature independent contributions, the frequencies of the corresponding 'external' low-frequency and 'internal' high-frequency vibrations and even to evaluate the thermodynamic parameters of the crystal, *e.g.*, the specific heat at constant volume,[227] from changes in the multiple-temperature anisotropic atomic displacement parameters. A drawback of this approach consists in the need to carry out multiple-temperature X-ray diffraction studies.

An alternative route is to use quantum chemically calculated anisotropic displacement parameters since they also give information on correlated motion of atoms in the crystal; at low temperatures, this motion can be treated as harmonic. The potential energy of a harmonic oscillator is proportional to its displacement from the equilibrium position

$$E = E_0 + \frac{1}{2} \sum_{ij} f_{ij} \mathbf{r}_{ij} \tag{30}$$

where E_0 is the vibrational energy at the equilibrium point (zero-point vibrational energy) and f_{ij} and $\mathbf{r}_{ij}$ are the force constants and corresponding coordinates, respectively. The force constants are obtained by differentiating energy with respect to atomic displacements. This procedure underlies all conventional algorithms for vibrational frequency calculations.

The atomic displacement parameters for organic molecules were for the first time obtained [228] from the molecular mechanics calculations. At present, this can be done using hybrid approaches that combine molecular mechanics with *ab initio* quantum chemical calculations.[197, 229] Examples are provided by the ONIOM method † where the central molecule in the cluster is described within the framework of the DFT while the surrounding molecules are described by a

¶ Abbreviation for 'thermal motion analysis', a program for analyzing anisotropic displacement parameters of atoms.[221]

† Abbreviation for 'our *N*-layered integrated molecular orbital and molecular mechanics'.[230]

force field [230] and by the methods based on the DFT calculations with periodic boundary conditions [231–237] that directly take into account the influence of crystal packing. This is a default feature of the CRYSTAL09 program [143] and its more recent versions [*e.g.*, CRYSTAL14 (Ref. 238)] that use Gaussian basis sets. As to software for plane-wave quantum chemical calculations of crystals, this possibility is implemented in, *e.g.*, the PHONOPY program.‡ In particular, the anisotropic atomic displacement parameters for crystals of organic compounds of different 'rigidity' (urea, urotropin, L-alanine and benzene) were obtained [237] from normal vibrational frequencies calculated using the CRYSTAL09 program and different functional/basis set combinations.

In classical physics the energy of normal vibrational mode is function of the wave vector **q**

$$E_j(\mathbf{q}) = h\omega_j(\mathbf{q})\left[\frac{1}{2} + \left(\exp\frac{h\omega_j(\mathbf{q})}{k_B T} - 1\right)^{-1}\right] \quad (31)$$

where $\omega_j(\mathbf{q})$ is the normal mode frequency. The matrix of root-mean-square displacements of the kth atom in the crystal composed of N unit cells containing n atoms each is given by the sum of contributions from all $3nN$ normal vibrational modes

$$B_{\text{atom}}(k) = \frac{1}{Nm_k}\sum_{i\mathbf{q}}\frac{E_j(\mathbf{q})}{\omega_j^2(\mathbf{q})}\mathbf{e}(k|i\,\mathbf{q})\left[\mathbf{e}^*(k|j\,\mathbf{q})\right]^{\mathrm{T}} \quad (32)$$

where m_k is the mass of the kth atom and $\mathbf{e}*(k|j\,\mathbf{q})$ is the unit vector corresponding to the kth component of the eigenvector $\mathbf{e}(j\mathbf{q})$ and normal mode j along the wave vector **q**. In the coordinate system of the unit cell the $B_{\text{atom}}(k)$ matrix corresponds to the tensor U describing anisotropic thermal vibrations of atoms in routine X-ray diffraction experiments. Since 'external' vibrations in molecular crystals (generally, so-called phonon spectrum) are anisotropic (phonon dispersion), quantum chemical calculations should be carried out for a set of ***q***-points of the reciprocal space to properly describe the first Brillouin zone. The ***q***-point set depends on the space group of the crystal. In addition, the authors of Ref. 237 used the supercell approach where the supercell included several unit cells; this allows one to carry out calculations at the corresponding number of ***q***-points.

The anisotropic atomic displacement parameters obtained from calculations with optimization of atomic coordinates at fixed unit cell parameters [237] were in reasonable agreement with the results of neutron diffraction studies even at $T \leqslant 150$ K. Irrespective of the functional and basis set used [the B3LYP/6-31G(d,p) combination was optimum from the standpoint of accuracy and computational cost] [237] the contributions of 'internal' vibrations were consistent with experimental data. Agreement for the contributions of 'external' vibrations was much worse due to anharmonicity [240] and known drawbacks of the present-day exchange-correlation functionals in the description of weak intermolecular interactions. An attempt to change the situation by applying an empirical correction failed.[237]

‡ Abbreviation for combination 'phonon and Python' — a program for calculating phonon spectra of crystals and related physicochemical properties written in Python programming language.[239]

As a result, hybrid approaches are widely used at present. The contributions of 'internal' vibrations are obtained from quantum chemical calculations of crystals,[85, 241, 242] molecular cluster [243] (to take account of the crystal field effect) or even isolated molecules from the invariom database.[244] The contributions of 'external' vibrations are determined from the TLS-refinement of X-ray diffraction data containing information on lattice vibrations. Separation of the two types of vibrations is based on the recommendations,[223] according to which for 'rigid' crystals containing Z independent molecules in the unit cell, a total of $6 \times Z$ lowest-frequency vibrations (usually, their frequencies are lower than 200 cm^{-1}) correspond to vibrations of the entire molecules, *viz.*, three translational vibrations and three rotations about the centre of mass. It is this approach that is implemented in the SHADE3 (Ref. 85) and APD-Toolkit (Ref. 244) programs to evaluate anisotropic displacement parameters of hydrogen atoms from X-ray diffraction data and quantum chemical calculations of crystals or isolated model molecules from the invariom database. Using the vibrational frequencies thus obtained, conventional-resolution X-ray diffraction data and the databases of multipole parameters,[241] one can determine the vibrational entropy of the crystal,[177] which is necessary, *e.g.*, to analyze the thermodynamic stability of polymorphs.[242]

An obvious disadvantage of the hybrid approaches for estimation of anisotropic atomic displacement parameters and thermodynamic properties of crystals is the separation of vibrations into 'internal' high-frequency and 'external' low-frequency ones. However, except a few true 'rigid' molecules (*e.g.*, benzene), vibrations in crystals are coupled and therefore it is impossible to unambiguously select vibrations necessary for quantum chemical calculations of crystals and those needed for TLS-fit of X-ray diffraction data.

The authors of the normal mode refinement (NoMoRe) method [245] implemented in the same-name program rejected the separation but retained referencing against experimental data. The method is based on the refinement of the normal mode frequencies ω_j obtained from DFT calculations of crystals from the available X-ray diffraction or neutron diffraction [245] data. It was proposed to carry out single-point calculations at the Γ point of the Brillouin zone in order to significantly decrease the computing time and to enable calculations of crystals with large unit cells. In this case, the matrix of root-mean-square atomic displacements is given by

$$B_{\text{atom}}(k) = \frac{1}{Nm_k}\sum_{j}\frac{E_j}{\omega_j^2}\mathbf{e}(k|j)\left[\mathbf{e}^*(k|j)\right]^{\mathrm{T}} \quad (33)$$

where

$$E_j = h\omega_j\left[\frac{1}{2} + \left(\exp\frac{h\omega_j}{k_B T} - 1\right)^{-1}\right] \quad (34)$$

At the Γ point, the calculated vibrational frequencies corresponding to translational motion of molecules in the crystal are equal to zero. Prior to refinement they were assigned an initial value of 50 cm^{-1}, which is close to the frequencies in real (*e.g.*, naphthalene) crystals.[246, 247]

Similarly to routine X-ray diffraction studies, the refined parameters include atomic coordinates and possibly,

atomic site occupancies for disordered fragments or, *e.g.*, the extinction coefficient. However, refinement of anisotropic displacement parameters is replaced by the least-squares refinement of the scale factors for a certain set of frequencies ω_j to minimize the weighted *R*-factor, wR_2. The scale factors can be refined for all possible normal vibrations, but usually, it is sufficient to include only a relatively small number of vibrations that make the major contribution to anisotropic displacement parameters. These are vibrations with frequencies lower than 150 cm^{-1} (Refs 246 and 247); however, the addition of certain higher-frequency vibrations with frequencies of up to 500 cm^{-1} improves agreement with the experiment. These vibrations are chosen based on the contribution of each vibration to the anisotropic atomic displacement parameters rather than subjective opinion of a researcher.[245] In addition, refinement of the overall scale factor for other vibrations in this frequency range significantly decreases the number of refined parameters compared to the number of measured reflections. It should be noted that fixed values of the normal mode coordinates $\mathbf{e}(k|j)$ in expression (33) can introduce systematic errors observed in the ED distribution near atomic positions;[245, 248] however, the influence of diffuse scattering should also not be excluded.[9]

This method for normal mode refinement was tested for urea,[245] naphthalene, L-alanine and xylitol.[248] The inclusion of the anisotropic atomic displacement parameters thus determined in subsequent refinement of the model from X-ray diffraction data (including high-resolution data) in all cases led to larger *R*-factor values; however, the results of neutron diffraction studies were reproduced with reasonable accuracy. In particular, agreement with experimental data attained for hydrogen atoms was even better than after quantum chemical calculations for the entire first Brillouin zone,[237] SHADE3 computations [85] or ONIOM calculations with TLS-fit (ONIOM + TLS).[243] The normal vibrational frequencies refined against X-ray diffraction data can also be used to determine thermodynamic properties of crystals. For instance, the heat capacity at constant pressure [248] calculated for naphthalene for the temperature range 0 – 250 K differs from the results of thermochemical measurements by less than 0.5 kcal $(mol\ K)^{-1}$, as in the case of analysis of multi-temperature data (see above).[227]

Among the methods for calculations of anisotropic atomic displacement parameters and thermochemical properties of crystals described above, the NoMoRe approach seems to be the most promising. It includes the contributions of all possible vibrations irrespective of their nature ('external' or 'internal') in explicit form and partially eliminates the drawbacks of the DFT in the description of weak intermolecular interactions owing to refinement of low-frequency vibrations against X-ray diffraction data. However, quantum chemical calculations of crystals make the method time-consuming and the computational cost of the technique can further increase if quantum chemical calculations for the entire Brillouin zone are needed. The current version of the NoMoRe method is inapplicable to disordered systems, being, however, suitable for studies of multicomponent crystals in contrast to TLS-analysis or analysis of multi-temperature anisotropic displacement parameters.[225]

Nevertheless, the possibility to calculate anisotropic displacement parameters, especially for hydrogen atoms, is of great importance for high-resolution charge-density studies. In particular, this gave an impetus to the development of methods based on the density functional calculations of molecular crystals.[237, 245] Unfortunately, these methods are labourious and thus of limited use. The ONIOM calculations of a molecular cluster [229] are characterized by lower computational cost and shorter computing time; however, the influence of crystal packing is included by introducing a scale factor, which leads to systematic errors (however, these errors are rather small at very low temperatures of 10 – 20 K).

Besides, the inclusion of calculated anisotropic atomic displacement parameters [229, 237, 245, 248] (except those of hydrogen atoms) [85] in the refinement of X-ray diffraction data (by analogy with the databases of multipole parameters described above) still did not lead to improvement of the ED model even when compared to routine X-ray diffraction data.

8. The Hirshfeld atom refinement

To solve this problem, an approach termed the Hirshfeld atom refinement (HAR) [§] was proposed.[249] It allows one to determine coordinates and anisotropic displacement parameters of all atoms including H atoms [250] in routine X-ray diffraction experiment with an accuracy comparable with that of neutron diffraction studies.[251] The approach is based on partitioning the space of the molecule into atomic regions called the stockholder partitioning procedure.[252] This is a logical development of the ideas of Politzer and Harris,[253] who treated the molecule as superposition of noninteracting atoms (promolecule model [91] or the independent atom model in X-ray crystallography) and assigned each atom to a spatial region whose charge is the same as the charge of the free atom. The main drawback of such a partition scheme is the use of hypothetical planes separating atoms from one another, which makes it applicable to linear molecules only.[254] Hirshfeld assumed [252] that 'like partners in a stockholders' corporation, each atom thus partakes of the local gain or loss in direct proportion to its share in the capital investment'. Mathematically, this means that the contribution of an atom to the observed ED distribution in the molecule at any point (ρ^{mol}) is proportional to its contribution to the ED distribution in the promolecule (ρ^{pro}) at the same point

$$\rho_i(\mathbf{r}) = w_i(\mathbf{r})\rho^{mol}(\mathbf{r}) \tag{35}$$

where the weighting function $w_i(\mathbf{r})$, which takes values in the interval from 0 to 1 (for isolated atom), characterizes the relative contribution of the *i*th atom at the point **r**

$$w_i(\mathbf{r}) = \frac{\rho_i^0(\mathbf{r})}{\rho^{pro}(\mathbf{r})} \tag{36}$$

The electron density of the promolecule is the superposition of EDs of noninteracting spherically symmetric atoms in the ground state (ρ_i^0), placed in the same positions as in the real molecule,

§ Strictly speaking, this is 'structure refinement based on the Hirshfeld atom model'. For brevity, from this point on we will use the three-word term indicated in the title of Section 8.

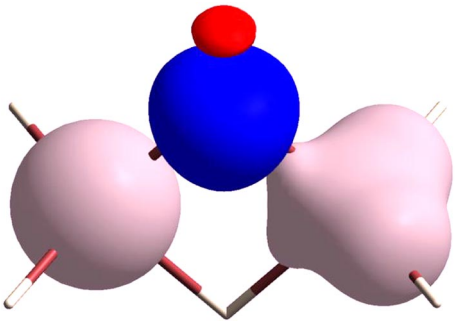


Figure 22. Electron density isosurfaces (ρ = 0.08 e Å^{-3}) of boron in diborane B_2H_6 calculated using the independent atom model (left) and obtained after Hirshfeld atom refinement (right).[250]

$$\rho^{\text{pro}}(\mathbf{r}) = \sum_i \rho_i^0(\mathbf{r}) \tag{37}$$

Using the stockholder scheme (or Hirshfeld partition), for any experimental or theoretical ED distribution in arbitrary complex molecules one can unambiguously select overlapping atomic domains ρ_i called Hirshfeld atoms[249] characterizing the asphericity of atoms (Fig. 22) due to the formation of chemical bonds. It is possible to evaluate the charge, multipole moments, the electrostatic potential and the intermolecular interaction energy for each Hirshfeld atom.[252]

The stockholder scheme also underlies an analysis of Hirshfeld surfaces (not to be confused with Hirshfeld atoms!) implemented in the CrystalExplorer program.[255] This is a convenient tool for 'visualization' of intermolecular interactions using X-ray diffraction data. Within the framework of this approach a molecule in a crystal is confined by a surface such that in the enclosed region the molecule contribution to the ED distribution of the crystal exceeds that of the crystalline environment,[256] *i.e.*, $w_i(\mathbf{r}) \geqslant 0.5$. The weighting function $w_i(\mathbf{r})$ is the ratio of the ED of the promolecule formed by noninteracting spherically symmetric atoms [see expression (36)] to the superposition of atomic EDs for the entire crystal (procrystal)

$$w_i(\mathbf{r}) = \frac{\rho_{\text{promol}}(\mathbf{r})}{\rho_{\text{procryst}}(\mathbf{r})} = \frac{\sum\limits_{i\in\text{mol}} \rho_i^0(r)}{\sum\limits_{i\in\text{cryst}} \rho_i^0(r)} \tag{38}$$

The Hirshfeld surface thus defined characterizes not only the molecular geometry,[257] but also the intermolecular interactions the molecule is involved in owing to 'mapping' of various parameters on this surface (first of all, distances to the nearest atom inside and outside the molecule). Interestingly, the notion of atomic Hirshfeld surface was introduced more recently[258] to analyze non-molecular crystals (*e.g.*, minerals[259]). As an example, Fig. 23 presents the atomic Hirshfeld surfaces for lead atom.[260]

In the method proposed much more recently[249] the Hirshfeld atoms [$\rho_i(\mathbf{r})$ in expression (35)] are used to calculate the aspherical atomic scattering factors that are included in the refinement of positional and anisotropic atomic displacement parameters against the available X-ray diffraction data (that is why 'the Hirshfeld atom refinement'). The corresponding molecular distribution $\rho^{\text{mol}}(\mathbf{r})$ is

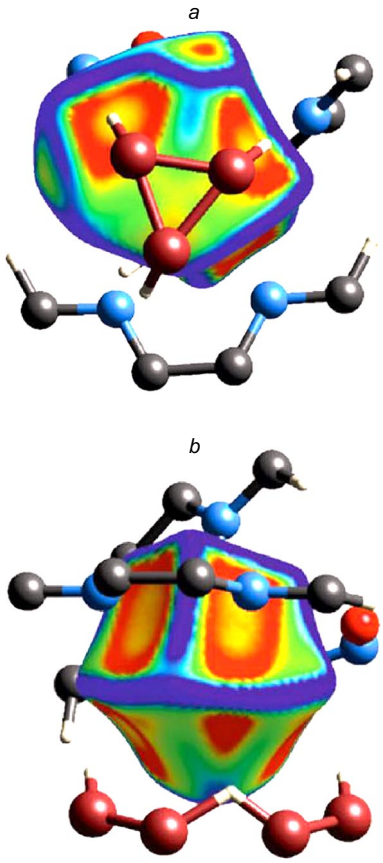


Figure 23. Hirshfeld atomic surface of lead in complexes with $[B_{20}H_{18}]^{2-}$ (*a*) and 2,2′-bipyridine (*b*).[260]

determined from quantum chemical calculations of a molecule whose geometry matches its geometry in the crystal using, *e.g.*, the atomic coordinates obtained in routine X-ray diffraction experiment using the spherical atom model as the initial approximation.

Within the framework of this approach the ED distribution in the unit cell of a crystal is treated as the sum of Hirshfeld atoms. They can be combined with the probability density function to locate the atom at a certain point by deconvolution (*), which gives the expression for the 'thermally smeared' Hirshfeld atom

$$\langle \rho_i \rangle = \rho_i^* P \tag{39}$$

The Fourier transforms of these functions $\langle f_i \rangle$ represent 'thermally smeared' aspherical atomic scattering factors that are used to obtain the structure factors [see expression (3)]. The structure factors (F_i^{C}) are calculated as products of the scale factor s and the function $X_i(\xi,|F_i|)$, which includes the influence of extinction and depends on the empirical parameter ξ,

$$F_i^{\text{C}} = sX_i(\xi, |F_i|)|F_i| \tag{40}$$

where the structure factor F_i is related to the 'thermally smeared' ED distribution of the unit cell $<\rho_{\text{cell}}>$ through the Fourier transform [see expression (4)]. Since 'thermally smeared' atomic scattering factors $<f_i>$ only depend on the atomic coordinates and atomic displacement parame-

ters, the corresponding ED distribution in the unit cell can be expressed through these quantities taking into account the scale factor and extinction correction.

If the atomic coordinates change only slightly upon subsequent refinement against X-ray diffraction data, it is assumed that the functions $\rho_i(\mathbf{r})$ remain almost unchanged and therefore it is sufficient to calculate the Hirshfeld atoms once for the starting geometry. This is the 'rigid' Hirshfeld atom model used in the initial version of this approach.[249] More recently, an iterative procedure was proposed, which involves successive cycles of quantum chemical calculations of the molecule under study, calculations of the scattering factors for the Hirshfeld atoms in the molecule and the least-squares refinement of their positional and anisotropic displacement parameters.[251] The minimizing parameter is the difference χ^2, which depends on the theoretical structure factors calculated using the Hirshfeld atom model (F_i^{C}) and on the experimental structure factors (F_i^{exp}) taking into account their standard deviations (σ), the number of reflections (N_{r}) and the number of refined parameters (N_{p})

$$\chi^2 = \frac{1}{N_{\mathrm{r}} - N_{\mathrm{p}}} \sum_i \frac{(F_i^{\mathrm{C}} - F_i^{\mathrm{exp}})}{\sigma_i^2} \qquad (41)$$

At present, this type of Hirshfeld atom refinement is implemented only in the TONTO program,¶ which is available as either original software or part of the OLEX2 program package.[262] Although the 'fitting' of atomic coordinates and anisotropic atomic displacement parameters takes the same time as routine structure refinement, quantum chemical calculations of the molecule and atomic scattering factors for Hirshfeld atoms are labour-consuming; therefore, Hirshfeld atom refinement is now available only for small organic and inorganic molecules.[250] The TONTO program¶ allows one to carry out these calculations in different approximations;[261] however, Hirshfeld atom refinement is at present performed only using the Hartree–Fock method and a few most widely used DFT functionals.[249] There is a wide range of available basis sets (at least for atoms of Period 1–3 elements). For organic compounds it is recommended to use the BLYP functional and the cc-pVTZ basis set[251] because calculations with larger basis sets (*e.g.*, cc-pVQZ) do not significantly improve the results.[251] Since quantum chemical calculations of molecules are carried out in the Cartesian coordinate system rather than fractional coordinates as in X-ray crystallography, the positional and atomic displacement parameters are refined in the same system which excludes the influence of errors in determination of the unit cell parameters.[251]

A significant drawback of Hirshfeld atom refinement associated with quantum chemical calculations of the molecular ED is not the best method for taking account of the crystal field effect[251] implemented in the TONTO program. To this end, the molecule is surrounded by a cluster of point charges equal to the charges of corresponding Hirshfeld atoms and atomic dipoles placed at positions occupied by atoms of the neighbouring molecules in the crystal. The cluster size is a user-defined parameter, although there is a trend towards increasing the cluster radius from 5 Å in the earlier studies[249] to 15 Å in more recent ones.[137] This procedure is iterative and follows the ED calculations for the molecule in each cycle of the refinement. Usually, the charges of Hirshfeld atoms are somewhat smaller than those obtained using other ED partitioning schemes.[263] Nevertheless, the quality of the structure model is significantly improved,[264] especially if strong intermolecular interactions occur in the crystal.[137,249] To obtain the best results, it is recommended to carry out quantum chemical calculations of molecules in the cluster approximation using the BLYP functional that includes the electron correlation effects.[249]

Molecular nature of the ED distribution used in calculations of aspherical atomic scattering factors based on the Hirshfeld partitioning makes the Hirshfeld atom refinement for crystals with more than one independent molecule in the unit cell not a trivial task. At present, the only way to solve this problem is to calculate a molecular cluster rather than a single molecule (generally, to calculate the unique part of the unit cell[265] of even the entire crystal[266]) surrounded by point charges. Of course, this is accompanied by proportional increase in the computational cost which can be to some extent reduced by using a smaller basis set, *e.g.*, def2-SVP, as implemented in the OLEX2 program package,[267] without significant loss of quality for compounds where no strong intermolecular interactions occur. Unfortunately, the problem of description of disorder frequently occurring in molecular crystals is still to be solved.

In spite of these drawbacks, the Hirshfeld atom refinement proved itself as the approach for accurate determination of atomic coordinates and anisotropic displacement parameters for Period 1–4 elements[250] (anharmonic description of thermal motion of these atoms will be available in the nearest future[267]) from X-ray diffraction data collected in routine experiments[267] similarly to the independent atom model. The ED distribution obtained as 'side product' is in essence equivalent to the static ED determined from the multipole refinement; however, it can be described using functions similar to the basis set ones. Consequently, this distribution appears to be potentially more convenient for subsequent analysis using the AIMALL software package.† However, unlike the multipole refinement of high-resolution X-ray diffraction data, the Hirshfeld atom refinement eliminates the drawbacks of X-ray diffraction technique due to the nature of X-rays scattered by electrons rather than atomic nuclei. This leads to a well-known problem of underestimation of the length of bonds involving hydrogen atoms and incorrect evaluation of corresponding H-atom displacement parameters (correct description of these parameters is necessary to determine and predict the properties of compounds).[81,84,109]

If Hirshfeld atom refinement is performed using theoretical aspherical atomic scattering factors for a particular molecule rather than databases of multipole parameters, the X–H bond lengths in organic compounds characterized by both weak intermolecular interaction (*e.g.*, benzene)[249] and strong hydrogen bonds (*e.g.*, L-phenylalaninium hydrogen

¶ TONTO is a powerful computational chemistry package for quantum chemical calculations of the wave functions and various physical properties of crystals.[261]

† A software package for topological analysis of analytical ED distribution function.[268]

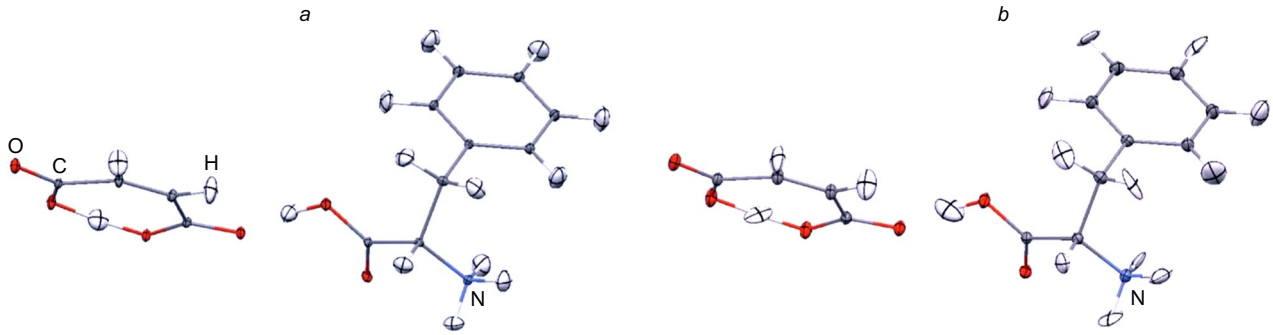


Figure 24. Structure of L-phenylalaninium hydrogen maleate molecule obtained after multipole refinement using the atomic displacement parameters of H evaluated by the SHADE (*a*) and after Hirshfeld atom refinement (*b*).[265]

maleate)[265] almost match the X–H bond lengths from neutron diffraction data. Quantum chemical calculations of molecules surrounded by point charges using the recommended computational method and basis set (BLYP/cc-pVTZ) can lead to differences smaller than 0.01 Å.[251] The lengths of the bonds involving bridging hydrogen atoms or H atoms located near metal ions can be evaluated analogously,[250] although the Hirshfeld atom refinement for transition metal complexes and heavy-element compounds is not recommended (in the latter case, due to relativistic effects).[267]

The accuracy in determination of anisotropic H-atom displacement parameters upon Hirshfeld atom refinement is often comparable with the accuracy in their determination by neutron diffraction [*e.g.*, within 0.006 Å^2 (Ref. 251)]. In some cases anisotropic H-atom displacement parameters were determined from X-ray diffraction data collected using Cu K_α-radiation.[196] However, the corresponding thermal ellipsoids (Fig. 24) were too prolate or too oblate compared to the ellipsoids obtained by combining the SHADE method[85] with the multipole model or TAAM,[265] which preclude unconstrained refinement of H-atom positions. A possible way to solve the problem[197] is to use anisotropic displacement parameters of hydrogen atoms calculated using the invariom database and TLS-analysis of X-ray diffraction data. Fortunately, this problem concerns only 5% of conventional-resolution data sets.[250]

Neutron diffraction studies still remain the most reliable source of information on the lengths of bonds involving hydrogen atoms and the anisotropic H-atom displacement parameters.[265] However, the Hirshfeld atom refinement is at present the best method to extract this information from more readily available X-ray diffraction data.[269] Besides, the Hirshfeld atom refinement allows one to solve the scaling factor problem[270] associated with the use of anisotropic H-atom displacement parameters determined from neutron diffraction data.

The main application field of Hirshfeld atom refinement is the determination of coordinates and anisotropic displacement parameters of all atoms in the crystal. In addition, the corresponding ED distribution can quite correctly reproduce the ED obtained from the multipole refinement of high-resolution X-ray diffraction data.[264] The observed differences between topological parameters (usually, to within 3σ) are associated with insufficient 'flexibility' of the multipole model. In some cases the ED model obtained after Hirshfeld atom refinement describes the observed diffraction pattern as well as or even better than the approaches based on the multipole model (including unconstrained refinement of multipole parameters and the use of databases of multipole parameters).[264, 267]

In spite of the drawbacks mentioned above the Hirshfeld atom refinement is a useful tool for the emerging quantum crystallography.[271] It almost does not require user intervention, which still to a great extent specifies the procedure and influences the results of multipole refinement of high-resolution X-ray diffraction data. Convenient implementation of Hirshfeld atom refinement in the widely used OLEX2 program package[267] makes it candidate for being a conventional tool for routine X-ray diffraction analysis and, probably, put competitive pressure on the multipole model in the studies of the ED distribution. Besides, the atomic coordinates thus determined are ideally suited[264, 272] for X-ray constrained wave function fit (XCW).[273] A HAR + XCW combination is called X-ray constrained wave function refinement (XWR).

9. X-Ray constrained wave function refinement

The method proposed by Jaayatilaka and Grimwood[273] and implemented in the TONTO program[261] is based on the concept of X-ray constrained wave function or density matrix.[274] Experimental data can be collected using any physicochemical methods and their combinations [*e.g.*, polarized neutron diffraction[275] or Compton (inelastic) scattering];[276] however, single-crystal X-ray diffraction is most often used since it is readily available and related to the ED distribution. The advantage of such a hybrid approach over high-resolution X-ray diffraction studies is the possibility to determine those physicochemical properties of crystals (*e.g.*, optical properties) that require knowledge of the wave function rather than the ED distribution only. However, unlike quantum chemical calculations of crystals,[37] the X-ray constrained wave function refinement (XWR) method takes into account the effects of thermal motion of atoms and other peculiar features of real crystals.[274]

The first attempts to extract the wave function from experimental data date back to the mid-1960s,[277–280] however, the principles of the XWR method were reported in a series of pioneering studies by Clinton *et al.*,[281–285] who developed a semiempirical method for extracting the density matrices from theoretical ED distribution. Subsequent improvements of the technique allowed one to use quantum

chemically calculated structure factors [286] and the structure factors measured for beryllium crystal.[287] Aleksandrov *et al.*[288] determined the density matrix from X-ray diffraction data for diamond and silicon. The main drawback of these and related approaches is the impossibility to choose the one and only wave function that reproduces the ED distribution from X-ray diffraction data.[289] A possible way to solve this problems was the assumption that this wave function should simultaneously minimize the energy of the system.[290, 291]

A logical development of this idea is the implementation of the XWR method.[273, 292–294] Within the framework of this approach a crystal is composed of identical noninteracting fragments, each fragment being described by the wave function $|\Psi_j\rangle$. In this case the wave function of the crystal is given by

$$|\Psi\rangle = \prod_j |\Psi_j\rangle \tag{42}$$

The ED function, ρ_{cell}, of the unit cell containing N_f fragments can be expressed as the sum of their electron densities (ρ_j) related to ρ_0, the ED function of the unique part of the unit cell, by the symmetry operations R_j.

$$\rho_{\text{cell}}(\mathbf{r}) = \sum_{j=1}^{N_f} \rho_j(\mathbf{r}) = \sum_{j=1}^{N_f} \rho_0 \frac{r - r^j}{R_j} \tag{43}$$

In the single-determinant approximation, the wave function corresponding to this density, $|\Psi_0\rangle$, is obtained by minimizing the functional $J[\Psi_j]$

$$J[\Psi_0] = E_0[\Psi_0] + \lambda_i\left(\chi^2[\Psi_0] - \Delta\right) \tag{44}$$

Here the first term is the total energy of the system, which is obtained from quantum chemical (*e.g.*, Hartree–Fock) calculations, while the second term specifies the agreement between the experimental and theoretically calculated structure factors (for notations, see below).

Thus, the functional (44) can be represented by a Lagrangian (L) which depends on the Lagrange multiplier (λ_i) associated with the experimental constraints and on the number of unconstrained variables (c) and factors associated with orbital orthogonality (ε),

$$L(\lambda_i, c, \varepsilon) = E(c, \varepsilon) - \lambda_i(\chi^2 - \Delta) \tag{45}$$

where E is the total energy of the system, c are molecular-orbital coefficients in the molecular orbitals as linear combination of atomic orbitals (MO LCAO) approximation, Δ is the desired error (it is usually chosen to be 1.0 or one standard deviation [274]), and χ^2 is the measure of statistical agreement between the theoretical and experimental structure factors

$$\chi^2 = \frac{1}{N_{\text{r}} - N_{\text{p}}} \sum_h \frac{(s|F_h^{\text{calc}}| - |F_h^{\text{exp}}|)^2}{\sigma_h^2} \tag{46}$$

In this expression, N_{r} is the number of measured reflections included in X-ray wave function refinement and N_{p} is the number of refined parameters (*e.g.*, one Lagrange multiplier λ_i).

Theoretical structure factors F_h^{calc} are calculated with inclusion of correction for thermal motion of atoms; this quantity is difficult to calculate by quantum chemistry methods but can be evaluated using the anisotropic displacement parameters obtained from X-ray diffraction experiments.[295–297] Minimization of functional (44) gives the wave function $|\Psi_0\rangle$ in analytical form (a set of MOs with corresponding coefficients and energies) which also minimizes the energy of the system E_0 [or $E(c, \varepsilon)$ in expression (45)] in the Hartree–Fock calculations and reproduces the experimentally measured structure factors with the desired accuracy. It should be noted that the corresponding energy E_0 is always higher than the energy obtained from unconstrained quantum chemical calculations.[274]

To date, the XWR method with inclusion of crystal field effects [298] was successfully used in studies of beryllium,[292] ammonia,[294] urea [299] and other organic crystals.[300] This made it possible to analyze the bond orders and the electron localizability indicator (ELI) function,[300, 301] to evaluate the dipole moments and polarizability of molecules in crystals, as well as the refractive indices of molecular crystals.[298, 302, 303] There properties cannot be reliably determined only from the experimental ED distribution obtained upon multipole refinement of high-resolution X-ray diffraction data.[304]

The most interesting example of application of the XWR technique is the description of open-shell systems.[305] Within the framework of unrestricted Hartree–Fock method it allows one to obtain the experimental spin density distribution (earlier, this was possible only using less available polarized neutron diffraction method) [275] and to include relativistic effects (*e.g.*, within the framework of the DKH2 approach ‡).[306] The latter is of particular importance for the description of the ED in crystals of compounds containing heavy-element atoms abundant in core electrons. Besides, when using various post-Hartree–Fock methods (*e.g.*, the coupled cluster approach) the XWR method also includes the electron correlation effects.[307] Recently attempts to overcome the limitations of the single-determinant approximation have been undertaken.[308]

Various localization techniques [309–311] that can be applied to the XWR wave function eliminate the main drawback of the XWR approach, *viz.*, full delocalization of the MOs in the molecule and difficulties in the interpretation of the corresponding ED distribution.[274] Among them, an approach [312] based on the extremely localized molecular orbitals (ELMO) [313] seems to be the most appropriate. The ELMOs are specified prior to carrying out quantum chemical calculations of structure factors, they are strictly localized on small fragments such as atoms, chemical bonds or functional groups (Fig. 25) and can therefore be transferred from one molecule to another [314] (by analogy with the databases of experimental or theoretical multipole parameters, see above) provided that both contain equivalent chemical fragments. The ELMO can also be used to obtain the XWR wave functions for the closed-shell systems [274] if no high-quality X-ray diffraction data are available and quantum chemical calculations are too labour-consuming (these are, *e.g.*, biomacromolecules repeatedly mentioned above).[315]

‡ DKH is a method for calculating the relativistic correction to the total energy of a molecule or crystal (Douglas–Kroll–Hess scalar relativistic Hamiltonian).

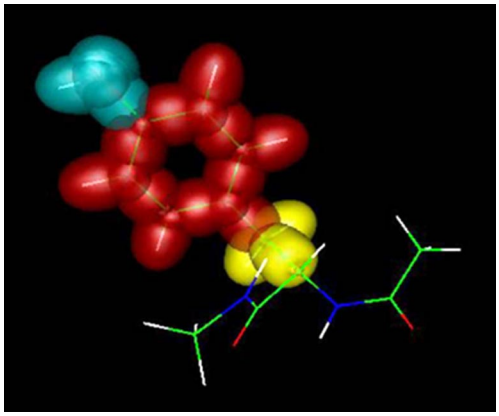


Figure 25. Extremely localized molecular orbitals of thyrosine. The ELMO describing the hydroxyl, phenyl and methylene groups are given in blue, red and yellow, respectively.[315]

Like databases of multipole parameters,[39, 128, 163] the ELMO database includes, first of all, MOs localized on the chemical bonds and functional groups from twenty amino acids and proteins formed from them (see Fig. 25).[315] From practical considerations, the database was constructed using the wave functions calculated for isolated molecules in small STO-4G basis sets. To obtain better convergence, is it recommended to use larger basis sets [*e.g.*, 6-311G++(2d,2p)[274]]. Nevertheless, utilization of different types of ELMO from this database made possible a very accurate (the similarity index comparing the ED values at each point[316] was at least 99.2) reproduction of the ED distribution corresponding to the total wave function for different polypeptides and a small model protein containing 56 amino acid residues.[315] The wave function calculations for this protein using the ELMO database took one hour *vs.* one week for conventional calculations.

An improved version of the ELMO database[317] includes the model molecules for the ELMO calculations in the 6-311+G(2d,2p) basis set chosen taking into account the nearest functional groups and represents a good alternative to the databases of experimental (ELMAM2 and SBFA) and theoretical (invariom database and UBDB) multipole parameters when obtaining the ED distribution and performing structure refinement of biomacromolecules from X-ray diffraction data. In particular, the ED values at the (3,−1)BCP obtained for the crystal of polypeptide Tyr-Gly-Gly-Phe-Leu upon transfer of results corresponding multipole parameters from the ELMO, ELMAM2 and UBDB databases[318] differed by less than 6%. A comparison of the results of Hartree–Fock and DFT (with the B3LYP functional) calculations of this polypeptide revealed a similar difference.[317] The ELMO excellently described the ED distribution in the region of intermolecular hydrogen bonds in the polypeptide crystal but overestimated the charges of the polypeptide fragments.[318] Attempts to solve this problem were undertaken earlier.[319, 320]

The major drawback of the ELMO approach is non-orthogonality of the ELMO. This precludes obtaining the ED distribution in the entire molecule of interest by summation of the pre-calculated ED distributions for molecular fragments[315] in contrast to the approach using databases of multipole parameters. In the latter case, the existence of a local coordinate system[121] allows one to specify the same local axes for each pseudoatom in different molecules in advance, whereas the ELMO database requires that rotation and translation operations be done[321] to minimize the shape differences between the fragment of the model compound and the molecule of interest.[315] At the same time, the ELMO approach provides not only the ED distribution, but also the wave function of the crystal and thus significantly extends the range of physicochemical properties of compounds that can be determined from X-ray diffraction data including conventional-resolution data.

10. Conclusion

To date, high-resolution X-ray diffraction studies that make it possible to elucidate the ED distribution in small-molecule crystals firmly established themselves in modern chemical science.[6] The advances made in the field are to a great extent supported by the results of quantum chemical calculations that are traditionally used to confirm the reliability of structural information concerning chemical bonds and properties of compounds. Recently, hybrid approaches involving refinement of experimentally measured structure factors using quantum chemistry methods have been utilized (they were considered in detail in this review). This made it possible to extend the range of objects under study to complex systems (polypeptides, metal-organic frameworks, inclusion compounds, *etc.*) that are thought to be unsuitable for high-resolution X-ray diffraction studies even taking into account recent technological advances in the field of high-brilliance X-ray radiation sources, sensitive detectors, *etc.*

In this review we have shown that quantum chemical calculations can serve a source of the multipole parameters[172, 190] or atomic displacement parameters[245, 249] that are independent of the nature and quality of crystalline samples (low scattering power, strong absorption, twinning, *etc.*) and not influenced by experimental errors (diffuse X-ray scattering or permeation of low-energy photons through focusing multilayer optics). At the same time, refinement against X-ray diffraction data allows one to account for the effects observed in real crystals (*e.g.*, translational vibrations ignored by calculations at the point Γ)[245] or to partially compensate the drawbacks of the DFT in the description of weak intermolecular interactions responsible for the existence of molecular crystals and many properties of these systems.

The choice of optimum combination from the standpoint of computing time, total computational cost and accuracy of the expected results depends on the problem to be solved. In particular, the Hirshfeld atom refinement[249] is the most reliable method for the determination of anisotropic H-atom displacement parameters that cannot be obtained in routine X-ray diffraction experiment owing to low scattering power of these atoms. A faster method to reach the goal is to go to anisotropic displacement parameters calculated using the invariom database and TLS-analysis of X-ray diffraction data.[197]

Hybrid methods combining quantum chemical calculations and X-ray diffraction data deserve particular attention since in this case one can extract information that is difficult or impossible to obtain using only one method. For

instance, refinement of normal vibrations [245] allows one to determine the vibrational entropy and other thermodynamic properties of a crystal from the results of a single X-ray diffraction experiment, while the XWR approach [272] makes it possible to study those properties of compounds (*e.g.*, optical properties) that require the total wave function. To solve many problems, there is no need to carry out complicated calculations that require specialists with high skills in quantum chemistry. For instance, the Hirshfeld atom refinement [249] is implemented in the popular OLEX2 program package in user-friendly form.

The UBDB database of theoretical multipole parameters,[172] the invariom database [190] or the ELMO database,[317] which provide the ED distribution and even thermodynamic properties (or other only-wave-function-derived properties) of crystals from conventional-resolution X-ray diffraction data that are mainly used only for structure determination, offer great prospects for researchers. Making them an integral part of X-ray diffraction studies will help to extend them to new classes (*e.g.*, biomacromolecules since their quantum chemical calculations are still unreasonably expensive) or series of related compounds,[35] which is a necessary condition for revealing common regularities and using them in the design of novel materials.

The potential of hybrid methods is far from being exhausted. One can assume that progress in this field will lead to transformation of X-ray crystallography into a branch of 'quantum crystallography' [322] that goes far beyond high-resolution X-ray diffraction studies when analyzing chemical bonding in crystals of different chemical nature (from elements to DNA) and various properties (thermochemical, optical, magnetic, transport *etc.*). In the future one can also expect that the hybrid approaches will be used in studies of partially ordered systems and even solutions based on the structural or thermochemical information provided by spectroscopic methods.

The review has been written with the financial support from the Russian Foundation for Basic Research (Project No. 16-03-00691).

Figure 20 is courtesy of The Royal Society of Chemistry. Figures 3, 12, 14 – 16 are courtesy of the American Chemical Society. Figures 2 and 21 are courtesy of IOP Science. Figures 20 and 23 are courtesy of Wiley Interscience. Figure 25 is courtesy of Elsevier. Figure 22 is courtesy of AAAS Publishing. Figures 4 – 11, 13, 17 – 19, 24 are courtesy of the International Union of Crystallography.

References

1. P.Debye. *Ann. Phys.*, **351**, 809 (1915)
2. P.Hohenberg, W.Kohn. *Phys. Rev. B: Condens. Matter*, **136**, 864 (1964)
3. P.Coppens. *Science*, **158**, 1577 (1967)
4. N.K.Hansen, P.Coppens. *Acta Crystallogr., Sect. A*, **34**, 909 (1978)
5. R.F.W.Bader. *Atoms in Molecules: A Quantum Theory*. (Clarendon Press, 1994)
6. P.Coppens. *Angew. Chem., Int. Ed.*, **44**, 6810 (2005)
7. M.Y.Antipin. *Russ. Chem. Rev.*, **59**, 607 (1990)
8. L.A.Aslanov, G.V.Fetisov, A.V.Laktionov, V.T.Markov, V.V.Chernyshev, S.G.Zhukov, A.P.Nesterenko, A.I.Chulikov, N.M.Chulikova. *Pretsizionnyi Rentgendifraktsionnyi Eksperiment*. (High-Resolution X-Ray Diffraction Experiment) (Moscow: Moscow State University, 1989)
9. V.G.Tsirelson, R.P.Ozerov. *Electron Density and Bonding in Crystals: Principles, Theory, and X-Ray Diffraction Experiments in Solid State Physics and Chemistry*. (Bristol, Philadelphia: Institute of Physics Pub., 1996)
10. P.Coppens. *X-Ray Charge Densities and Chemical Bonding*. (Chester, Oxford, New York: International Union of Crystallography, Oxford University Press, 1997)
11. *Modern Charge-Density Analysis*. (Eds C.Gatti, P.Macchi). (Dordrecht, New York: Springer, 2012)
12. G.A.Jeffrey, J.F.Piniella. *The Application of Charge Density Research to Chemistry and Drug Design*. (Boston: Springer, 1991)
13. *Electron Density and Chemical Bonding I*. Vol. 146. (Ed. D.Stalke). (Berlin, Heidelberg: Springer, 2012)
14. *Electron Density and Chemical Bonding. 2: Theoretical Charge Density Studies*. (Eds M.Chodkiewicz, D. Stalke). (Berlin: Springer, 2012)
15. D.Stalke. In *The Chemical Bond I*. Vol. 169. (Ed D.M.P.Mingos). (Cham: Springer International Publishing, 2016). P. 57
16. T.S.Koritsanszky, P.Coppens. *Chem. Rev.*, **101**, 1583 (2001)
17. D.Chopra. *J. Phys. Chem. A*, **116**, 9791 (2012)
18. A.S.Chimpri, P.Macchi. *Phys. Sci.*, **87**, 048105 (2013)
19. A.Krawczuk, P.Macchi. *Chem. – Cent. J.*, **8**, 68 (2014)
20. B.Dittrich. *Acta Crystallogr., Sect. B*, **73**, 325 (2017)
21. M.R.V.Jørgensen, V.R.Hathwar, N.Bindzus, N.Wahlberg, Y.-S.Chen, J.Overgaard, B.B.Iversen. *IUCrJ*, **1**, 267 (2014)
22. M.S.Schmøkel, L.Bjerg, J.Overgaard, F.Krebs Larsen, G.K.Hellerup Madsen, K.Sugimoto, M.Takata, B.Brummerstedt Iversen. *Angew. Chem., Int. Ed.*, **52**, 1503 (2013)
23. G.K.Fukin, M.A.Samsonov, A.V.Arapova, A.S.Mazur, T.O.Artamonova, M.A.Khodorkovskiy, A.V.Vasilyev. *J. Solid State Chem.*, **254**, 32 (2017)
24. G.K.Fukin, E.V.Baranov, C.Jelsch, B.Guillot, A.I.Poddel'sky, V.K.Cherkasov, G.A.Abakumov. *J. Phys. Chem. A*, **115**, 8271 (2011)
25. A.A.Korlyukov, V.N.Khrustalev, A.V.Vologzhanina, K.A.Lyssenko, M.S.Nechaev, M.Y.Antipin. *Acta Crystallogr., Sect. B*, **67**, 315 (2011)
26. S.V.Gruener, D.V.Airapetyan, A.A.Korlyukov, A.G.Shipov, Y.I.Baukov, V.S.Petrosyan. *Appl. Organomet. Chem.*, **24**, 888 (2010)
27. A.O.Borissova, A.A.Korlyukov, M.Y.Antipin, K.A.Lyssenko. *J. Phys. Chem. A*, **112**, 11519 (2008)
28. Y.V.Nelyubina, L.N.Puntus, K.A.Lyssenko. *Chem. – Eur. J.*, **20**, 2860 (2014)
29. L.N.Puntus, K.A.Lyssenko, M.Y.Antipin. J.G.Bünzli. *Inorg. Chem.*, **47**, 11095 (2008)
30. H.Kasai, E.Nishibori. *Sci. Rep.*, **7**, 41375 (2017)
31. B.B.Iversen, F.K.Larsen, A.A.Pinkerton, A.Martin, A.Darovsky, P.A.Reynolds. *Acta Crystallogr., Sect. B*, **55**, 363 (1999)
32. V.V.Zhurov, E.A.Zhurova, A.I.Stash, A.A.Pinkerton. *J. Phys. Chem. A*, **115**, 13016 (2011)
33. V.V.Zhurov, E.A.Zhurova, A.I.Stash, A.A.Pinkerton. *Acta Crystallogr., Sect. A*, **67**, 160 (2011)
34. C.G.Gianopoulos, V.V.Zhurov, S.G.Minasian, E.R.Batista, C.Jelsch, A.A.Pinkerton. *Inorg. Chem.*, **56**, 1775 (2017)
35. I.L.Kirby, M.B.Pitak, S.J.Coles, P.A.Gale. *Chem. Lett.*, **44**, 2 (2015)
36. B.Dittrich, C.F.Matta. *IUCrJ*, **1**, 457 (2014)
37. A.A.Korlyukov, M.Y.Antipin. *Russ. Chem. Rev.*, **81**, 105 (2012)

38. A.Volkov, M.Messerschmidt, P.Coppens. *Acta Crystallogr., Sect. D*, **63**, 160 (2007)
39. B.Dittrich, C.B.Hübschle, P.Luger, M.A.Spackman. *Acta Crystallogr., Sect. D*, **62**, 1325 (2006)
40. S.B.Novaković, G.A.Bogdanović, C.Heering, G.Makhloufi, D.Francuski, C.Janiak. *Inorg. Chem.*, **54**, 2660 (2015)
41. Y.V.Nelyubina, A.S.Shaplov, E.I.Lozinskaya, M.I.Buzin, Y.S.Vygodskii. *J. Am. Chem. Soc.*, **138**, 10076 (2016)
42. D.Yu. Pushcharovskii. *Rentgenografiya Mineralov*. (X-Ray Diffraction of Minerals) (Moscow: Geoinformmark, 2000)
43. *Crystal Structure Analysis: Principles and Practice*. (Eds A.J.Blake, W.Clegg). (Oxford, New York: Oxford University Press, 2009)
44. G.B.Bokii, M.A.Parai-Koshits. *Rentgenostrukturnyi Analiz*. (X-Ray Diffraction Analysis). (Moscow: Moscow State University, 1964) Vol. 1
45. B.K.Vainshtein. *Sovremennaya Kristallografiya. Simmetriya Kristallov, Metody Strukturnoi Kristallografii*. (Modern Crystallography. Symmetry of Crystals, Methods of Structural Crystallography) (Moscow: Nauka, 1979) Vol. 1
46. G.V.Fetisov. *Sinkhrotronnoe Izluchenie. Metody Issledovaniya Struktury Veshchestva*. (Synchrotron Radiation. Methods for Studying the Structure of Substances). (Moscow: Fizmatlit, 2007)
47. *Fundamentals of Crystallography*. (Ed. C.Giacovazzo). (Oxford, New York: Oxford University Press, 2011)
48. *International Tables for Crystallography. Vol. B: Reciprocal Space*. (Ed. U.Shmueli). (Dordrecht: Springer, 2008)
49. E.Clementi, C.Roetti. *Atom. Data Nuclear Data Tabl.*, **14**, 177 (1974)
50. L.Bindi, M.Evain. *Am. Mineral.*, **92**, 886 (2007)
51. U.H.Zucker, H.Schulz. *Acta Crystallogr., Sect. A*, **38**, 568 (1982)
52. S.C.Abrahams. *Acta Crystallogr., Sect. A*, **25**, 165 (1969)
53. J.Henn. *Acta Crystallogr., Sect. A*, **72**, 696 (2016)
54. S.R.Hall, F.H.Allen, I.D.Brown. *Acta Crystallogr., Sect. A*, **47**, 655 (1991)
55. A.L.Spek. *J. Appl. Crystallogr.*, **36**, 7 (2003)
56. P.G.Jones. *Chem. Soc. Rev.*, **13**, 157 (1984)
57. V.V.Zhurov, E.A.Zhurova, A.A.Pinkerton. *J. Appl. Crystallogr.*, **41**, 340 (2008)
58. K.N.Jarzembska, R.Kamiński, L.Dobrzycki, M.K.Cyrański. *Acta Crystallogr., Sect. B*, **70**, 847 (2014)
59. M.S.Schmøkel, J.Overgaard, B.B.Iversen. *Z. Anorg. Allg. Chem.*, **639**, 1922 (2013)
60. B.Niepötter, R.Herbst-Irmer, D.Stalke. *J. Appl. Crystallogr.*, **48**, 1485 (2015)
61. L.Krause, R.Herbst-Irmer, D.Stalke. *J. Appl. Crystallogr.*, **48**, 1907 (2015)
62. P.Macchi, H.-B.Bürgi, A.S.Chimpri, J.Hauser, Z.Gál. *J. Appl. Crystallogr.*, **44**, 763 (2011)
63. B.Dawson. *Acta Crystallogr.*, **17**, 990 (1964)
64. R.F.Stewart. *Acta Crystallogr., Sect. A*, **32**, 565 (1976)
65. F.L.Hirshfeld. *Acta Crystallogr., Sect. B*, **27**, 769 (1971)
66. Z.Su, P.Coppens. *Acta Crystallogr., Sect. A*, **54**, 357 (1998)
67. P.Macchi, P.Coppens. *Acta Crystallogr., Sect. A*, **57**, 656 (2001)
68. V.G.Tsirelson. *Kvantovaya Khimiya. Molekuly, Molekulyarnye Sistemy i Tverdye Tela*. (Quantum Chemistry. Molecules, Molecular Systems and Solids) (Moscow: Binom, 2010)
69. K.Kurki-Suonio. *Isr. J. Chem.*, **16**, 115 (1977)
70. V.V.Zhurov, A.A.Pinkerton. *Z. Anorg. Allg. Chem.*, **639**, 1969 (2013)
71. P.Macchi. *Acta Crystallogr., Sect. B*, **73**, 330 (2017)
72. P.Macchi, J.-M.Gillet, F.Taulelle, J.Campo, N.Claiser, C.Lecomte. *IUCrJ*, **2**, 441 (2015)
73. L.J.Farrugia, H.M.Senn. *J. Phys. Chem. A*, **116**, 738 (2012)
74. A.Volkov, Y.A.Abramov, P. Coppens. *Acta Crystallogr., Sect. A*, **57**, 272 (2001)
75. A.Fischer, D.Tiana, W.Scherer, K.Batke, G.Eickerling, H.Svendsen, N.Bindzus, B.B.Iversen. *J. Phys. Chem. A*, **115**, 13061 (2011)
76. J.Overgaard, C.Jones, D.Dange, J.A.Platts. *Inorg. Chem.*, **50**, 8418 (2011)
77. J.A.Platts, M.K.Thomsen, J.Overgaard. *Z. Anorg. Allg. Chem.*, **639**, 1979 (2013)
78. L.Krause, B.Niepötter, C.J.Schürmann, D.Stalke, R.Herbst-Irmer. *IUCrJ*, **4**, 420 (2017)
79. L.J.Farrugia, C.Evans, D.Lentz, M.Roemer. *J. Am. Chem. Soc.*, **131**, 1251 (2009)
80. A.O.Borissova, M.Y.Antipin, K.A.Lyssenko. *J. Phys. Chem. A*, **113**, 10845 (2009)
81. A.A.Hoser, P.M.Dominiak, K.Woźniak. *Acta Crystallogr., Sect. A*, **65**, 300 (2009)
82. R.F.Stewart. *J. Chem. Phys.*, **51**, 4569 (1969)
83. F.H.Allen, I.J.Bruno. *Acta Crystallogr., Sect. B*, **66**, 380 (2010)
84. A.Ø.Madsen, H.O.Sørensen, C.Flensburg, R.F.Stewart, S.Larsen. *Acta Crystallogr., Sect. A*, **60**, 550 (2004)
85. A.Ø.Madsen, A.A.Hoser. *J. Appl. Crystallogr.*, **47**, 2100 (2014)
86. P.Munshi, A.Ø.Madsen, M.A.Spackman, S.Larsen, R.Destro. *Acta Crystallogr., Sect. A*, **64**, 465 (2008)
87. M.S.Schmøkel, S.Cenedese, J.Overgaard, M.R.V.Jørgensen, Y.-S.Chen, C.Gatti, D.Stalke, B.B.Iversen. *Inorg. Chem.*, **51**, 8607 (2012)
88. P.R.Mallinson, T.Koritsanszky, E.Elkaim, N.Li, P.Coppens. *Acta Crystallogr., Sect. A*, **44**, 336 (1988)
89. R.Herbst-Irmer, J.Henn, J.J.Holstein, C.B.Hübschle, B.Dittrich, D.Stern, D.Kratzert, D.Stalke. *J. Phys. Chem. A*, **117**, 633 (2013)
90. F.L.Hirshfeld. *Acta Crystallogr., Sect. A*, **32**, 239 (1976)
91. M.A.Spackman. *Chem. Phys. Lett.*, **301**, 425 (1999)
92. *Applications of Topological Methods in Molecular Chemistry*. (Eds R.Chauvin, C.Lepetit, B.Silvi, E.Alikhani). (Cham: Springer, 2016)
93. A.M.Pendás, E.Francisco, M.A.Blanco, C.Gatti. *Chem. – Eur. J.*, **13**, 9362 (2007)
94. D.Cremer, E.Kraka. *Angew. Chem., Int. Ed. Engl.*, **23**, 627 (1984)
95. M.V.Vener, E.O.Levina, A.A.Astakhov, V.G.Tsirelson. *Chem. Phys. Lett.*, **638**, 233 (2015)
96. Y.A.Abramov. *Acta Crystallogr., Sect. A*, **53**, 264 (1997)
97. E.Espinosa, I.Alkorta, J.Elguero, E.Molins. *J. Chem. Phys.*, **117**, 5529 (2002)
98. F.Bertolotti, A.V.Shishkina, A.Forni, G.Gervasio, A.I.Stash, V.G.Tsirelson. *Cryst. Growth Des.*, **14**, 3587 (2014)
99. K.A.Lyssenko, A.A.Korlyukov, D.G.Golovanov, S.Y.Ketkov, M.Y.Antipin. *J. Phys. Chem. A*, **110**, 6545 (2006)
100. K.A.Lyssenko, A.A.Korlyukov, M.Y.Antipin. *Mendeleev Commun.*, **15**, 90 (2005)
101. I.V.Glukhov, K.A.Lyssenko, A.A.Korlyukov, M.Y.Antipin. *Faraday Discuss.*, **135**, 203 (2007)
102. Y.V.Nelyubina, I.V.Glukhov, M.Y.Antipin, K.A.Lyssenko. *Chem. Commun.*, **46**, 3469 (2010)
103. Y.V.Nelyubina, I.V.Ananyev, V.V.Novikov, K.A.Lyssenko. *RSC Adv.*, **6**, 91694 (2016)

104. V.Tsirelson, A.Stash. *Chem. Phys. Lett.*, **351**, 142 (2002)
105. V.Tsirelson, A.Stash. *Acta Crystallogr., Sect. B*, **58**, 780 (2002)
106. V.G.Tsirelson, Á.Nagy. *J. Phys. Chem. A*, **113**, 9022 (2009)
107. E.D.Stevens, P.Coppens. *Acta Crystallogr., Sect. A*, **35**, 536 (1979)
108. A.Holladay, P.Leung, P.Coppens. *Acta Crystallogr., Sect. A*, **39**, 377 (1983)
109. M.A.Spackman, P.Munshi, B.Dittrich. *ChemPhysChem*, **8**, 2051 (2007)
110. A.Volkov, T.Koritsanszky, P.Coppens. *Chem. Phys. Lett.*, **391**, 170 (2004)
111. H.Wolf, M.R.V.Jørgensen, Y.-S.Chen, R.Herbst-Irmer, D.Stalke. *Acta Crystallogr., Sect. B*, **71**, 10 (2015)
112. S.C.Abrahams, E.T.Keve. *Acta Crystallogr., Sect. A*, **27**, 157 (1971)
113. K.Diederichs. *Acta Crystallogr., Sect. D*, **66**, 733 (2010)
114. J.Henn, K.Meindl. *Acta Crystallogr., Sect. A*, **70**, 499 (2014)
115. J.Henn, K.Meindl. *Acta Crystallogr., Sect. A*, **70**, 248 (2014)
116. J.Henn, K.Meindl. *Acta Crystallogr., Sect. A*, **71**, 203 (2015)
117. K.Meindl, J.Henn. *Acta Crystallogr., Sect. A*, **64**, 404 (2008)
118. R.Herbst-Irmer, D.Stalke. *Acta Crystallogr., Sect. B*, **73**, 531 (2017)
119. J.M.Bak, S.Domagaa, C.Hübschle, C.Jelsch, B.Dittrich, P.M.Dominiak. *Acta Crystallogr., Sect. A*, **67**, 141 (2011)
120. C.F.Matta, R.F.W.Bader. *Prot. Struct. Funct. Bioinform.*, **40**, 310 (2000)
121. V.Pichon-Pesme, C.Lecomte, H.Lachekar. *J. Phys. Chem.*, **99**, 6242 (1995)
122. M.Ahmed, S.Noureen, P.C.Gros, B.Guillot, C.Jelsch. *Acta Crystallogr., Sect. C*, **67**, o329 (2011)
123. C.P.Brock, J. D.Dunitz, F.L.Hirshfeld. *Acta Crystallogr., Sect. B*, **47**, 789 (1991)
124. C.Jelsch, V.Pichon-Pesme, C.Lecomte, A.Aubry. *Acta Crystallogr., Sect. D*, **54**, 1306 (1998)
125. C.Lecomte, B.Guillot, N.Muzet, V.Pichon-Pesme, C.Jelsch. *Cell. Mol. Life Sci.*, **61**, 774 (2004)
126. B.Guillot, C.Jelsch, A.Podjarny, C.Lecomte. *Acta Crystallogr., Sect. D*, **64**, 567 (2008)
127. N.Muzet, B.Guillot, C.Jelsch, E.Howard, C.Lecomte. *Proc. Natl. Acad. Sci. USA*, **100**, 8742 (2003)
128. B.Zarychta, V.Pichon-Pesme, B.Guillot, C.Lecomte, C.Jelsch. *Acta Crystallogr., Sect. A*, **63**, 108 (2007)
129. D.Liebschner, C.Jelsch, E.Espinosa, C.Lecomte, E.Chabriùre, B.Guillot. *J. Phys. Chem. A*, **115**, 12895 (2011)
130. S.Domagaa, B.Fournier, D.Liebschner, B.Guillot, C.Jelsch. *Acta Crystallogr., Sect. A*, **68**, 337 (2012)
131. S.Domagaa, P.Munshi, M.Ahmed, B.Guillot, C.Jelsch. *Acta Crystallogr., Sect. B*, **67**, 63 (2011)
132. S.Jagannatha Prathapa, J.Held, S.van Smaalen. *Z. Anorg. Allg. Chem.*, **639**, 2047 (2013)
133. C.Jelsch, B.Guillot, A.Lagoutte, C.Lecomte. *J. Appl. Crystallogr.*, **38**, 38 (2005)
134. V.R.Hathwar, T.S.Thakur, T.N.G.Row, G.R.Desiraju. *Cryst. Growth Des.*, **11**, 616 (2011)
135. V.R.Hathwar, T.S.Thakur, R.Dubey, M.S.Pavan, T.N.Guru Row, G.R.Desiraju. *J. Phys. Chem. A*, **115**, 12852 (2011)
136. R.Dubey, M.S.Pavan, T.N.Guru Row, G.R.Desiraju. *IUCrJ*, **1**, 8 (2014)
137. B.Dittrich, E.Sze, J.J.Holstein, C.B.Hübschle, D.Jayatilaka. *Acta Crystallogr., Sect. A*, 68, 435 (2012)
138. G.S.Chandler, M.A.Spackman. *Acta Crystallogr., Sect. A*, **34**, 341 (1978)
139. L.J.Farrugia, H.M.Senn. *J. Phys. Chem. A*, **114**, 13418 (2010)
140. P.Coppens, A.Volkov. *Acta Crystallogr., Sect. A*, **60**, 357 (2004)
141. K.Batke, G.Eickerling. *J. Phys. Chem. A*, **117**, 11566 (2013)
142. D.Ayma, M.Rérat, R.Orlando, A.Lichanot. *Acta Crystallogr., Sect. A*, **54**, 1019 (1998)
143. R.Dovesi, B.Orlando, B.Civalleri, R.Roetti, V.R.Saunders, C.M.Zicovich-Wilson. *Z. Kristallogr.*, **220**, 571 (2005)
144. M.Catti, A.Pavese. *Acta Crystallogr., Sect. A*, **52**, 413 (1996)
145. G.Kresse, J.Furthmuller. *Phys. Rev. B*, **54**, 11169 (1996)
146. P.Blaha, K.Schwarz, G.K.H.Madsen, D.Kvasnicka, J.Luitz. *WIEN2k, An Augmented Plane Wave + Local Orbitals Program for Calculating Crystal Properties*. (Wien: Technische Universität Wien, 2001)
147. G.S.Chandler, B.N.Figgis, Z.Li. *Phys. Chem. Chem. Phys.*, **2**, 3743 (2000)
148. V.Zavodnik, A.Stash, V.Tsirelson, R.de Vries, D.Feil. *Acta Crystallogr., Sect. B*, **55**, 45 (1999)
149. S.J.van Reeuwijk, K.G.van Beek, D.Feil. *J. Phys. Chem. A*, **104**, 10901 (2000)
150. Y.A.Abramov, F.P.Okamura. *Acta Crystallogr., Sect. A*, **53**, 187 (1997)
151. V.G.Tsirelson, A.S.Avilov, Y.A.Abramov, E.L.Belokoneva, R.Kitaneh, D.Feil. *Acta Crystallogr., Sect. B*, **54**, 8 (1998)
152. V.G.Tsirelson, A.S.Avilov, G.G.Lepeshov, A.K.Kulygin, J.Stahn, U.Pietsch, J.C.H.Spence. *J. Phys. Chem. B*, **105**, 5068 (2001)
153. R.Boese, D.Bläser, O.Heinemann, Y.Abramov, V.Tsirelson, P.Blaha, K.Schwarz. *J. Phys. Chem. A*, **103**, 6209 (1999)
154. P.Coppens, T.N.Guru Row, P.Leung, E.D.Stevens, P.J.Becker, Y.W.Yang. *Acta Crystallogr., Sect. A*, **35**, 63 (1979)
155. E.D.Voronova, A.A.Golovanov, K.Y.Suponitsky, I.V.Fedyanin, A.V.Vologzhanina. *Cryst. Growth Des.*, **16**, 3859 (2016)
156. A.Volkov, Y.A.Abramov, P.Coppens, C.Gatti. *Acta Crystallogr., Sect. A*, **A56**, 332 (2000)
157. M.S.Schmøkel, L.Bjerg, F.K.Larsen, J.Overgaard, S.Cenedese, M.Christensen, G.K.H.Madsen, C.Gatti, E.Nishibori, K.Sugimoto, M.Takata, B.B.Iversen. *Acta Crystallogr., Sect. A*, **69**, 570 (2013)
158. E.Aubert, S.Lebègue, M.Marsman, T.T.T.Bui, C.Jelsch, S.Dahaoui, E.Espinosa, J.G.Ángyán. *J. Phys. Chem. A*, **115**, 14484 (2011)
159. T.T.T.Bui, S.Dahaoui, C.Lecomte, G.R.Desiraju, E.Espinosa. *Angew. Chem., Int. Ed.*, **48**, 3838 (2009)
160. M.E.Brezgunova, E.Aubert, S.Dahaoui, P.Fertey, S.Lebègue, C.Jelsch, J.G.Ángyán, E.Espinosa. *Cryst. Growth Des.*, **12**, 5373 (2012)
161. M.E.Brezgunova, J.Lieffrig, E.Aubert, S.Dahaoui, P.Fertey, S.Lebègue, J.G.Ángyán, M.Fourmigué, E.Espinosa. *Cryst. Growth Des.*, **13**, 3283 (2013)
162. A.Volkov, T.Koritsanszky, M.Chodkiewicz, H.F.King. *J. Comput. Chem.*, **30**, 1379 (2009)
163. T.Koritsanszky, A.Volkov, P.Coppens. *Acta Crystallogr., Sect. A*, **58**, 464 (2002)
164. P.M.Dominiak, A.Volkov, X.Li, M.Messerschmidt, P.Coppens. *J. Chem. Theor. Comput.*, **3**, 232 (2007)
165. B.Dittrich, T.Koritsanszky, A.Volkov, S.Mebs, P.Luger. *Angew. Chem., Int. Ed.*, **46**, 2935 (2007)
166. P.V.Afonine, R.W.Grosse-Kunstleve, P.D.Adams, V.Y.Lunin, A.Urzhumtsev. *Acta Crystallogr., Sect. D*, **63**, 1194 (2007)
167. B.Dittrich, T.Koritsánszky, P.Luger. *Angew. Chem., Int. Ed.*, **43**, 2718 (2004)

168. A.Volkov, X.Li, T.Koritsanszky, P.Coppens. *J. Phys. Chem. A*, **108**, 4283 (2004)
169. V.Pichon-Pesme, C.Jelsch, B.Guillot, C.Lecomte. *Acta Crystallogr., Sect. A*, **60**, 204 (2004)
170. A.Volkov, T.Koritsanszky, X.Li, P.Coppens. *Acta Crystallogr., Sect. A*, **60**, 638 (2004)
171. P.M.Dominiak, A.Volkov, A.P.Dominiak, K.N.Jarzembska, P.Coppens. *Acta Crystallogr., Sect. D*, **65**, 485 (2009)
172. K.N.Jarzembska, P.M.Dominiak. *Acta Crystallogr., Sect. A*, **68**, 139 (2012)
173. S.A.Bojarowski, P.Kumar, P.M.Dominiak. *Acta Crystallogr., Sect. B*, **73**, 598 (2017)
174. P.Kumar, S.A.Bojarowski, K.N.Jarzembska, S.Domagaa, K.Vanommeslaeghe, A.D.MacKerell, P.M.Dominiak. *J. Chem. Theor. Comput.*, **10**, 1652 (2014)
175. M.Malinska, Z.Dauter. *Acta Crystallogr., Sect. D*, **72**, 770 (2016)
176. W.F.Sanjuan-Szklarz, A.A.Hoser, M.Gutmann, A.Ø.Madsen, K.Woźniak. *IUCrJ*, **3**, 61 (2016)
177. A.Ø.Madsen, S.Larsen. *Angew. Chem., Int. Ed.*, **46**, 8609 (2007)
178. J.M.Bak, P.M.Dominiak, C.C.Wilson, K.Woźniak. *Acta Crystallogr., Sect. A*, **65**, 490 (2009)
179. E.Rödel, M.Messerschmidt, B.Dittrich, P.Luger. *Org. Biomol. Chem.*, **4**, 475 (2006)
180. S.J.Prathapa, S.Mondal, S.van Smaalen. *Acta Crystallogr., Sect. B*, **69**, 203 (2013)
181. A.Hofmann, R.Kalinowski, P.Luger, S.van Smaalen. *Acta Crystallogr., Sect. B*, **63**, 633 (2007)
182. B.Dittrich, C.B.Hübschle, M.Messerschmidt, R.Kalinowski, D.Girnt, P.Luger. *Acta Crystallogr., Sect. A*, **61**, 314 (2005)
183. P.Luger. *Org. Biomol. Chem.*, **5**, 2529 (2007)
184. K.Pröpper, J.J.Holstein, C.B.Hübschle, C.S.Bond, B.Dittrich. *Acta Crystallogr., Sect. D*, **69**, 1530 (2013)
185. B.Dittrich, C.S.Bond, R.Kalinowski, M.A.Spackman, D.Jayatilaka. *CrystEngComm*, **12**, 2419 (2010)
186. S.Mebs, A.Lüth, P.Luger. *Bioorg. Med. Chem.*, **18**, 5965 (2010)
187. M.Woińska, P.M.Dominiak. *J. Phys. Chem. A*, **117**, 1535 (2013)
188. C.M.Wandtke, J.Lübben, B.Dittrich. *ChemPhysChem*, **17**, 2238 (2016)
189. A.Warshel, P.K.Sharma, M.Kato, W.W.Parson. *Biochim. Biophys. Acta — Proteins Proteomics*, **1764**, 1647 (2006)
190. B.Dittrich, C.B.Hübschle, K.Pröpper, F.Dietrich, T.Stolper, J.Holstein. *Acta Crystallogr., Sect. B*, **69**, 91 (2013)
191. B.Dittrich, M.Strumpel, M.Schäfer, M.A.Spackman, T.Koritsánszky. *Acta Crystallogr., Sect. A*, **62**, 217 (2006)
192. H.D.Flack. *Acta Crystallogr., Sect. A*, 39, 876 (1983)
193. B.Dittrich, P.Munshi, M.A.Spackman. *Acta Crystallogr., Sect. B*, **63**, 505 (2007)
194. B.Dittrich, J.J.McKinnon, J.E.Warren. *Acta Crystallogr., Sect. B*, **64**, 750 (2008)
195. J.Lübben, C.Volkmann, S.Grabowsky, A.Edwards, W.Morgenroth, F.P.A.Fabbiani, G.M.Sheldrick, B.Dittrich. *Acta Crystallogr., Sect. A*, **70**, 309 (2014)
196. C.M.Orben, B.Dittrich. *Acta Crystallogr., Sect. C*, **70**, 580 (2014)
197. B.Dittrich, J.Lübben, S.Mebs, A.Wagner, P.Luger, R.Flaig. *Chem. – Eur. J.*, **23**, 4605 (2017)
198. W.Hummel, J.Hauser, H.B.Bürgi. *J. Mol. Graph.*, **8**, 214 (1990)
199. B.Dittrich, C.B.Hübschle, J.J.Holstein, F.P.A.Fabbiani. *J. Appl. Crystallogr.*, **42**, 1110 (2009)
200. B.Dittrich, M.Weber, R.Kalinowski, S.Grabowsky, C.B.Hübschle, P.Luger. *Acta Crystallogr., Sect. B*, **65**, 749 (2009)
201. Y.V.Nelyubina, K.A.Lyssenko. *Chem. – Eur. J.*, **21**, 9733 (2015)
202. Y.V.Nelyubina, A.A.Korlyukov, K.A.Lyssenko. *Chem. – Eur. J.*, **20**, 6978 (2014)
203. S.Grabowsky, R.Kalinowski, M.Weber, D.Förster, C.Paulmann, P.Luger. *Acta Crystallogr., Sect. B*, **65**, 488 (2009)
204. Y.V.Nelyubina, A.A.Korlyukov, K.A.Lyssenko. *Mendeleev Commun.*, **24**, 286 (2014)
205. C.J.Schürmann, K.Pröpper, T.Wagner, B.Dittrich. *Acta Crystallogr., Sect. B*, **68**, 313 (2012)
206. P.Luger, M.Weber, C.Hübschle, R.Tacke. *Org. Biomol. Chem.*, **11**, 2348 (2013)
207. B.Dittrich, J.E.Warren, F.P.A.Fabbiani, W.Morgenroth, B.Corry. *Phys. Chem. Chem. Phys.*, **11**, 2601 (2009)
208. B.Dittrich, C. Schürmann, C. B. Hübschle. *Z. Kristallogr. — Cryst. Mater.*, **231**, 725 (2016)
209. B.Dittrich, M.A.Spackman. *Acta Crystallogr., Sect. A*, **63**, 426 (2007)
210. Y.V.Nelyubina, A.A.Korlyukov, K.A.Lyssenko, I.V.Fedyanin. *Inorg. Chem.*, **56**, 4688 (2017)
211. B.Dittrich, C.M.Wandtke, A.Meents, K.Pröpper, K.C.Mondal, P.P.Samuel, N.A.SK, A.P.Singh, H.W.Roesky, N.Sidhu. *ChemPhysChem*, **16**, 412 (2015)
212. B.Dittrich, E.Ruf, T.Meller. *Struct. Chem.*, **28**, 1333 (2017)
213. J.J.Holstein, C.B.Hübschle, B.Dittrich. *CrystEngComm*, **14**, 2520 (2012)
214. K.N.Jarzembska, M.Kubsik, R.Kamiåski, K.Woźniak, P.M.Dominiak. *Cryst. Growth Des.*, **12**, 2508 (2012)
215. G.Cavallo, P.Metrangolo, R.Milani, T.Pilati, A.Priimagi, G.Resnati, G.Terraneo. *Chem. Rev.*, **116**, 2478 (2016)
216. Y.V.Nelyubina, A.A.Korlyukov, K.A.Lyssenko. *RSC Adv.*, **5**, 75360 (2015)
217. C.B.Hübschle, B.Dittrich. *J. Appl. Crystallogr.*, **44**, 238 (2011)
218. *APEX3 Suite for Crystallographic Software — Single Crystal X-Ray Diffraction*. (Karlsruhe: Bruker AXS, 2014)
219. A.Ø.Madsen. *J. Appl. Crystallogr.*, **39**, 757 (2006)
220. V.Schomaker, K.N.Trueblood. *Acta Crystallogr., Sect. B*, **24**, 63 (1968)
221. K.N.Trueblood, E.Huber-Buser. *THMA11, Program for Analysing Thermal Parameters*. (Los Angeles, CA: University of California, 1987)
222. V.Schomaker, K.N.Trueblood. *Acta Crystallogr., Sect. B*, **54**, 507 (1998)
223. B.T.M.Willis, A.W.Pryor. *Thermal Vibrations in Crystallography*. (London, New York: Cambridge University Press, 1975)
224. K.N.Trueblood, J.D.Dunitz. *Acta Crystallogr., Sect. B*, **39**, 120 (1983)
225. H.B.Bürgi, S.C.Capelli. *Acta Crystallogr., Sect. A*, **56**, 403 (2000)
226. S.C.Capelli, M.Förtsch, H.B.Bürgi. *Acta Crystallogr., Sect. A*, **56**, 413 (2000)
227. T.Aree, H.-B.Bürgi. *J. Phys. Chem. B*, **110**, 26129 (2006)
228. G.Filippini, C.M.Gramaccioli, M.Simonetta, G.B.Suffritti. *J. Chem. Phys.*, **59**, 5088 (1973)
229. B.Dittrich, S.Pfitzenreuter, C.B.Hübschle. *Acta Crystallogr., Sect. A*, **68**, 110 (2012)
230. M.Svensson, S.Humbel, R.D.J.Froese, T.Matsubara, S.Sieber, K.Morokuma. *J. Phys. Chem.*, **100**, 19357 (1996)

231. V.L.Deringer, R.P.Stoffel, A.Togo, B.Eck, M.Meven, R.Dronskowski. *CrystEngComm*, **16**, 10907 (2014)
232. V.L.Deringer, A.Wang, J.George, R.Dronskowski, U.Englert. *Dalton Trans.*, **45**, 13680 (2016)
233. J.George, A.Wang, V.L.Deringer, R.Wang, R.Dronskowski, U.Englert. *CrystEngComm*, 17, 7414 (2015)
234. K.B.Sterri, V.L.Deringer, A.Houben, P.Jacobs, C.M.N.Kumar, R.Dronskowski. *Z. Naturforsch., Ser. B*, **71**, 431 (2016)
235. A.F.Zurhelle, V.L.Deringer, R.P.Stoffel, R.Dronskowski. *J. Phys.: Condens. Matter*, **28**, 115401 (2016)
236. J.George, V.L.Deringer, A.Wang, P.Müller, U.Englert, R.Dronskowski. *J. Chem. Phys.*, **145**, 234512 (2016)
237. A.Ø.Madsen, B.Civalleri, M.Ferrabone, F.Pascale, A.Erba. *Acta Crystallogr., Sect. A*, **69**, 309 (2013)
238. R.Dovesi, R.Orlando, A.Erba, C.M.Zicovich-Wilson, B.Civalleri, S.Casassa, L.Maschio, M.Ferrabone, M.D.L.Pierre, P.D'Arco, Y.Noël, M.Causá, M.Rérat, B.Kirtman. *Int. J. Quant. Chem.*, **114**, 1287 (2014)
239. A.Togo, I.Tanaka. *Scr. Mater.*, **108**, 1 (2015)
240. J.George, R.Wang, U.Englert, R.Dronskowski. *J. Chem. Phys.*, **147**, 074112 (2017)
241. K.N.Jarzembska, A.A.Hoser, R.Kamiåski, A.Ø.Madsen, K.Durka, K.Woźniak. *Cryst. Growth Des.*, **14**, 3453 (2014)
242. L.Mazur, K.N.Jarzembska, R.Kamiński, A.A.Hoser, A.Ø.Madsen, E.Pindelska, M.Zielińska-Pisklak. *Cryst. Growth Des.*, **16**, 3101 (2016)
243. A.E.Whitten, M.A.Spackman. *Acta Crystallogr., Sect. B*, **62**, 875 (2006)
244. J.Lübben, L.J.Bourhis, B.Dittrich. *J. Appl. Crystallogr.*, **48**, 1785 (2015)
245. A.A.Hoser, A.Ø.Madsen. *Acta Crystallogr., Sect. A*, **72**, 206 (2016)
246. H.-B.Bürgi. *Acta Crystallogr., Sect. B*, **45**, 383 (1989)
247. S.C.Capelli, A.Albinati, S.A.Mason, B.T.M.Willis. *J. Phys. Chem. A*, **110**, 11695 (2006)
248. A.A.Hoser, A.Ø.Madsen. *Acta Crystallogr. Sect. A*, **73**, 102 (2017)
249. D.Jayatilaka, B.Dittrich. *Acta Crystallogr., Sect. A*, **64**, 383 (2008)
250. M.Woińska, S.Grabowsky, P.M.Dominiak, K.Woźniak, D.Jayatilaka. *Sci. Adv.*, **2**, e1600192 (2016)
251. S.C.Capelli, H.-B.Bürgi, B.Dittrich, S.Grabowsky, D.Jayatilaka. *IUCrJ*, **1**, 361 (2014)
252. F.L.Hirshfeld. *Theor. Chim. Acta*, **44**, 129 (1977)
253. P.Politzer, R.R.Harris. *J. Am. Chem. Soc.*, **92**, 6451 (1970)
254. P.Politzer. *Theor. Chim. Acta*, **23**, 203 (1971)
255. M.A.Spackman, J.J.McKinnon. *CrystEngComm*, **4**, 378 (2002)
256. M.A.Spackman, P.G.Byrom. *Chem. Phys. Lett.*, **267**, 215 (1997)
257. P.R.Spackman, S.P.Thomas, D.Jayatilaka. *Sci. Rep.*, **6**, 22204 (2016)
258. I.Skovsen, M.Christensen, H.F.Clausen, J.Overgaard, C.Stiewe, T.Desgupta, E.Mueller, M.A.Spackman, B.B.Iversen. *Inorg. Chem.*, **49**, 9343 (2010)
259. M.Stachowicz, J.Parafiniuk, C.Wilson, S.Coles, K.Woźniak. *Am. Mineral.*, **100**, 110 (2015)
260. V.V.Avdeeva, M.I.Buzin, A.O.Dmitrienko, P.V.Dorovatovskii, E.A.Malinina, N.T.Kuznetsov, E.D.Voronova, Y.V.Zubavichus, A.V.Vologzhanina. *Chem. – Eur. J.*, **23**, 16819 (2017)
261. D.Jayatilaka, D.J.Grimwood. In *Computational Science — ICCS 2003*. (Berlin, Heidelberg: Springer, 2003). P. 142
262. O.V.Dolomanov, L.J.Bourhis, R.J.Gildea, J.A.K.Howard, H.Puschmann. *J. Appl. Crystallogr.*, **42**, 339 (2009)
263. P.Bultinck, D.L.Cooper, D.V.Neck. *Phys. Chem. Chem. Phys.*, **11**, 3424 (2009)
264. L.Checińska, W.Morgenroth, C.Paulmann, D.Jayatilaka, B.Dittrich. *CrystEngComm*, **15**, 2084 (2013)
265. M.Woińska, D.Jayatilaka, M.A.Spackman, A.J.Edwards, P.M.Dominiak, K.Woźniak, E.Nishibori, K.Sugimoto, S.Grabowsky. *Acta Crystallogr., Sect. A*, **70**, 483 (2014)
266. M.E.Wall. *IUCrJ*, **3**, 237 (2016)
267. M.Fugel, D.Jayatilaka, E.Hupf, J.Overgaard, V.R.Hathwar, P.Macchi, M.J.Turner, J.A.K.Howard, O.V.Dolomanov, H.Puschmann, B.B.Iversen, H.-B.Bürgi, S.Grabowsky. *IUCrJ*, **5**, 32 (2018)
268. T.A.Keith. *AIMALL, Version 09.04.23*, ttp://aim.tkgristmill.com (Last accessed on 15.01.2019)
269. I.Sovago, M.J.Gutmann, H.M.Senn, L.H.Thomas, C.C.Wilson, L.J.Farrugia. *Acta Crystallogr., Sect. B*, **72**, 39 (2016)
270. R.H.Blessing. *Acta Crystallogr., Sect. B*, **51**, 816 (1995)
271. S.Grabowsky, A.Genoni, H.-B.Bürgi. *Chem. Sci.*, **8**, 4159 (2017)
272. S.Grabowsky, P.Luger, J.Buschmann, T.Schneider, T.Schirmeister, A.N.Sobolev, D.Jayatilaka. *Angew. Chem., Int. Ed.*, **51**, 6776 (2012)
273. D.Jayatilaka, D.J.Grimwood. *Acta Crystallogr., Sect. A*, **57**, 76 (2001)
274. A.Genoni, B.Meyer. In *Advances in Quantum Chemistry. Vol. 73*. (Eds P.E.Hoggan, T.Ozdogan). (London: Academic Press, 2016). P. 333
275. P.Cassam-Chenaï, S.K.Wolff, G.S.Chandler, B.N.Figgis. *Int. J. Quantum Chem.*, **60**, 667 (1996)
276. G.Loupias, J.Chomilier. *Z. Phys. At. Mol. Clust.*, **2**, 297 (1986)
277. A.Mukherji, M.Karplus. *J. Chem. Phys.*, **38**, 44 (1963)
278. Y.Rasiel, D.R.Whitman. *J. Chem. Phys.*, **42**, 2124 (1965)
279. D.P.Chong, W.B.Brown. *J. Chem. Phys.*, **45**, 392 (1966)
280. D.P.Chong, Y.Rasiel. *J. Chem. Phys.*, **44**, 1819 (1966)
281. W.L.Clinton, J.Nakhleh, F.Wunderlich. *Phys. Rev.*, **177**, 1 (1969)
282. W.L.Clinton, A.J.Galli, L.J.Massa. *Phys. Rev.*, **177**, 7 (1969)
283. W.L.Clinton, G.A.Henderson, J.V.Prestia. *Phys. Rev.*, **177**, 13 (1969)
284. W.L.Clinton, G.B.Lamers. *Phys. Rev.*, **177**, 19 (1969)
285. W.L.Clinton, A.J.Galli, G.A.Henderson, G.B.Lamers, L.J.Massa, J.Zarur. *Phys. Rev.*, **177**, 27 (1969)
286. C.Frishberg, L.J.Massa. *Phys. Rev. B*, **24**, 7018 (1981)
287. L.Massa, M.Goldberg, C. Frishberg, R.F.Boehme, S.J.L.Placa. *Phys. Rev. Lett.*, **55**, 622 (1985)
288. Y.V.Aleksandrov, V.G.Tsirelson, I.M.Reznik, R.P.Ozerov. *Basic Solid State Phys.*, **155**, 201 (1989)
289. T.L.Gilbert. *Phys. Rev. B*, **12**, 2111 (1975)
290. G.A.Henderson, R.K.Zimmerman. *J. Chem. Phys.*, **65**, 619 (1976)
291. M.Levy. *Proc. Natl. Acad. Sci. USA*, **76**, 6062 (1979)
292. D.Jayatilaka. *Phys. Rev. Lett.*, **80**, 798 (1998)
293. I.Bytheway, D.J.Grimwood, D.Jayatilaka. *Acta Crystallogr., Sect. A*, **58**, 232 (2002)
294. I.Bytheway, D.J.Grimwood, B.N.Figgis, G.S.Chandler, D.Jayatilaka. *Acta Crystallogr., Sect. A*, **58**, 244 (2002)
295. R.F.Stewart. *J. Chem. Phys.*, **57**, 1664 (1972)
296. P.Coppens, T.V.Willoughby, L.N.Csonka. *Acta Crystallogr., Sect. A*, **27**, 248 (1971)
297. K.Tanaka. *Acta Crystallogr., Sect. A*, **44**, 1002 (1988)

298. D.Jayatilaka, P.Munshi, M.J.Turner, J.A.K.Howard, M.A.Spackman. *Phys. Chem. Chem. Phys.*, **11**, 7209 (2009)
299. D.Jayatilaka, D.Grimwood. *Acta Crystallogr., Sect. A*, **60**, 111 (2004)
300. S.Grabowsky, D.Jayatilaka, S.Mebs, P.Luger. *Chem. – Eur. J.*, **16**, 12818 (2010)
301. S.P.Thomas, D.Jayatilaka, T.N.Guru Row. *Phys. Chem. Chem. Phys.*, **17**, 25411 (2015)
302. A.E.Whitten, D.Jayatilaka, M.A.Spackman. *J. Chem. Phys.*, **125**, 174505 (2006)
303. D.D.Hickstein, J.M.Cole, M.J.Turner, D.Jayatilaka. *J. Chem. Phys.*, **139**, 064108 (2013)
304. F.Hamzaoui, A.Zanoun, G.Vergoten. *J. Mol. Struct.*, **697**, 17 (2004)
305. M.Hudák, D.Jayatilaka, L.Perašnová, S.Biskupič, J.Kožíšek, L.Bučinský. *Acta Crystallogr., Sect. A*, **66**, 78 (2010)
306. M.Reiher, A.Wolf. *Relativistic Quantum Chemistry: The Fundamental Theory of Molecular Science*. (Weinheim: Wiley, 2014)
307. A.Genoni, L.H.R.Dos Santos, B.Meyer, P.Macchi. *IUCrJ*, **4**, 136 (2017)
308. A.Genoni. *Acta Crystallogr., Sect. A*, **73**, 312 (2017)
309. S.F.Boys. *Rev. Mod. Phys.*, **32**, 296 (1960)
310. C.Edmiston, K.Ruedenberg. *Rev. Mod. Phys.*, **35**, 457 (1963)
311. J.Pipek, P.G.Mezey. *J. Chem. Phys.*, **90**, 4916 (1989)
312. A.Genoni. *J. Phys. Chem. Lett.*, **4**, 1093 (2013)
313. H.Stoll, G.Wagenblast, H.Preuß. *Theor. Chim. Acta*, **57**, 169 (1980)
314. M.Sironi, A.Famulari, M.Raimondi, S.Chiesa. *J. Mol. Struct. (THEOCHEM)*, **529**, 47 (2000)
315. M.Sironi, M.Ghitti, A.Genoni, G.Saladino, S.Pieraccini. *J. Mol. Struct. (THEOCHEM)*, **898**, 8 (2009)
316. P.D.Walker, P.G.Mezey. *J. Am. Chem. Soc.*, **116**, 12022 (1994)
317. B.Meyer, B.Guillot, M.F.Ruiz-Lopez, A.Genoni. *J. Chem. Theor. Comput.*, **12**, 1052 (2016)
318. B.Meyer, B.Guillot, M.F.Ruiz-Lopez, C.Jelsch, A.Genoni. *J. Chem. Theor. Comput.*, **12**, 1068 (2016)
319. A.Genoni, M.Sironi. *Theor. Chem. Acc.*, **112**, 254 (2004)
320. A.Genoni, A.Fornili, M.Sironi. *J. Comput. Chem.*, **26**, 827 (2005)
321. D.M.Philipp, R.A.Friesner. *J. Comput. Chem.*, **20**, 1468 (1999)
322. A.Genoni, L.Bučinský, N.Claiser, J.Contreras-García, B.Dittrich, P.M.Dominiak, E.Espinosa, C.Gatti, P.Giannozzi, J.-M.Gillet, D.Jayatilaka, P.Macchi, A.Ø.Madsen, L.Massa, C.F.Matta, K.M.Merz, P.N.H.Nakashima, H.Ott, U.Ryde, K.Schwarz, M.Sierka, S.Grabowsky. *Chem. – Eur. J.*, **24**, 10881 (2018)